Technical Report Documentation Page

1. Report No.	2. Government Accession No.	3. Recipient's Catalog No.
FHWA/TX-03/0-4203-2		

4. Title and Subtitle	5. Report Date
AS-BUILT PROPERTIES OF TEST PAVEMENTS ON IH-20 IN ATLANTA DISTRICT	March 2003
	6. Performing Organization Code
7. Author(s)	8. Performing Organization Report No.
Arif Chowdhury, Amit Bhasin, and Joe W. Button	Report 0-4203-2
9. Performing Organization Name and Address	10. Work Unit No. (TRAIS)
Texas Transportation Institute The Texas A&M University System College Station, Texas 77843-3135	11. Contract or Grant No. Project No. 0-4203
12. Sponsoring Agency Name and Address	13. Type of Report and Period Covered
Texas Department of Transportation Research and Technology Implementation Office P.O. Box 5080 Austin, Texas 78763-5080	Research: September 2001-August 2002
	14. Sponsoring Agency Code

15. Supplementary Notes

Research performed in cooperation with the Texas Department of Transportation and the U.S. Department of Transportation, Federal Highway Administration.
Research Project Title: Strategic Study for Resolving Hot Mix Related Issues

16. Abstract

The primary objectives of this research project were to measure as-built properties of nine test pavements and populate a database to be used in a future project for evaluating relationships between pavement performance and measured properties during construction. Texas Department of Transportation (TxDOT) Atlanta District constructed nine test sections on IH-20 in Harrison County. These sections were constructed with nine (three mixture types × three aggregate types) different mixtures as surface courses. Type B limestone mixture was used as asphaltic concrete pavement base for all nine test sections. Several agencies participated in both field and lab testing and data collection. Different field and lab tests were performed before, during, and after construction. Researchers from Texas Transportation Institute conducted several laboratory tests including asphalt pavement analyzer (APA), permeability, mixture proportion, and indirect tensile tests on both roadway cores and plant mixes. Dynamic modulus tests were conducted only on plant mix materials. Results from the tests performed by other agencies were collected for analysis and populating the database. This report documents the as-built properties. Detailed test results and as-built properties were recorded in electronic format on a compact disk and provided to TxDOT with this report.

Nine test sections were grouped and ranked on the basis of their laboratory test results. All the mixtures were of good quality; so their lab test results were not much different from each other. Preliminary assessment reveals that field air void contents affect performance significantly, especially permeability and indirect tensile strength. Another important factor for quality control is to maintain proper asphalt content during plant production.

17. Key Words	18. Distribution Statement
Dynamic Modulus, Pavement Performance, Permeability of HMA	No restrictions. This document is available to the public through NTIS: National Technical Information Service 5285 Port Royal Road Springfield, Virginia 22161

19. Security Classif.(of this report)	20. Security Classif.(of this page)	21. No. of Pages	22. Price
Unclassified	Unclassified	122	

Form DOT F 1700.7 (8-72) Reproduction of completed page authorized

AS-BUILT PROPERTIES OF TEST PAVEMENTS ON IH-20 IN ATLANTA DISTRICT

by

Arif Chowdhury
Associate Transportation Researcher

Amit Bhasin
Graduate Research Assistant

and

Joe W. Button
Senior Research Engineer

Report 0-4203-2
Project Number 0-4203
Research Project Title: Strategic Study for Resolving Hot Mix Related Issues

Sponsored by the
Texas Department of Transportation
In Cooperation with the
U.S. Department of Transportation
Federal Highway Administration

March 2003

TEXAS TRANSPORTATION INSTITUTE
The Texas A&M University System
College Station, Texas 77843-3135

DISCLAIMER

The contents of this report reflect the views of the authors, who are responsible for the facts and the accuracy of the data presented herein. The contents do not necessarily reflect the official view or policies of the Federal Highway Administration (FHWA) or the Texas Department of Transportation (TxDOT). This report does not constitute a standard, specification, or regulation. The engineer in charge of the project was Joe W. Button, P.E., (Texas, # 40874).

ACKNOWLEDGMENTS

This project was conducted in cooperation with the Texas Department of Transportation and the Federal Highway Administration. The researchers gratefully acknowledge the support and guidance of Mr. Dale Rand, project director during this phase of the project. Mr. Miles Garrison's contribution during every stage of the project is highly appreciated. The researchers are also thankful to Mr. Greg Cleveland, Dr. Dar Hao Chen, Mr. James Voss, Dr. Yetkin Yildirim, and Dr. Soheil Nazarian.

TABLE OF CONTENTS

Page

LIST OF FIGURES

Page

LIST OF TABLES

Page

CHAPTER 1: INTRODUCTION

GENERAL

Performance-related specifications (PRS), a recently introduced idea, have become increasingly popular in the pavements industry. Implementation of PRS requires that key quality characteristics used to establish conformance are measurable factors controlled by the contractor's operations or decisions in hot-mix asphalt (HMA) construction (*1*).

BACKGROUND

Hot-mix asphalt is used extensively throughout the United States as a cost-effective pavement surfacing material. Each year more than 550 million tons of HMA are placed in the United States at a cost of nearly 18 billion dollars (*2*). Small improvements in the life of HMA can result in substantial cost savings and economic benefit to the public agencies and private groups associated with HMA construction and maintenance. During the 1980s, the Strategic Highway Research Program (SHRP) initiated a major research effort to improve the life of HMA. This five-year research effort resulted in an improved binder specification and mixture design and analysis system known as Superpave. In the past, the Texas Department of Transportation (TxDOT) undertook several research projects to improve the life of HMA. The combination of changes in specification and construction practices and the implementation of federal and state research findings have yielded higher performing asphalt pavements.

Characterization of HMA properties is very critical for predicting the performance of asphalt pavement. TxDOT initiated Research Project 0-1708, "Predicting Hot-Mix Performance from Measured Properties," to develop simple, practical, and reliable test procedures for evaluating the quality of finished asphalt concrete pavements on the basis of predicted performance. To accomplish this goal, the researchers proposed a three-phase work plan that called for:

- conducting a detailed review of recent and ongoing related studies at the state and federal level (Phase I);

- identifying mixture-, construction-, and structural-related properties that are significant predictors of pavement performance and are under the contractor's control (Phase II); and
- identifying/modifying existing procedures or developing new procedures that relate the properties from Phase II to the expected field performance (Phase III).

The vision of Project 0-1708 researchers was that TxDOT would use the results to develop PRS for asphalt concrete pavements and to support the implementation of such specifications in the state. According to the proposal, development efforts would concentrate on quality control/quality assurance (QC/QA) test methods for new flexible pavements and would target the following areas:

- identification of key quality characteristics consisting of mixture, construction, and structural-related properties that are significant predictors of field performance;
- rational and practical test methods for measuring construction quality characteristics; and
- performance-related acceptance criteria.

The TxDOT Research Monitoring Committee-1 (RMC-1) terminated Project 0-1708 on August 31, 2001 after Phase 1 completion. RMC-1 reduced the scope of the project and included it in the first year of Project 0-4203. This work was performed as Task 9 of Project 0-4203. The number of tests planned in this task was significantly less than the number originally proposed in Phase II of Project 0-1708.

RESEARCH OBJECTIVE

Research Project 0-4203, "Strategic Study for Resolving Hot Mix Related Issues" was initiated to provide the tools for TxDOT to design and control HMA materials for pavements that will meet the increasing performance demands. The objectives of Task 9 are significantly different from the objectives of the entire project. The objectives of Task 9 are to measure the as-built properties of the base and surface courses of nine test pavements and populate a database to be used in future projects for evaluating relationships between pavement performance and measured properties during construction.

SCOPE OF REPORT

This report documents the as-built properties of nine test sections on Interstate Highway 20 (IH-20) in Harrison County, Atlanta District. The projects populate a database to be used in a future project for evaluating relationships between measured properties and pavement performance. The properties were measured before, during, and shortly after construction. This report also ranks the HMA mixtures used in the construction project with respect to their rutting, cracking, and moisture damage potential on the basis of measured laboratory testing. Even though the Texas Transportation Institute (TTI) compiled the data collected by several agencies, this report will concentrate on the laboratory tests conducted at TTI using plant mixture and roadway cores. Detailed test results and as-built properties were recorded in electronic format and provided to TxDOT on a compact disk with this report.

CHAPTER 2:
IH-20 TEST SECTIONS

BACKGROUND

TxDOT Atlanta District undertook a project (IM 20-7(57)) in late 2000 for the reconstruction and rehabilitation of existing roadway on IH-20 in Harrison County. Several agencies initiated a number of research projects to conduct numerous tests for this project. The research projects were designed to collect data before, during, and after the construction. In fact, one of the projects was designed to collect long-term pavement distress and traffic data (*3*). Beyond the regular QC/QA and other routine laboratory tests, researchers performed a number of additional tests. The agencies involved in collecting data and conducting tests are: TxDOT in-house research group, TxDOT Atlanta District lab, TTI, Center for Transportation Research (CTR) at The University of Texas at Austin, and The University of Texas at El Paso (UTEP). TTI participated under Project 0-1708, Project 0-4203, and Project 0-4126; CTR participated under Project 0-4185; and UTEP participated under Project 0-1735.

PROJECT DESCRIPTION

The control number of this construction project was CSJ 495-08-074. The project site was located on IH-20 from 0.5 mile west of Farm to Market (FM) Road 3251 to 0.5 miles east of State Highway (SH) 43. Net length of the project was 18616.60 ft or 3.525 miles and consisted of reconstruction of westbound (WB) and eastbound (EB) lanes and shoulders on each direction. Figure 1 depicts the layout of the test sections. Figure 2 presents a typical cross-section of a test section. The major items included in this construction project were:

- mill the old 4-inch asphalt concrete pavement above the damaged 8-inch continuously reinforced concrete pavement (CRCP),
- repair the CRCP,
- apply a new HMA base, and
- place a new surface course overlay.

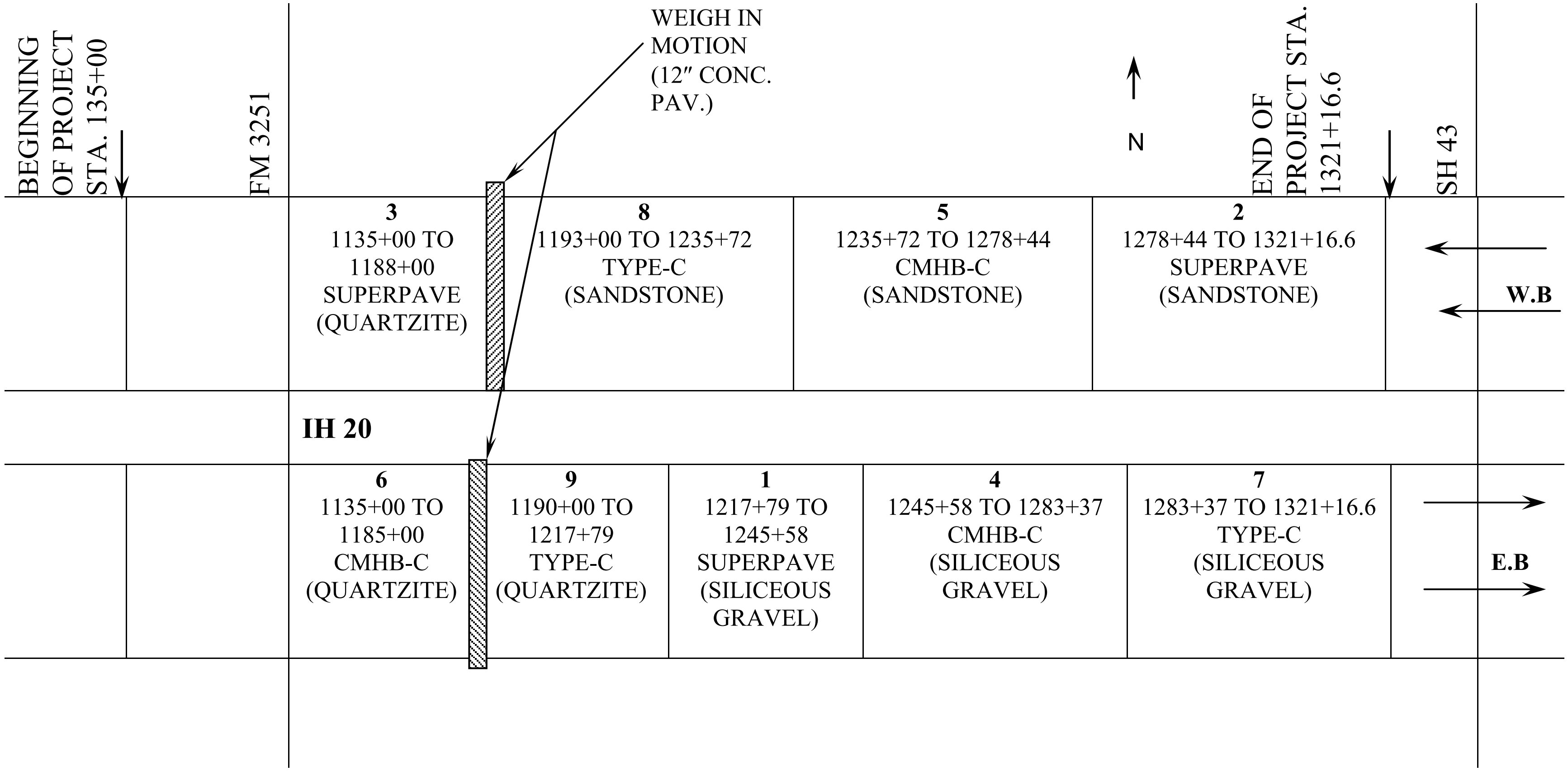

Figure 1. IH-20 Test Section Layout.

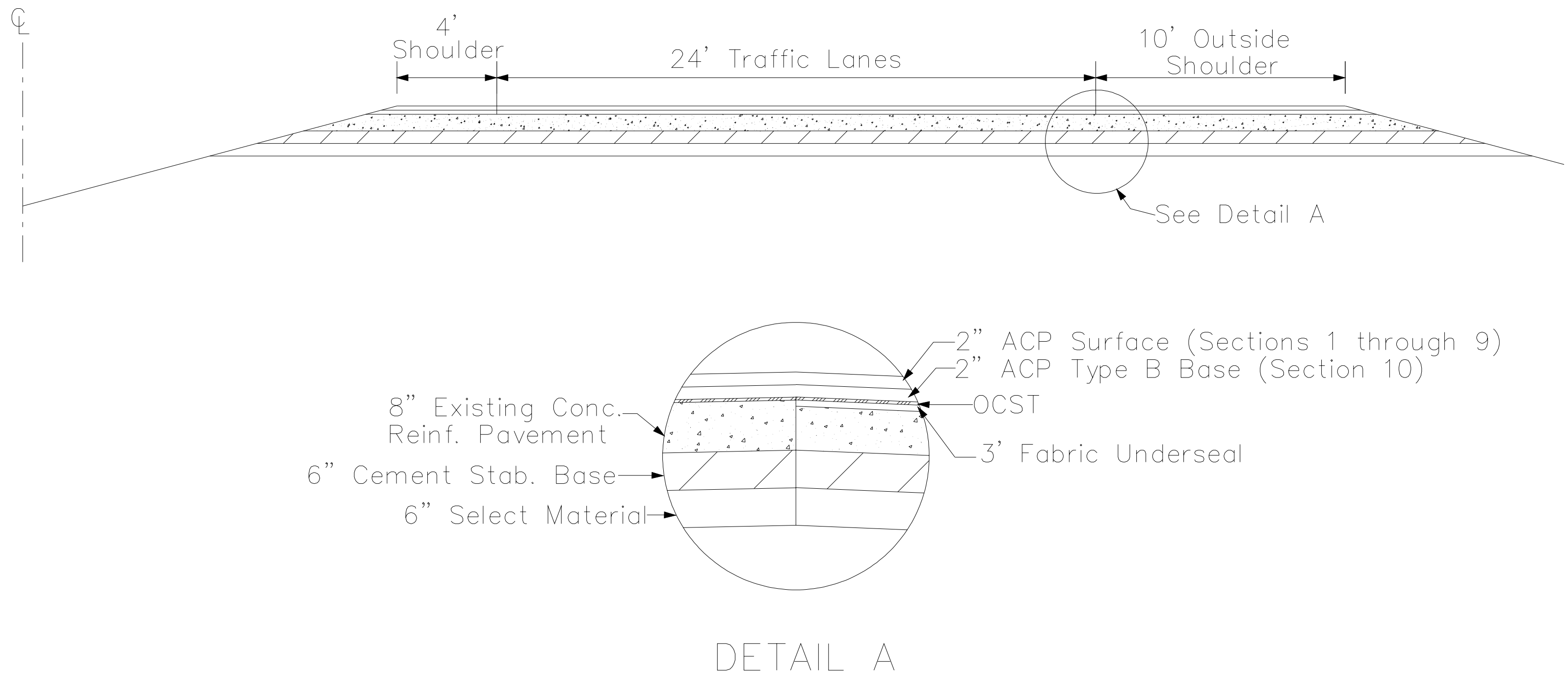

Figure 2. Typical Cross Section.

Construction Sequence

Construction began in the summer of 2001 and ended in December 2001. The prime contractor of this project was Maden Contracting Company. Longview Asphalt produced all the HMA mixture in their batch plant. The uppermost existing 4-inch (100 mm) HMA layer was milled out at the beginning. After milling off the top HMA layer, the CRCP layer was repaired as needed. Type B HMA base was placed above the repaired CRCP layer. The average thickness of this base course was 2 inches (50 mm). Fabric was placed between Type B mixture and the repaired CRCP layer at the shoulder. Finally, the surface course was placed above the base course. Average thickness of the surface course was 2 inches (50 mm). Nine different mixture designs were used to pave the surface layer. The contractor used a material transfer device during the paving operation in order to reduce HMA segregation. These nine surface mixtures constitute nine test sections. Researchers conducted a number of nondestructive tests (NDT) on existing pavements to collect data before milling, during construction of the different layers, and after the surface layer was completed.

MIXTURE DESIGN

Throughout the whole construction site, only one mixture design for the Type B base course was used. Each of the nine test sections had a different mixture as a surface course. Three different types of aggregate and three mixture designs constituted a matrix of nine (3 × 3) surface mixture designs (Table 1). All 10 mixtures were produced using one type of asphalt, i.e., PG 76-22 from Wright Asphalt in Houston, Texas.

Superpave Mixtures

Three Superpave mixtures were designed considering 30 million equivalent single axle load (ESAL) as Design ESAL. The number of gyrations as N_{ini}, N_{des}, and N_{max} were 9, 125, and 205, respectively. They were designed following the current Superpave mixture design procedure, Tex-204-F, Part IV. Table 2 lists aggregate gradations used for the three Superpave mixtures.

Table 1. Matrix of Mixture Types Used in Surface Course.

Aggregate Type	Aggregate Supplier	Aggregate Source	Test Section Number and Mixture Designation		
			12.5 mm Superpave	CMHB-C	Type C
Quartzite	Martin Marietta	Jones Mill	3 A0113 (H01-09)	6 A0115 (H01-16)	9 A0118 (H01-19)
Sandstone	Meridian	Sawyer, OK	2 A0112 (H01-08)	5 A016 (H01-17)	8 A0119 (H01-20)
Siliceous River Gravel	Hanson	Prescott, AK	1 A0111 (H01-07)	4 A0114 (H01-15)	7 A0117 (H01-18)

Table 2. Aggregate Gradations Used for Superpave Mixtures.

Sieve Size (mm)	Cumulative Percent Passing		
	Siliceous Gravel (Section 1)	Sandstone (Section 2)	Quartzite (Section 3)
19.0	100.0	100.0	100.0
12.5	92.0	92.1	93.7
9.5	84.8	79.4	81.7
4.75	52.4	49.0	45.5
2.36	30.9	29.2	31.4
1.18	20.4	22.4	21.0
0.6	13.9	18.9	17.7
0.3	8.8	14.9	11.8
0.15	4.5	10.2	8.2
0.075	3.2	6.5	5.6

The Section 1 Superpave mixture used 67 percent siliceous river gravel, 32 percent limestone screenings, and 1 percent hydrated lime. The Section 2 Superpave mixture used 91 percent sandstone, 8 percent igneous screenings, and 1 percent hydrated lime. The Section 3 Superpave mixture used 89 percent quartzite, 10 percent igneous screenings, and 1 percent hydrated lime. Combined aggregate gradation for each of the three Superpave mixtures passed below the restricted zone. Table 3 summarizes all Superpave mixture designs. Appendix A shows the details of these mixture designs.

Table 3. Superpave Mixture Design Summary.

Mixture	AC (%)	Air Void (%)	VMA (%)	VFA (%)	Percent G_{mm} at N_{ini}	Percent G_{mm} at N_{max}	Dust Proportion
Section 1, Siliceous Gravel	5.0	3.7	15.3	73.9	86.9	97.5	0.6
Section 2, Sandstone	5.1	3.8	15.1	73.1	86.0	97.4	1.3
Section 3, Quartzite	5.1	3.8	15.6	73.1	86.5	97.4	1.1
Specification	N/A	4.0±1.0	14.0 Min	65-75	89.0 Max	98.0 Max	0.6 – 1.2

CMHB-C Mixtures

Three CMHB-C mixtures were designed using three different types of aggregates. The design procedure followed TxDOT mixture design method Tex-204-F, Part II. Table 4 describes the aggregate gradations used for three CMHB mixtures. The Section 4 mixture is composed of 79 percent siliceous gravel, 20 percent igneous screenings, and 1 percent hydrated lime. The Section 5 CMHB mixture is composed of 87 percent sandstone, 12 percent igneous screenings,

Table 4. Aggregate Gradations Used for CMHB-C Mixtures.

Sieve Size	Cumulative Percent Passing		
	Siliceous Gravel (Section 4)	Sandstone (Section 5)	Quartzite (Section 6)
7/8 in	100.0	100.0	100.0
5/8 in	99.7	100.0	99.6
3/8 in	64.5	65.4	65.6
# 4	34.3	38.0	34.2
# 10	21.8	24.0	24.0
# 40	16.2	16.4	14.5
# 80	9.8	10.9	9.1
# 200	6.4	6.4	5.9

and 1 percent hydrated lime. The Section 6 mixture uses 87 percent quartzite, 12 percent igneous screenings, and 1 percent hydrated lime. Table 5 summarizes the three CMHB mixtures. Appendix A documents details of the mixture designs.

Table 5. CMHB-C Mixture Design Summary.

Mixture	Optimum Asphalt Content (%)	Design Air Void (%)	VMA (%)
Section 4 (Siliceous Gravel)	4.7	3.5	14.1
Section 5 (Sandstone)	4.8	3.5	14.6
Section 6 (Quartzite)	4.8	3.5	14.1

Type C Mixtures

Three newly designed Type C mixtures used the same three types of aggregates used for Superpave mixture and CMHB-C mixtures. Table 6 describes the aggregate gradations of these mixtures. The Section 7 Type C mixture is composed of 61 percent siliceous gravel, 30 percent limestone screenings, 8 percent igneous screenings, and 1 percent hydrated lime. The Section 8 Type C mixture was designed using 99 percent sandstone and 1 percent hydrated lime. The Section 9 Type C mixture was designed using 91 percent quartzite, 8 percent igneous screenings, and 1 percent hydrated lime.

Table 6. Aggregate Gradations Used for Type C Mixtures.

Sieve Size	Cumulative Percent Passing		
	Siliceous Gravel (Section 7)	Sandstone (Section 8)	Quartzite (Section 9)
7/8 in	100.0	100.0	100.0
5/8 in	100.0	99.8	99.8
3/8 in	75.8	80.7	79.1
# 4	49.2	46.2	51.4
# 10	31.5	30.9	34.0
# 40	18.2	15.6	17.9
# 80	11.7	9.6	10.0
# 200	5.8	5.8	5.3

Table 7 summarizes the Type C mixtures. Appendix A presents the details of these mixture designs.

Table 7. Type C Mixture Design Summary.

Mixture	Optimum Asphalt Content (%)	Design Air Void (%)	VMA (%)
Section 7 (Siliceous Gravel)	4.4	4.0	14.0
Section 8 (Sandstone)	4.5	4.0	14.1
Section 9 (Quartzite)	4.6	4.0	14.6

Type B Mixture

The Type B base mixture was designed using about 90 percent limestone aggregate from Hanson (Perch Hill) and 10 percent field sand from Marshall, Texas. In this report, the Type B base mixture is termed Section 10. In fact, this section represents all nine base course sections. Table 8 presents the combined design gradation and other mixture design data of Type B mixture.

Table 8. Type B Mixture Design Summary.

<table>
<tr><th>Sieve Size</th><th>Percent Passing</th><th colspan="2">Design Summary</th></tr>
<tr><td>7/8 in</td><td>100.0</td><td rowspan="2">Optimum Asphalt Content (%)</td><td rowspan="2">3.8</td></tr>
<tr><td>5/8 in</td><td>90.1</td></tr>
<tr><td>3/8 in</td><td>79.4</td><td rowspan="2">Design Air Void (%)</td><td rowspan="2">4.0</td></tr>
<tr><td>#4</td><td>52.9</td></tr>
<tr><td>#10</td><td>31.9</td><td rowspan="2">Design VMA (%)</td><td rowspan="2">13.0</td></tr>
<tr><td>#40</td><td>19.4</td></tr>
<tr><td>#80</td><td>9.8</td><td rowspan="2">Rice Specific Gravity (gm/cc)</td><td rowspan="2">2.516</td></tr>
<tr><td>#200</td><td>3.8</td></tr>
</table>

DATA COLLECTION

An ambitious plan was undertaken for data collection on this construction project. Researchers collected data before, during, and after the construction. Several agencies collected laboratory and field data. During construction, several types of data were collected at different stages. There is also a long-term plan to monitor pavement performance. So, the data collection process will be continued. Initially, a few more types of data collection were in plan; however, due to a shortage of funding, some of them were omitted by TxDOT.

Table 9 shows the type of data for which each agency was responsible. Some of the data mentioned in Table 9 is still in the collection phase and some data collection will be continued for several more years. This report focuses primarily on the laboratory tests performed by TTI. Researchers collected test data available from different sources. These data (raw and analyzed) are compiled on a compact disc and will be delivered to TxDOT as a deliverable product (P2).

Researchers at TTI made a sincere effort to gather all test results from the other agencies, but sometimes all the necessary data were not readily available. Table 10 describes the construction limits, chronology, and weather condition during the paving of surface courses. Table 11 describes similar information obtained during paving of the base course (Type B mixture). Information presented in Table 10 and Table 11 was excerpted from a TxDOT construction diary.

Table 9. Data Collection Scheme for IH-20 Project.

Test/Data	Laboratory Tests			Construction Related Tests			Pavement Condition Moni-toring
	Molded Specimens		AC Cores Random Sample				
	Mix Design	As-Produced Plant Mix		Existing Pave-ment	After CRCP Repair	Over-lay	
Engineering Properties (Potential Performance Indicator)							
• Permeability		TTI	TTI				
• APA Rutting Test		TTI	TTI				
• Dynamic Modulus		TTI					
• Indirect Tensile Strength		TTI	TTI				
• Hamburg	TxDOT	CTR	CTR				
• Moisture Sensitivity (531-C)	TxDOT						
• Binder Properties from Cores	TxDOT		TTI				
Mixture Proportion							
• Binder Content		TTI	TTI				
• Air Voids (Molded Specimen)			TTI				
• Gradation		TxDOT	TTI				
Nondestructive Testing							
• Ground Penetrating Radar				TxDOT		TTI	TxDOT
• Seismic Pavement Analyzer						UTEP	
• Infrared						TTI	
• Nuclear Density Gauge						TxDOT	
• PaveTracker						TTI	
• Falling Weight Deflectometer				TxDOT			
• Rolling Depth Deflectometer				TxDOT	TxDOT	TxDOT	
• P-SPA						UTEP	
Pavement Performance Indicator							
• Ride Quality				TxDOT	TxDOT	TxDOT	TxDOT
• Distress				CTR		CTR	CTR
• Traffic – WIM Data						TxDOT	TxDOT

Table 10. Construction Records for Surface Courses.

Date	Section	Station	Principal Item of Work	Time		Weather/Comment
				Start	End	
11.06.2001	2	1321+16 – 1278+44	ACP Surface WB and shoulder	6:30 am	5:30 pm	Clear and Mild, Air Temp at start 50°F+, Surface Temp at start 56°F+
11.08.2001	5	1235+72 – 1278+44	ACP Surface at WB lanes and shoulders	7:00 am	--	Cloudy and Mild, Temp 50°F and rising at the start
11.12.2001	8	1236+00 – 1193+00	ACP Surface at WB IS lane and shoulder	10:00 am	1:40 pm	Cloudy and Mild, Temp 60°F and rising at the start
11.13.2001	8	1236+45 – 1193+00	ACP Surface at WB OS lane and shoulder	7:00 am	12:30 pm	Clear and Warm, 60°F rising
11.13.2001	3	1188+00 – 1135+00	ACP Surface at WB IS lane and shoulder	1:00 pm	5:30 pm	Same as above
11.14.2001	3	1188+00 – 1135+00	ACP Surface at WB lanes, shoulders, & ramps	7:00 am	5:00 pm	Cloudy and Warm, Temp 60°F and rising at start
11.15.2001	6	1135+00 – 1185+00	ACP Surface at EB lanes	7:00 am	1:00 pm	Clear and Warm
11.16.2001	6	1135+00 – 1190+00	ACP surface at EB lane and Ramp	9:00 am	5:00 pm	Cloudy and Mild, Temp 60°F and rising at start
11.19.2001	9	1190+00 – 1217+79	ACP Surface at EB lanes	7:00 am	5:00 pm	Cloudy and mild, Temp 50°F throughout the day, Rain
11.20.2001	1	1217+79 – 1245+58	ACP surface at EB	8:30 am	3:30 pm	Clear and Cool, Low 30s, Temp 40°F and rising at start
11.26.2001	4	1245+58 – 1281+75	ACP Surface at EB	7:00 am	6:00 pm	Cloudy and Mild, Temp 60°F and rising at start
11.27.2001	7	1281+75 – 1321+16	ACP Surface EB lanes and shoulders	9:00 am	4:30 pm	Cloudy and Mild, Temp 50°F throughout the day
11.27.2001	7	1281+75 – 1321+16	ACP Surface at EB lanes and shoulders	9:00 am	4:30 pm	Cloudy and Mild, Temp 50°F+ throughout the day
11.30.2001	7	1298+50 – 1321+16	ACP Surface EB OS shoulder	10:00 am	11:45 am	Clear and Cold, Temp Low 34°F and high 61°F
11.30.2001	7	1294+00 – 1304+50	ACP Surface EB IS lane	1:00 pm	4:30 pm	Same as above

WB – Westbound, EB – Eastbound, OS – Outside, IS – Inside, -- data not available

Table 11. Construction Records for Type B Base Courses.

Date	Sec-tion	Station	Principal Item of Work	Time		Weather/Comment
				Start	End	
09.06.2001	10	1371+17 – 1255+00	ACP Base and Fabric Underseal	7:00 am	4:30 pm	Cloudy and Hot Rain late afternoon
09.07.2001	10	1235+00 – 1135+00	ACP Base at WB OS lane	7:00 am	5:00 pm	Partly Cloudy and Hot
09.07.2001	10	1135+00 – 1278+00	ACP Base at WB OS shoulder	7:00 am	6:30 pm	Partly Cloudy and Hot
10.01.2001	10	1135+00 – 1263+60	ACP Base at EB OS lane	--	--	Clear and Warm Temp 60°F+ at Start of work
10.02.2001	10	1263+60 – 1321+16	ACP Base at EB OS lane	7:00 am	--	Clear and Warm, Morning Temp 50°F+
10.02.2001	10	1321+10 – 1252+00	ACP Base at WB IS lane and shoulder	--	3:00 pm	Same as above
10.10.2001	10	1135+00 – 1321+16	ACP Base at EB OS shoulder	7:00 am	6:00 pm	Cloudy and Warm
10.12.2001	10	1290+00 – 1227+00	ACP Base at WB IS lane and shoulder	11:30 am	5:00 pm	Cloudy and Mild
10.15.2001	10	1227+00 – 1135+00	ACP Base WB IS	7:30 am	--	Clear and Warm, Temp 50°F+ at the start
10.15.2001	10	FM 3251 Ramps	ACP Base at Exit and Entrance Ramp	--	6:30 pm	Same as above

WB – Westbound, EB – Eastbound, OS – Outside, IS – Inside, -- data not available

CHAPTER 3:
LABORATORY TESTS

GENERAL

TTI researchers conducted several laboratory tests to evaluate the rutting, fatigue, and moisture damage resistance potential of 10 different mixtures used in the test sections. According to Project 0-1708, Phase II proposal, researchers planned to conduct tests on virgin materials, plant mix, and roadway cores. Originally, roadway cores were supposed to be collected from potentially best, potentially worst, and random locations of each test section. This task was significantly scaled down due to a shortage of funding. The number of tests and locations of core specimens were reduced as well. After consulting with the project director and project monitoring committee, the researchers decided to conduct tests on only plant mix materials and roadway cores collected from random locations.

The Atlanta District laboratory collected loose plant mix material on the same day the mixture was used in the actual roadway. The loose mix was sealed in 5-gallon metallic buckets and later shipped to TTI. During collection of the loose plant mix, Atlanta District technicians made a great effort to avoid segregated mix to gather representative samples. While using the plant mix for specimen compaction, researchers reheated one bucket at a time to minimize aging. The Atlanta District lab also collected 4-inch and 6-inch cores from the surface course of each section and cores from the base course. Collection of cores from the Type B base was difficult due to thin layers and the underlying fabric. As a result, the bottom part of each of the Type B cores was damaged and unsuitable for further testing. District lab technicians gave up their effort of getting those cores after several unsuccessful attempts. Appendix C documents the locations of cores tested and their physical characteristics.

TESTS PERFORMED AT TTI

In the project kick-off meeting, the researchers, project director, and project monitoring committee agreed to conduct the following laboratory tests at TTI:

1) permeability tests on both roadway cores and lab compacted specimens,

2) asphalt pavement analyzer (APA) tests on both roadway cores and lab compacted specimens,
3) indirect tensile (IDT) strength test on both roadway cores and lab compacted specimens,
4) dynamic modulus testing using the lab compacted specimens,
5) asphalt content determination from cores,
6) aggregate gradation from cores, and
7) dynamic shear modulus on extracted asphalt from roadway cores.

TTI also prepared lab compacted specimens (four from each of the 10 sections) using the plant mix materials. These specimens were sent to Dr. Soheil Nazarian at The University of Texas at El Paso. He conducted permanent deformation/dynamic modulus tests on those specimens. Dr. Nazarian conducted the Portable Seismic Pavement Analyzer (P-SPA) on the compacted roadway surfaces for all nine test sections. Appendix C contains a summary of the test results performed by UTEP. The detailed results can be found in Report TX-02-1735-3F (*4*).

CTR conducted a visual inspection at different stages of construction. They also conducted tests using the Hamburg Wheel Tracking Device (HWTD) on both plant mix and roadway cores. Appendix C contains the results from CTR.

The following sections briefly explain the tests conducted at TTI facilities.

Permeability Test

The mechanisms of moisture damage in HMA and the methods of prevention are not well understood (*5*). Moisture damage may result from stripping of the asphalt film off a hydrophilic (water-loving) aggregate surface, chemical degradation and resulting loss of binder cohesion due to water, and factors yet to be discovered. Movement of traffic exacerbates moisture damage by creating excessive pore pressure. The excessive pore water pressure weakens the pavement layer from the inside and scours binder off the aggregate surface by forcing liquid water to move small distances at very high speeds.

Many state highway agencies are experiencing problems with HMA moisture susceptibility, particularly those in the eastern US and mountainous areas where precipitation rates are higher. HMA factors favoring moisture resistance are low air voids (low permeability), harder asphalts, improved asphalt-aggregate adhesion (higher mixing temperatures, antistrip treatments, and harder asphalts), clean aggregates, low filler/asphalt ratio, controlled segregation, and minimal initial moisture at construction. Other pertinent factors include asphalt or aggregate chemistry, other permeable or impermeable layers in the pavement (trapped water), annual precipitation, and asphalt modifiers.

As discussed earlier, the effect of air voids on moisture susceptibility may increase with coarseness (larger size or coarser gradation) of dense-graded mixture. This increase occurs because, for a given air void content, permeability (i.e., interconnected voids) increases with coarseness of the mix. This phenomenon explains the fact that the coarser Superpave mixtures and CMHB, designed at 4 percent air voids, have exhibited more permeability than former conventional dense-graded mixtures.

Permeability of asphalt pavement is one of the indicators of its moisture damage susceptibility. Several research studies have been performed utilizing different methodologies and procedures for measuring the permeability constant of HMA pavement. Permeability tests have been performed with either water or air. In the past, most researchers used water for determining the permeability of HMA mixtures. Darcy's law is generally used when computing this value; however, assumptions are made such that Darcy's law will remain valid. These assumptions include full saturation of the test specimens prior to testing and laminar flow throughout the testing (*6*). Higher permeability may be an indication of higher moisture induced damage to HMA pavement. Researchers can determine permeability of HMA mixtures in two different ways in the laboratory: falling head and constant head methods. In this project, researchers chose the falling head method.

Researchers followed the ASTM PS 129-01 (Standard Provisional Test Method for Measurement of Permeability of Bituminous Paving Mixtures Using a Flexible Wall Permeameter) procedure to measure the permeability in the laboratory (*7*). This laboratory test determines the conductivity of a compacted HMA sample (either laboratory molded specimen or roadway core). Figure 3 shows the schematic diagram of a falling head permeability test apparatus used to determine the rate of flow of water through a specimen. Water in a graduated cylinder is allowed to flow through a saturated asphalt sample, and the interval of time required to reach a known change in head is recorded. The coefficient of permeability of the asphalt sample is then determined based on Darcy's law. In this test procedure, it is assumed that the water flow is one-dimensional and laminar. Figures 4 and 5 demonstrate the actual apparatus used in this project.

The Superpave gyratory compacted (lab molded) specimens used for this test procedure were 6 inches in diameter and 3 inches in height with 7±1 percent air voids. This air void level was selected to mimic field conditions at construction. The field cores were 6 inches in diameter and approximately 2 inches in height (since the surface layer thickness was only 2 inches). The same specimens were tested using the APA after performing the permeability test. The cylindrical sides of the core specimens were smooth, and there were no gaps between the specimen and membrane surrounding the specimen. As a result, the fluid flow is assumed to be downward perpendicular to the plane surface only. However, the lab compacted specimens did not have smooth cylindrical surface, and there were intermittent gaps between the specimen and membrane. Therefore, the researchers applied a small amount of petroleum jelly to the cylindrical surface of the specimen to minimize flow along the side of the specimen.

Asphalt Pavement Analyzer

For the last two decades, the use of laboratory-scale wheel testers to estimate the rutting potential of HMA mixtures has increased. Most of the wheel testers estimate rutting susceptibility of asphalt mixtures by applying repeated wheel passes in a comparatively short period and usually employ an elevated temperature to accelerate the damage. Many transportation agencies and pavement industrial firms have begun using loaded wheel testers (LWT) to supplement their mixture design procedure (*8*).

The APA is a multifunctional loaded wheel tester used for evaluating permanent deformation (Figure 6). The APA is basically a modified and improved version of the Georgia Loaded Wheel Tester (GLWT). Operation of the APA is similar to that of the GLWT. By far, the APA is the most popular and commonly used loaded wheel tester in the US. Oscillating beveled aluminum wheels apply a repetitive load through high-pressure hoses to generate the desired contact pressure. Rutting susceptibility of HMA can be assessed by the APA using beam or cylindrical specimens under repetitive wheel loads and measuring the amount of permanent deformation under the wheelpath.

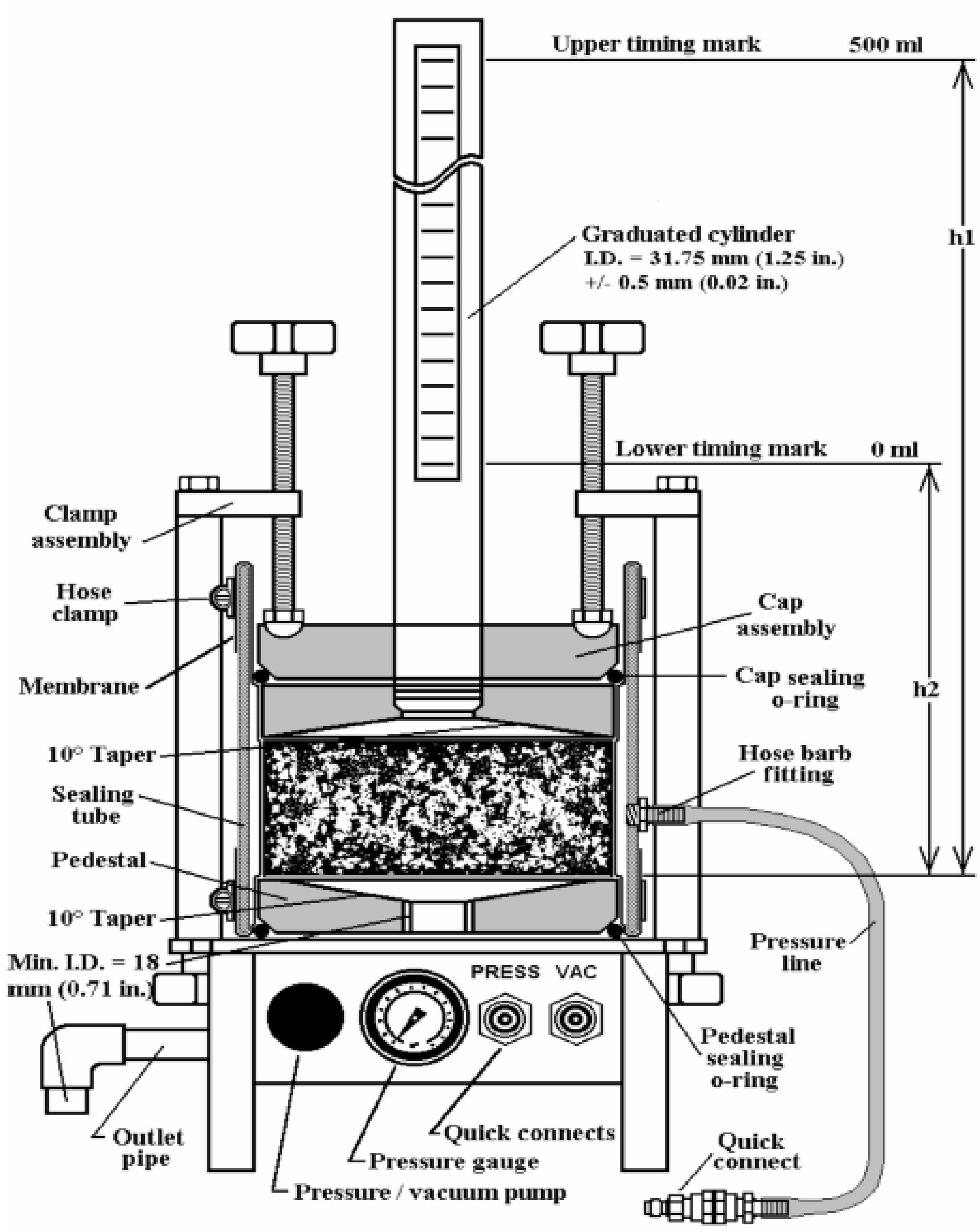

Figure 3. Falling Head Permeability Testing Apparatus.

Figure 4. Florida Permeability Test Apparatus.

Figure 5. Florida Permeability Test Setup.

Figure 7 shows the specimens set up in the APA machine. In this project, two types of specimens were tested using the APA: roadway cores and lab compacted cylindrical specimens. Before conducting the APA test, researchers measured permeability of these specimens. Six cylindrical specimens for each mixture were cored from each of the test sections. The cores were 6 inches (150 mm) in diameter and 2 inches (50 mm) in height. Standard APA testing requires 3-inch (75 mm) high specimens. Therefore, plaster of paris was added to the bottom surface of each of the roadway cores so that the overall height measured 3 inches (75 mm). Figure 8 shows a composite core specimen. The lab compacted specimens, prepared using the Superpave gyratory compactor, were 6 inches (150 mm) in diameter and 3 inches (75 mm) in height. The APA manufacturer recommends using three pairs of specimens for testing each mixture. Researchers prepared lab compacted specimens with 7±1 percent air voids. Seven percent air voids was chosen to conform to target field density. Rutting tests were performed at 147°F (64°C) for all the mixtures. The APA manufacturer suggests testing at the high temperature of the asphalt PG grade. In this case, the high temperature was 76°C (168.8°F). In fact, the asphalt PG grade for that particular location, according to the Superpave software, was 64°C (147°F). The asphalt was bumped up two grades due to high volume of traffic and the importance of the highway. Moreover, 168.8°F (76°C) was too high.

Each set of specimens was subjected to 8000 APA load cycles (*9*). One load cycle consists of one forward and one backward movement of the wheel. The wheel load and hose pressure were 100 lb (445 N) and 100 psi (690 kPa), respectively. The vertical linear variable distance transducer (LVDT) attached to the wheel measures the rut depth at four different points on each set of specimens. Two specimens in one mold form a set of specimens. The average of four readings is calculated as the rut depth of one set of specimens. The grand average of three rut depths measured on three sets of specimens is reported as mixture rut depth.

Figure 6. Asphalt Pavement Analyzer.

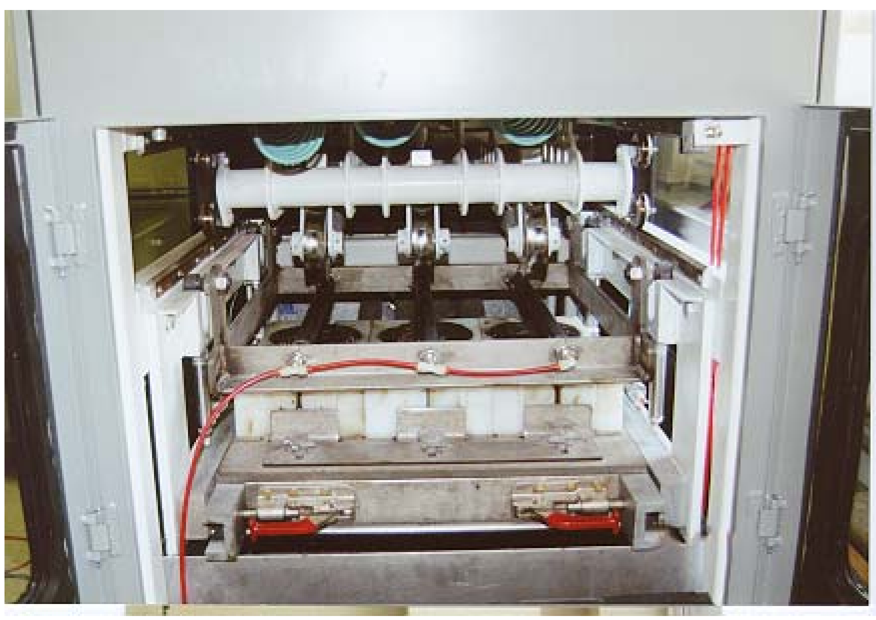

Figure 7. APA Test Setup.

Figure 8. Modified Roadway Core Specimen after APA Testing.

Indirect Tensile Test

Since the 1960s, the indirect tensile test has been extensively used in structural design, research of flexible pavement, and HMA mixture design (*10*). The SHRP Long-Term Pavement Performance (LTPP) program and AASHTO Guide for Design of Pavement Structures (1986 and 1993 versions) recommend an indirect tensile test for mixture characterization. The popularity of this test is mainly due to the fact that cores from thin lifts can be tested in the laboratory. This test is easy, quick, and characterized as less variable.

Some researchers correlated the indirect tensile strength with fatigue resistance of HMA pavements. Witczak et al. (*10*) reported a fair correlation between indirect tensile strength and fatigue resistance for the WesTrack site. Guddati et al. (*11*) indicated that there is good potential in predicting fatigue cracking using IDT strength results.

Researchers followed Tex-226-F (Indirect Tensile Strength Test) procedures to determine the tensile strength of lab compacted specimens and roadway cores. The specimens used in this test (both lab molded and roadway cores) were 4 inches in diameter and 2 inches in height. Figure 9 depicts IDT test setup. Lab prepared specimens were compacted to 7±1 percent air voids using the Superpave gyratory compactor. Researchers conducted the test at a strain rate of 2 inches/minute (50 mm/minute) at room temperature (77°F or 25°C).

Figure 9. Indirect Tensile Strength Test Setup.

Dynamic Modulus Test

Work initiated under Federal Highway Administration (FHWA) sponsorship and now continues under National Cooperative Highway Research Program (NCHRP) Project 9-19, "*Superpave Support and Performance Models Management.*" This project will lead to the development and validation of an advanced material characterization model and associated laboratory testing procedures for HMA. Researchers of NCHRP Project 9-19 developed a 'simple performance test' protocol to characterize both rutting and fatigue properties of HMA mixtures (*10, 14*). The dynamic modulus test procedure applies a sinusoidal axial compressive stress to a HMA specimen at a given spectrum of temperatures and loading frequencies. The measured applied stress and resulting recoverable strain responses are used to calculate the dynamic modulus and phase angle. Complex modulus, expressed as E^*, is a complex number defining the relationship between stress and strain for a linear viscoelastic material. Dynamic modulus, expressed as $|E^*|$, is the absolute value of complex modulus. Dynamic modulus is calculated by dividing the peak-to-peak stress by the peak-to-peak strain for a material subjected to sinusoidal loading. Phase angle (δ) is the lag time measured in degrees between a sinusoidally applied stress and resulting strain in a stress controlled test.

The results obtained from this test can be used to construct a master curve using the dynamic modulus value measured at different temperatures and frequencies. This master curve can be used for characterizing HMA mixtures for pavement thickness design and performance analysis. This master curve, in fact, characterizes both the rutting and fatigue performance of HMA mixtures.

Specimen Preparation

This test is conducted on a 4-inch (100 mm) diameter and 6-inch (150 mm) high compacted specimen. This size of specimen could not be obtained from a roadway core. So, the researchers used only specimens compacted at the lab using loose plant mix materials. Since the plant mix had already experienced the aging phase, further aging at the lab was not necessary. Researchers reheated the loose mixture to the compaction temperature (approximately 300°F). Initially, the specimens were compacted using the Superpave gyratory compactor at dimensions of 6-inch diameter and 7-inch height. The final specimen (4-inch diameter and 6-inch height) was obtained by coring from the 6-inch diameter specimen and sawing the two ends. The final air void contents of the cored specimens were maintained within +/-0.5 percent of the design air voids, which were typically 4 percent. Air void content of the cored specimen used for testing was typically 1.5 to 2 percent less than the larger size lab compacted specimen. The 6-inch diameter specimens were therefore compacted to approximately 6 percent air void content.

Three replicate specimens from each of the 10 sections were compacted. Coring and sawing made the specimen process somewhat complicated and time consuming, but the cored and sawed specimens typically have more uniform air void distribution (*10*). The smooth cylindrical surface was very conducive for attaching LVDTs.

Testing

Testing was performed on two replicates, each with three LVDTs for recording the strain. The LVDTs were fixed to the specimen using fastening clamps which were glued to the specimen surface (Figure10). A spacing of 4 inches (100 mm) between the studs was maintained which left about 1 inch (25 mm) from either face of the specimen. Care was taken to ensure that the studs where in vertical alignment. Each LVDT was placed at an equal distance (120°) around the cylindrical surface.

Each specimen was tested at six different frequencies of loading and four different temperatures. NCHRP researchers proposed five different temperatures for conducting this test including 10°F (-12°C) (*10*). The stress required to cause measurable strain at 10°F was beyond the capacity of the test equipment available at TTI at that time. Table 12 mentions the stress applied for each temperature and frequency.

The loads selected were such that the total strain in the specimen would be 50 to 150 microstrains. The NCHRP Project 9-19 researchers suggested this range of strain to keep sample deformation within the linear range. Loads causing smaller strains would not give accurate readings, and larger strains would cause the sample to deform permanently, thereby altering its properties. The third replicate was used for determining the loads required in order to keep the strain within these limits. Researchers performed the actual tests on two main replicates after determining the load ranges using the third replicate.

Table 12. Stresses Used for Dynamic Modulus Testing.

Temperature	Stress (psi) for different Frequency					
	25 Hz 200 cycles	10 Hz 200 cycles	5 Hz 100 cycles	1 Hz 20 cycles	0.5 Hz 15 cycles	0.1 & 0.2 Hz 7-15 cycles
40°F (4°C)	3.79	3.79	3.79	3.64	3.56	3.56
70°C (21°C)	1.65	1.65	1.65	1.65	1.65	1.65
100°F (37.7°C)	0.48	0.48	0.48	0.483	0.483	0.483
130°F (54.6°C)	0.14	0.14	0.14	0.14	0.14	0.14

The specimens were wrapped with cellophane and stored at room temperature to reduce unwanted aging before testing. The test specimens were brought to the required test temperature by placing them in an environmental test chamber for a minimum of two hours for 70, 100, and 130°F and for a period of four hours for 40°F.

To minimize damage to the specimens, researchers performed tests starting from the highest frequency to the lowest frequency at each temperature and then increased the temperature from the lowest to the highest level. Before application of axial load, researchers placed two thick latex sheets separated with silicone grease between each end of the specimen and loading platens. The objective of this end treatment was to reduce the shearing stresses at the specimen ends.

Data Acquisition and Data Analysis

The resulting strains were recorded using a data acquisition system and a desktop computer. The final values of the phase angle (δ) and dynamic modulus (|E*|) were calculated by using the average of the results from the last five loading cycles in accordance with recommendations of NCHRP Project 9-19.

The pneumatic system used for this test caused some "noise" in some cases during the recording of deformation. Due to this equipment error, researchers screened a number of readings manually to discard any outliers. In some cases, the final value was obtained by taking the average of three or four of the values from the last five loading cycles, after eliminating the outliers.

Figure 10. Dynamic Modulus Testing Setup.

The phase angle (*) was found to be very sensitive to the loading cycles and temperature. In certain cases, the variation in the last five values of * was so high that it was not possible to select any particular value for the purpose of analysis. This trend was more prominent in the case of very high loading frequencies, e. g., 25 Hz.

Researchers recorded the results of the two test replicates. The average of the modulus values obtained from each of the two replicates was used for plotting the master curve. Different shifting techniques can be used to construct the master curve on the basis of time-temperature superposition. In this project, sigmoidal function was employed for construction of the master curve. Pellinen et al. (*14*) showed that for the wide range of temperatures for the compressive dynamic modulus testing data, using the sigmoidal fitting function fit the data well because it followed the physical form of the measured data. Moreover, the proposed AASHTO 2002 Guide for Design of Pavement Structures utilizes the sigmoidal fitting function for the characterization of a HMA mixture. The master curve was plotted for each mix using a sigmoidal function described as follows (*14*):

$$\log(|E^*|) = \delta + \frac{\alpha}{1 + e^{\beta - \gamma \log \xi}}$$

where,

|E∗| = dynamic modulus

ξ = reduced frequency

δ = minimum modulus value

α = span of modulus values

γ = shape parameter governing slope

β = shape parameter governing horizontal position of turning point

This model typically represents a curve which is flat at very high and very low values of log(t), and typically represents the behavior of a viscoelastic material. The four variables involved in the model, i.e., δ, α, γ, and β along with the shift factors for the other three temperature ranges, are derived simultaneously using a nonlinear regression analysis supported by the solver function in the Microsoft Excel spreadsheet.

The reference temperature assumed in this case was 68°F (20°C). This temperature was selected arbitrarily. With the raw data available, a master curve can be created at different base temperatures. The dynamic modulus values for other temperatures were shifted to this value for plotting the master curve. The master curves along with the shift factors for all the mix designs from Sections 1 through 10 are attached as Appendix B.

Mixture Proportion and Binder Properties

During the QC/QA phase, it is important to make sure that construction follows agency specifications. TxDOT developed several different test procedures for its quality assurance program. Some important features of this QA program include checking the in-place air voids of a compacted layer, checking the asphalt content, and gradation of the mix.

Researchers examined the asphalt content of both loose plant mixtures and cores collected from the roadway. The gradation was checked using the cores collected for IDT testing. Asphalt recovered from the cores by the extraction procedure (Tex 210-F Part I, and Tex-211-F) was also tested using the dynamic shear rheometer (DSR) apparatus to determine the PG grading of the recovered asphalt. Researchers measured the asphalt content from the loose plant mix using the ignition oven. Results from all the tests are documented in the following chapter.

CHAPTER 4:
TEST RESULTS

GENERAL

Researchers conducted most of the lab tests using specimens compacted of plant mix materials and cores collected from roadways. Dynamic modulus tests could not be performed using cores due to the specimen size limitation discussed earlier. This chapter summarizes all test results, and provides graphical comparisons, and statistical analyses of the measured response parameters.

Permeability Testing

The research team conducted permeability tests using a falling head permeameter following ASTM Procedure PS 129-01 on lab molded and roadway cores (Table 13). The values shown in Table 13 are the averages of three replicates. Detailed results are given in Appendix B. Coefficient of variation of the permeability test for each mixture was calculated and reported in Table 13. Overall coefficient of variation of this test is very poor, which is common. Figures 11 and 12 illustrate the results of permeability tests conducted on cores and lab compacted samples,

Table 13. Falling-Head Permeability Test for Lab Molded Samples and Field Cores.

Section	Average Permeability (inch/sec)		Coefficient of Variation of Avg. Perm., (%)		Average Air Void (%)	
	Field Cores	Lab Molded	Field Cores	Lab Molded	Field Cores	Lab Molded
1	3.90E-03	1.38E-03	8.7	18.8	8.7	7.1
2	1.11E-02	1.39E-03	12.6	34.9	10.3	6.7
3	1.70E-03	8.11E-04	15.2	28.5	7.2	6.8
4	1.45E-03	1.99E-03	46.7	52.5	6.1	6.5
5	2.28E-02	1.87E-03	10.2	30.4	10.5	5.8
6	2.85E-03	1.01E-03	56.8	49.5	9.1	6.7
7	1.95E-03	1.19E-03	24.9	39.4	8.2	7.1
8	2.05E-03	7.91E-04	26.7	20.4	8.2	6.4
9	2.25E-03	1.45E-03	24.9	37.4	8.5	7.2
10	--	1.65E-03	--	18.3	--	6.9

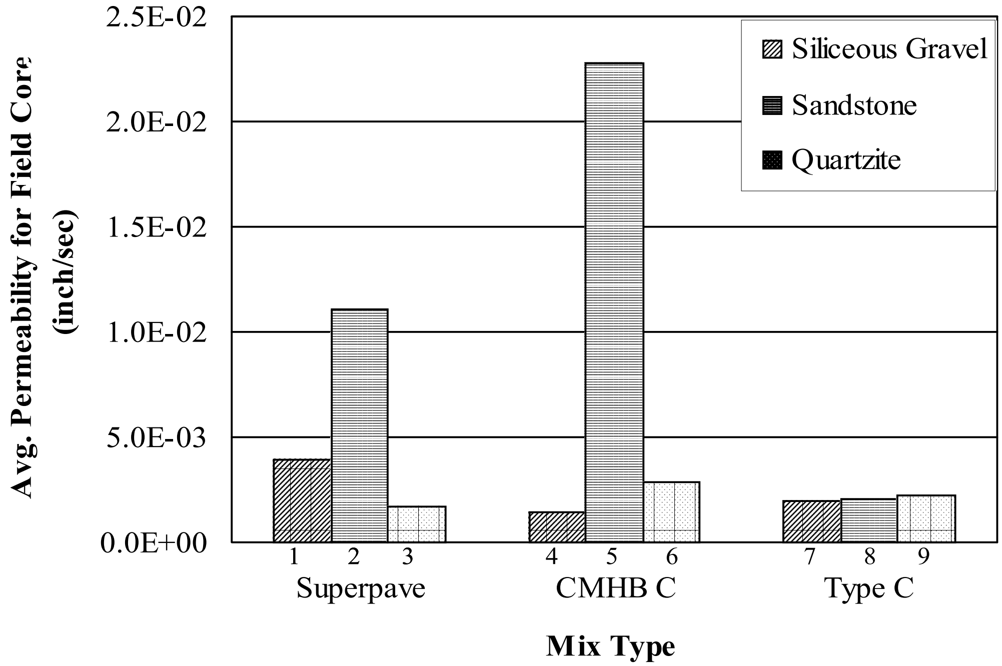

Figure 11. Field Core Permeability versus Mixture Type.

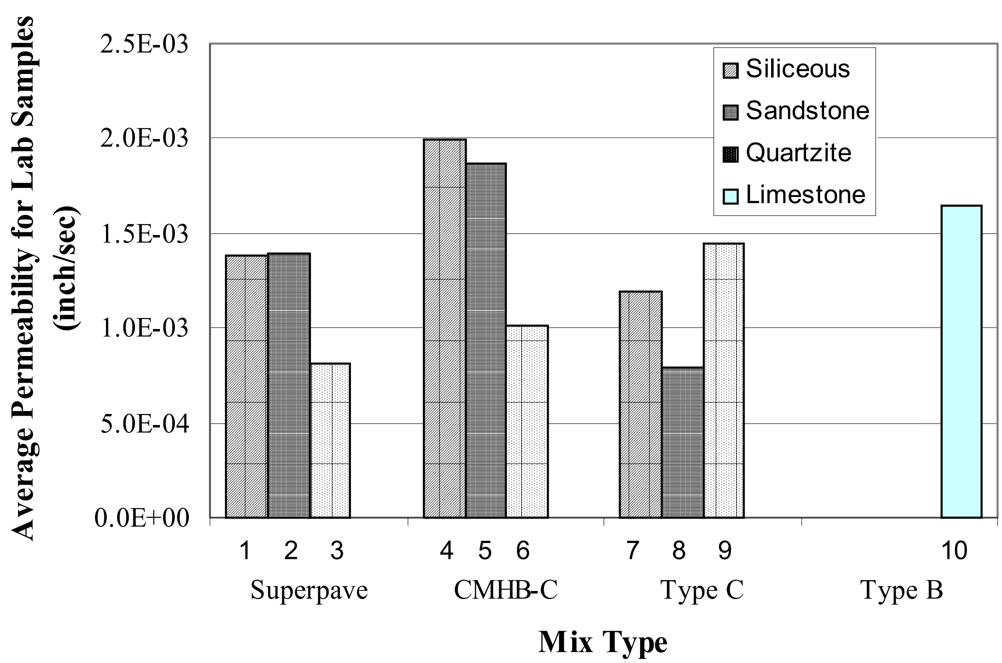

Figure 12. Lab Molded Permeability versus Mixture Type.

respectively. Roadway cores from Section 10 (Type B base) were badly damaged and not suitable for testing.

Figures 13 and 14 show the relation between permeability and air voids for field cores and lab compacted specimens, respectively. Figure 11 demonstrates a wide range of permeability for different field cores. The field cores of all three Type C mixtures show similar air voids and low permeability. CMHB-C sandstone mixture (Section 5) field core yielded the highest permeability and Superpave sandstone mixture core also yielded relatively higher permeability. There is no clear trend noticed among the permeability values of lab compacted specimens of different mixtures (Figure 12). The reason might be that all the specimens were compacted with 7±1 percent air voids to simulate those at construction. From the same figure it is noticed that CMHB specimens show higher permeability than the other types. This observation is supported by Figure 14, even though they have low air void contents.

Figure 13 demonstrates an interesting phenomenon. Because they have very high in-place air void contents, two field cores (CMHB-C sandstone and Superpave sandstone) show high permeability. So, in this case, air void content played the major role and not mixture type. In the same figure, it is noticed that the remaining seven cores have similar permeabilities as their air

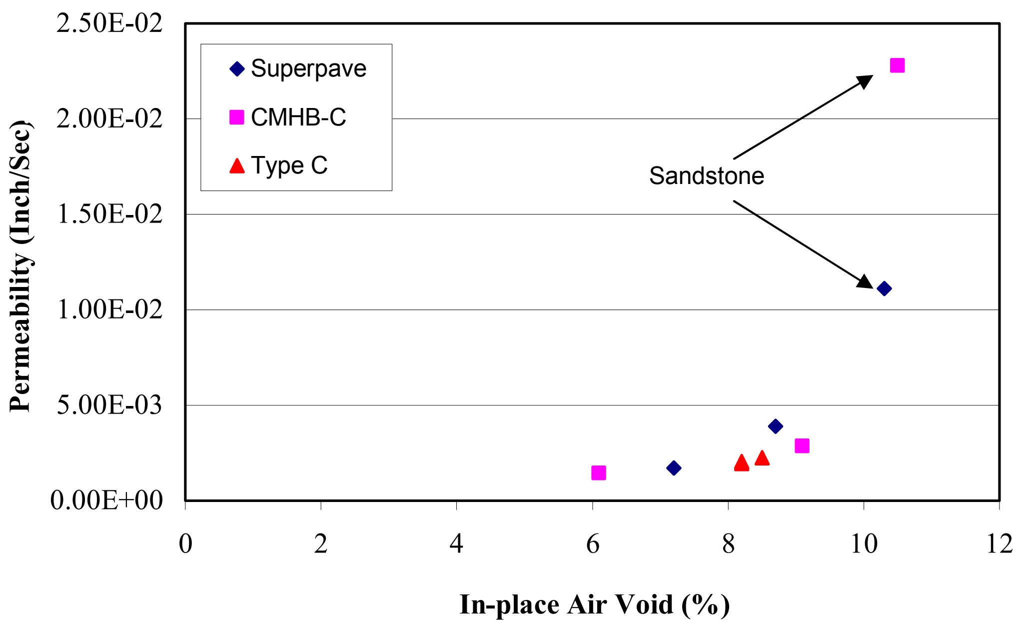

Figure 13. Permeability versus Air Void for Field Cores.

void contents measure less than 9.0 percent. A general trend appears that the permeability increases with increasing air void at linear rate up to a certain air void content after which it increases logarithmically. Mallick (*15*) found similar trends. Figure 14 does not reveal any clear trend between permeability and air void for the lab compacted specimens because they were prepared with narrow air void limits.

Figure 15 is constructed using permeability results of both lab compacted specimens and field cores for all mixtures. The field cores demonstrate an exponential correlation ($R^2 = 0.78$) between permeability and air voids. Notice from the figure that all lab compacted specimens are closely spaced at the bottom.

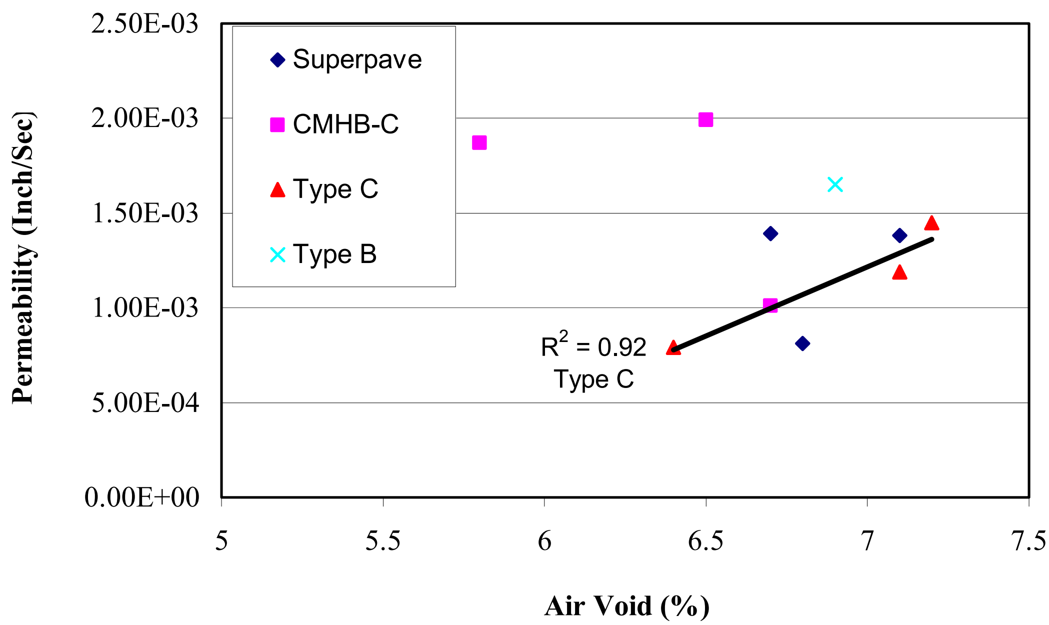

Figure 14. Permeability versus Air Void for Lab Molded Specimens.

APA Test Results

The researchers conducted dry APA tests on the same specimens used in the permeability tests. Researchers assumed that there should not be any damage to specimens by the permeability test. They provided ample time to dry out the specimens at ambient temperature. All the field samples and lab samples survived 8000 loading cycles. Table 14 summarizes the results from the APA test conducted on field cores.

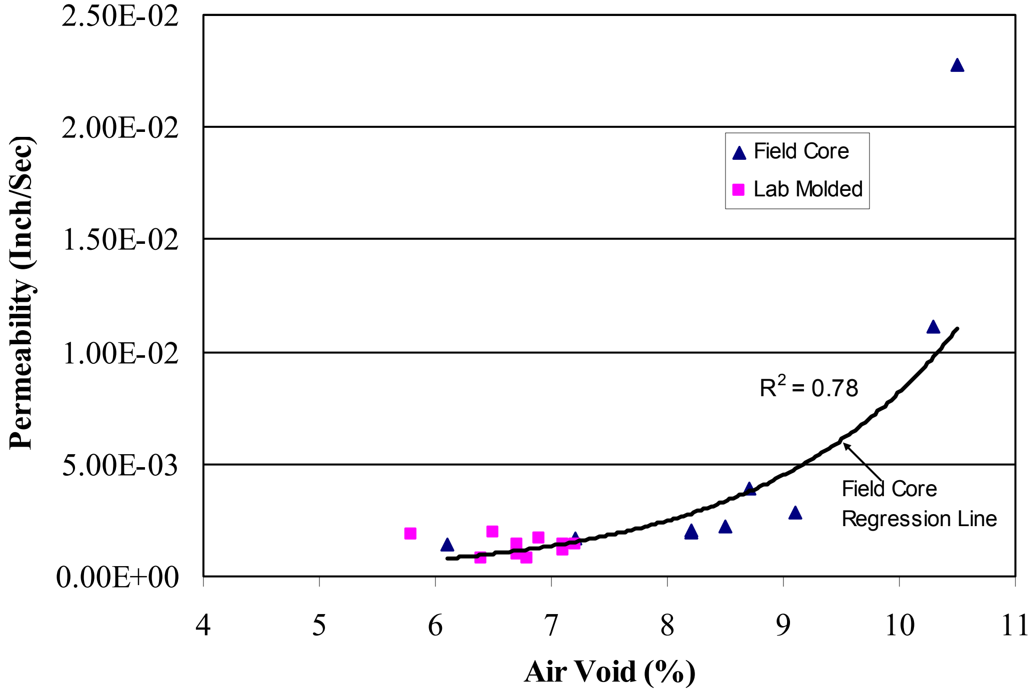

Figure 15. Comparison of Permeability between Field Core and Lab Molded Specimens.

Table 14. APA Rut Test Results for Field Cores.

Section	APA Rutting @ 8000 strokes (inches)				Creep Slope (strokes/inch) 1000s	Remarks
	Left	Middle	Right	Average		
1	0.18	0.09	0.13	0.11	135	Left reading omitted in average
2	0.16	0.13	0.18	0.15	142	Right reading omitted in average
3	0.13	0.12	0.13	0.12	115	
4	0.16	0.13	0.18	0.15	119	
5	0.18	0.18	0.19	0.18	138	
6	0.16	0.14	0.14	0.15	166	
7	0.14	0.12	0.15	0.14	165	
8	0.10	0.08	0.06	0.09	212	Right reading omitted in average
9	0.12	0.08	0.10	0.10	249	

During these tests, the APA equipment experienced some trouble with air pressure. One set (out of three) of specimens demonstrated unusually low rut depth. Researchers manually identified and excluded each of them during calculation of average rut depths (Table 15).

Figure 16 illustrates rut depths of different field cores. All the mixtures performed well in the APA test. There was no statistical difference among the test sections regardless of mixture type or aggregate type.

Table 14 documents results from the APA tests conducted with lab compacted specimens. The results are shown graphically in Figure 17. Most of the lab compacted specimens exhibited excellent rutting performance. Type C mixtures performed best followed by the Superpave mixtures with the CMHB-C mixture performing worst. The CMHB-C mixture containing siliceous river gravel (Section 4) exhibited the most rutting (less than 0.2 inches) followed by the Type B mixture. In certain cases, a large difference between the APA rut values for the lab molded specimens and the filed cores were observed. This difference could be accounted for, to some extent, by the difference in the compaction levels represented by the air voids in the laboratory samples and the field cores. In general, the lab compacted specimens performed better than field cores except for one mixture (Section 4). Again, in this case, the air voids of lab specimens were higher than those of field specimens.

Table 16 facilitates comparisons of results for lab compacted and field specimens. Detailed results from the APA machine are documented in Appendix B. Creep slope was calculated for each of the mixtures. At the beginning of the test, a specimen typically experiences very high deformation (due to initial compaction), and the curves usually flatten out with time. The curve slope (creep slope) is calculated from the relatively flat portion of the graph. This creep slope is useful for prediction of rut depth in a pavement (far beyond 8000 loading cycles). At the end of 8000 APA loading cycles, one mixture may have less rut depth than the other, but the first one may ultimately yield a higher rut depth if it has steeper creep slope and the test is continued far beyond 8000 cycles.

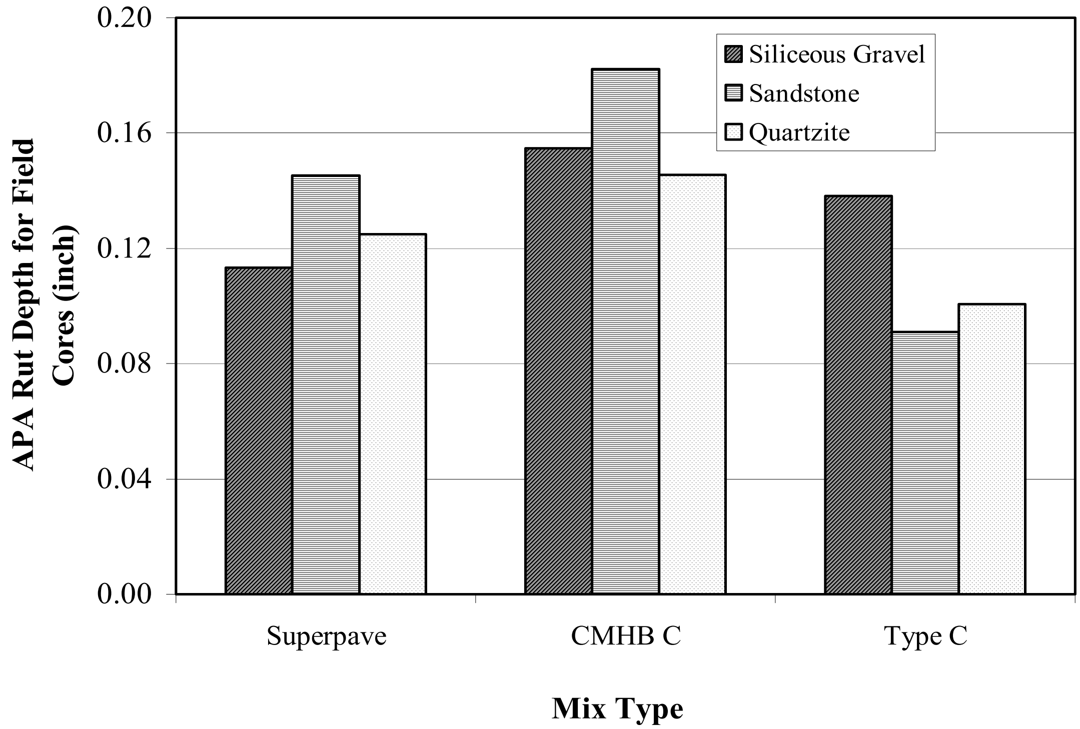

Figure 16. APA Rut Depth for Field Cores.

Table 15. APA Rut Test Results for Lab Molded Specimens.

Section	Rut Depth at 8000 strokes (inches)				Creep Slope (strokes/inch) 1000s	Remarks
	Left	Middle	Right	Average		
1	0.10	0.09	0.14	0.09	176	Right reading omitted in average
2	0.07	0.07	0.08	0.07	375	
3	0.10	0.08	0.09	0.09	249	
4	0.22	0.16	0.28	0.19	94	Right reading omitted in average
5	0.14	0.11	0.13	0.12	153	
6	0.13	0.08	0.11	0.10	178	
7	0.07	0.08	0.08	0.08	207	
8	0.07	0.06	0.05	0.05	306	Reading for middle taken @ 7985 strokes
9	0.08	0.08	0.07	0.08	316	
10	0.15	0.06	0.16	0.16	79	Middle reading omitted in average

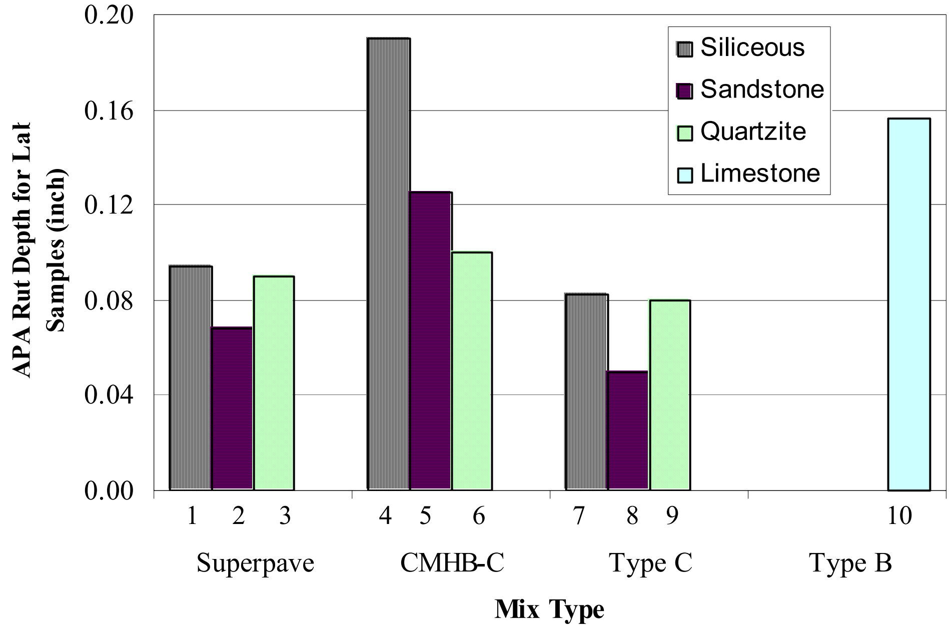

Figure 17. APA Rut Depth for Lab Compacted Specimens.

Table 16. APA Rut Test Comparison for Lab Molded Samples and Field Cores.

Section	APA Value (inch)		Creep Slope (strokes/inch) 1000s		Air Voids (%)	
	Field Cores	Lab Molded	Field Cores	Lab Molded	Field Cores	Lab Molded
1	0.11	0.09	135	176	8.7	7.1
2	0.15	0.07	142	375	10.3	6.7
3	0.12	0.09	115	249	7.2	6.8
4	0.15	0.19	119	94	6.1	6.5
5	0.18	0.12	138	153	10.5	5.8
6	0.15	0.10	166	178	9.1	6.7
7	0.14	0.08	165	207	8.2	7.1
8	0.09	0.05	212	306	8.2	6.4
9	0.10	0.08	249	316	8.5	7.2
10	--	0.16	--	79	7.3	6.9

Indirect Tensile Strength Test

The research team conducted indirect tensile tests on four specimens for each type of mixture. Table 17 exhibits the average of those four readings along with average air voids and coefficient of variation for each type of mixture. IDT test results for field cores and lab compacted specimens are presented in Figures 18 and 19, respectively. Figure 18 shows that most of the field cores have relatively similar IDT strengths. Section 2 (Superpave sandstone) and Section 5 (CMHB sandstone) have somewhat lower IDT values; they also contained higher air voids.

The coefficient of variation of field cores and lab molded specimens is reasonably good. IDT strengths of the lab compacted mixtures were much higher than those for field cores. Researchers identified two possible reasons for higher IDT strengths for lab molded specimens: lab prepared specimens were compacted by reheating of loose mixture and they were tested within relatively short period of compaction; their air voids content were lower than those of field cores. Figure 18 demonstrates that lab compacted mixtures show a comparatively wider range of IDT strength values than the field cores. Among the nine lab molded surface course mixtures, all three sandstone mixtures yielded the highest IDT values. The Type B mixture exhibits the lowest strength, and its optimum asphalt content was also relatively low.

Table 17. IDT Test for Lab Molded Samples and Field Cores.

Section	Average IDT Strength (psi)		Coefficient of Variation		Air Voids (%)	
	Field Cores	Lab Molded	Field Cores	Lab Molded	Field Cores	Lab Molded
1	91.1	174.0	10.15	5.9	8.9	6.9
2	75.2	226.4	11.28	3.3	10.6	7.9
3	101.3	154.2	7.41	1.0	6.8	6.1
4	103.2	168.9	11.13	14.7	5.0	6.5
5	72.1	205.2	14.49	6.9	9.4	7.0
6	88.2	159.1	3.46	13.7	8.6	7.3
7	103.6	173.6	3.93	11.6	8.3	7.4
8	99.9	213.7	14.50	4.9	8.5	7.4
9	97.8	176.1	10.28	9.1	9.4	7.2
10	--	138.8	--	12.1	7.7	6.7

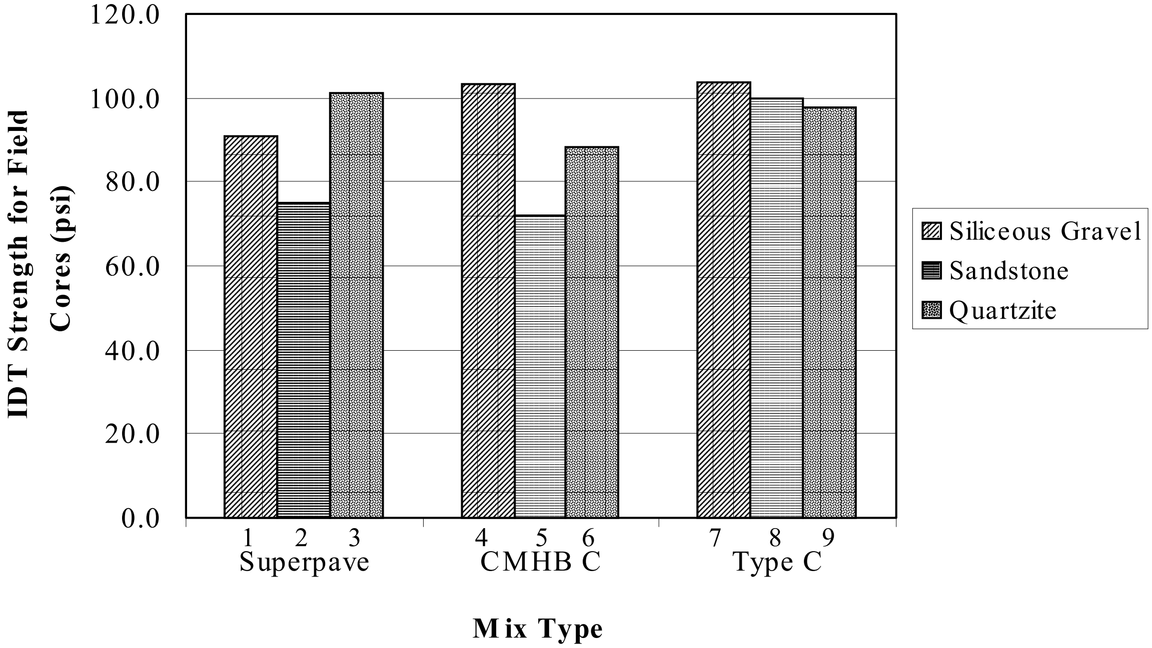

Figure 18. IDT Strength for Field Core Specimens.

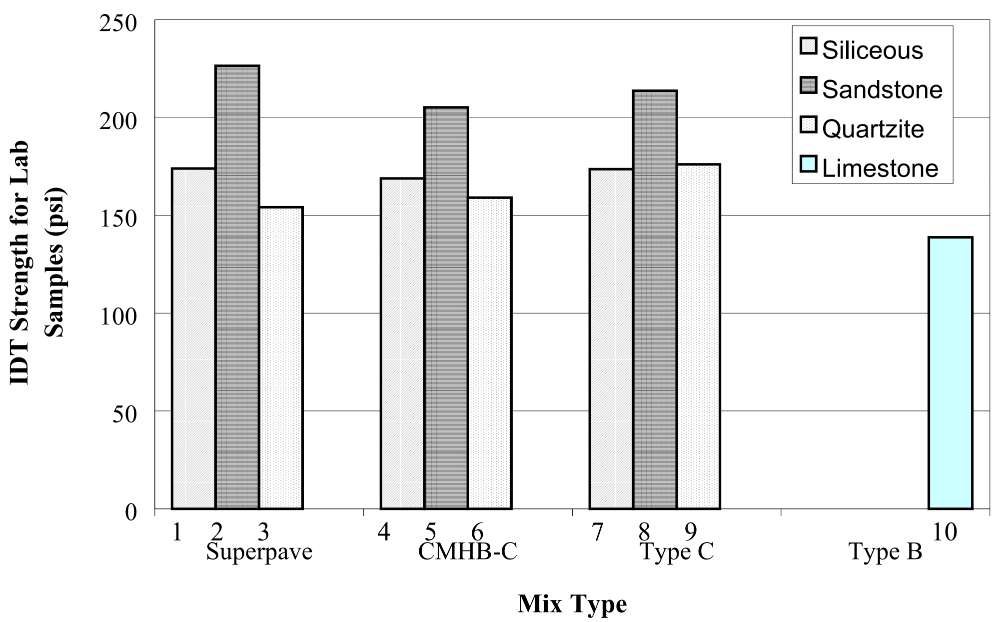

Figure 19. IDT Values for Lab Molded Specimens.

Dynamic Modulus Test

This test offers two main parameters: complex modulus and phase angle. According to the test protocol followed in this project, tests on each specimen yielded 24 (4 temp × 6 frequency) complex moduli and phase angles. Complex modulus and phase angle of a given mixture (section) were obtained by averaging results from two specimens. Appendix B provides detailed results from this test.

Each set of dynamic modulus values obtained from different frequencies at different temperatures was converted into one single 'master curve.' Master curves for each mixture and accompanying shift factors are documented in Appendix B. Figure 20 summarizes master curves for all 10 mixtures. Although all the mixes seem to have similar dynamic modulus values from the graph, it should be noted that the Y-axis represents the Log $|E^*|$ value. Therefore, even a small increase in the $|E^*|$ value in the graph may have significant affects on the actual value.

From the graph, it is also clear that the Type B mixture clearly shows higher $|E^*|$ values as compared to any other mixture for any given time of loading. However, this does not necessarily indicate improved performance towards rutting because, although the Type B mix has a higher E* value, it may also have a relatively higher value of the phase angle (δ) and may therefore have a larger component of viscous behavior. In this report, while making a comparison of permanent deformation characteristics among the mixtures, researchers selected E* values measured at 130°F temperature and 10 Hz loading frequency. Higher temperatures are critical for rutting; and at this temperature, modulus of mixture decreases. E* values measured at 40°F temperature and 10 Hz frequency were considered when ranking fatigue performance.

Figure 20 shows that most of the curves are closely clustered. One of the reasons is that all of these mixtures are of very good quality and designed with high-quality aggregate and the same relatively hard asphalt (PG 76-22). It is difficult to detect distinct differences in modulus values of lab specimens compacted to similar air voids when all the mixtures are of similar quality. Researchers attempted unsuccessfully to find correlations between APA rut depth and E* or E*/sinδ. Further they found no correlation between HWTD data and E*. These findings do not necessarily undermine the HMA characterization capability of the simple performance test (dynamic modulus). The HWTD test data was collected from CTR. The HWTD test results are included in Appendix C

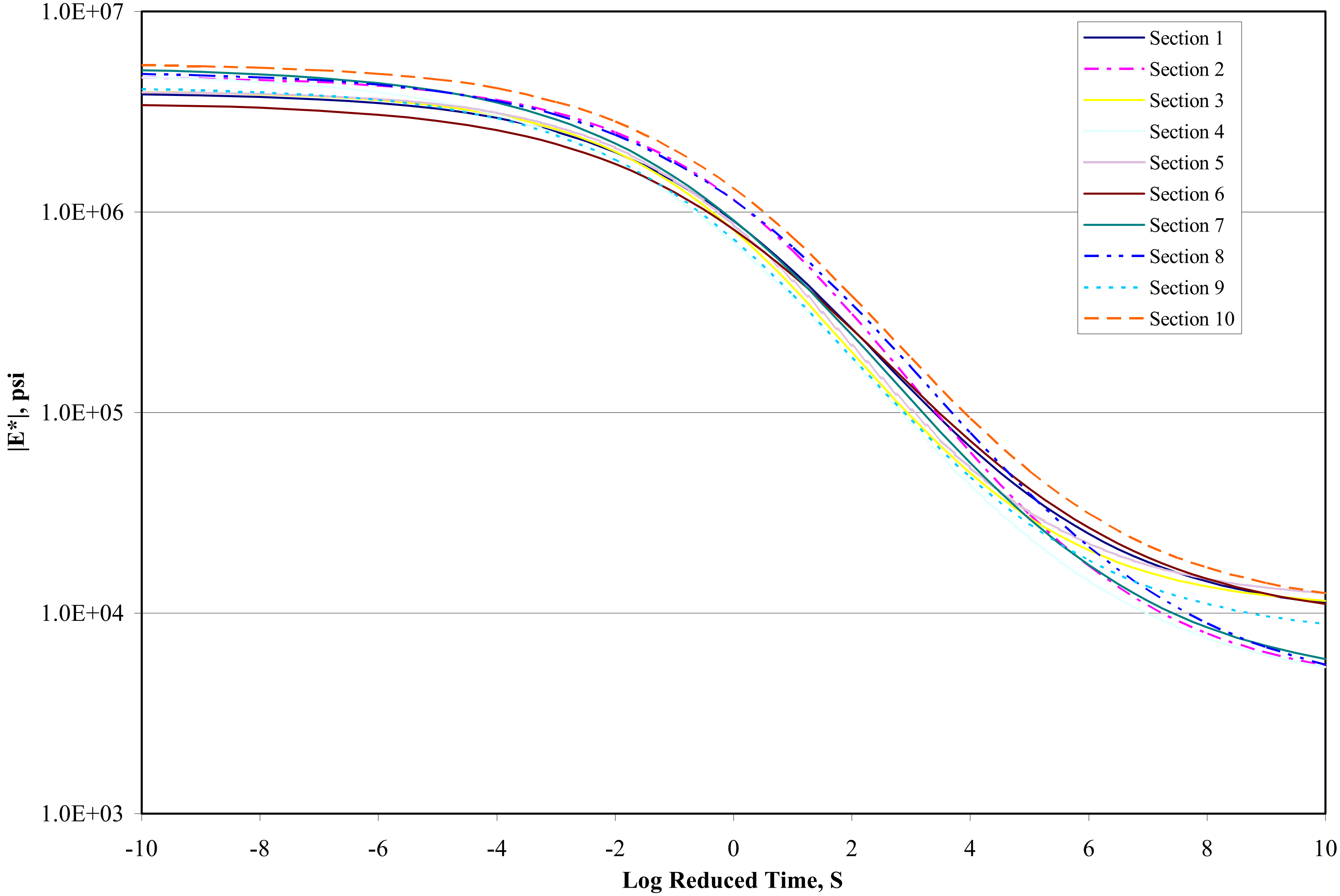

Figure 20. Master Curves for Mixes in All Sections (from Dynamic Modulus Test).

Mixture Proportion

IDT specimens collected from the field were used for determining mixture proportioning once the specimens were tested using the IDT. Four broken cores (4-inch diameter and 2-inch high) from each test section were used for asphalt recovery using the extraction procedure. The researchers followed the Tex-210-F, Part I and Tex-211-F test methods to extract asphalt from the roadway cores. Asphalts and aggregates recovered from this procedure were used for asphalt content determination, asphalt characterization, and aggregate grading. Asphalt recovered was tested using a DSR machine to determine its PG high-temperature grading. Table 18 describes the results of DSR testing on recovered asphalts.

Table 18. DSR Test on Asphalts Extracted from Field Cores.

Section	Passing Temperature (°C)	Passing Grade	G* at passing grade temp. (kPa)	Phase angle (δ) at passing temp.	G*/sinδ at passing temp (KPa)
1	70.0	70	2.01	65.60	2.21
2	71.1	70	2.28	67.80	2.46
3	69.3	64	3.35	65.20	3.69
4	68.5	64	3.15	66.00	3.45
5	70.8	70	2.20	67.80	2.38
6	75.0	70	3.38	64.70	3.74
7	81.8	76	1.63	70.30	1.73
8	87.2	82	1.44	65.80	1.58
9	69.3	64	3.18	65.10	3.51

The DSR results shown in Table 18 are somewhat erratic. Even though all nine HMA mixtures used one type of asphalt (PG 76-22 from Wright Asphalt), DSR tests on extracted asphalt yielded PG grades from PG 64 to PG 82. These anomalies suggest that asphalt found as soft (PG 64 or PG 70) was not properly recovered and contained small traces of tri-chloro-ethylene.

Researchers determined asphalt content in two different ways: solvent extraction using roadway cores and ignition oven using plant mixture. Due to the limitation of resources, researchers conducted only one of these tests for each type of mixture. Results of asphalt content determinations along with the design asphalt content are given in Table 19 and Figure 21. In most cases, asphalt content determined by extraction method is less than corresponding values measured by the ignition oven method. The ignition oven was not calibrated with the materials used in the study. If the solvent extraction method is considered to be more accurate, then Sections 1, 2, 3, 5, and 10 had contained more than 0.5 percentage point less asphalt than design asphalt content.

Table 19. Comparison of Asphalt Content and Rice Specific Gravity.

Section No.	Asphalt Content (%)			Rice Specific Gravity (gm/cc)	
	TTI (Extraction)	TTI (Ignition Oven)	TxDOT (Design)	TTI (Measured)	TxDOT (Interpolated)
1	4.43	4.66	5.00	2.440	2.425
2	4.53	5.27	5.10	2.404	2.367
3	4.45	5.75	5.10	2.463	2.455
4	4.60	4.80	4.70	2.418	2.416
5	3.94	5.19	4.80	2.394	2.387
6	4.75	4.79	4.80	2.474	2.464
7	3.98	4.17	4.40	2.462	2.453
8	4.62	4.90	4.50	2.421	2.404
9	4.65	4.75	4.60	2.475	2.478
10	3.10	3.58	3.80	2.502	2.516

Aggregates recovered from the extraction processes were used for sieve analysis following TxDOT procedure Tex-200-F Part II (Sieve Analysis of Fine and Coarse Aggregates – Washed Sieve Analysis). Comparative aggregate gradations (design versus extraction from cores) are presented in Tables 20 to 23. In most cases, the materials passing the No. 200 sieve found in the extracted sample were higher than the design percentage. This occurrence is not unusual as the aggregates degrade in each step of the construction and recovery process. In most cases, the final percentage conformed to TxDOT specifications. The Atlanta District lab also performed sieve analyses on the extracted aggregates collected from plant mixes. The results of

TxDOT sieving are documented in Appendix C. TxDOT results also indicate the increase of finer aggregate in plant mix sample from the design gradation. CMHB mixtures were more consistent when comparing design gradation and TxDOT plant mix sample sieving. The differences in gradation (passing No. 200 sieve) measured at TTI were higher than those measured at TxDOT. This discrepancy could be attributed to the fact that TxDOT measured plant mixes and TTI measured cores. Aggregates from core samples were subjected to compaction by roller and specimen breaking at the lab. As a result, more aggregate particles might have been broken into smaller sizes.

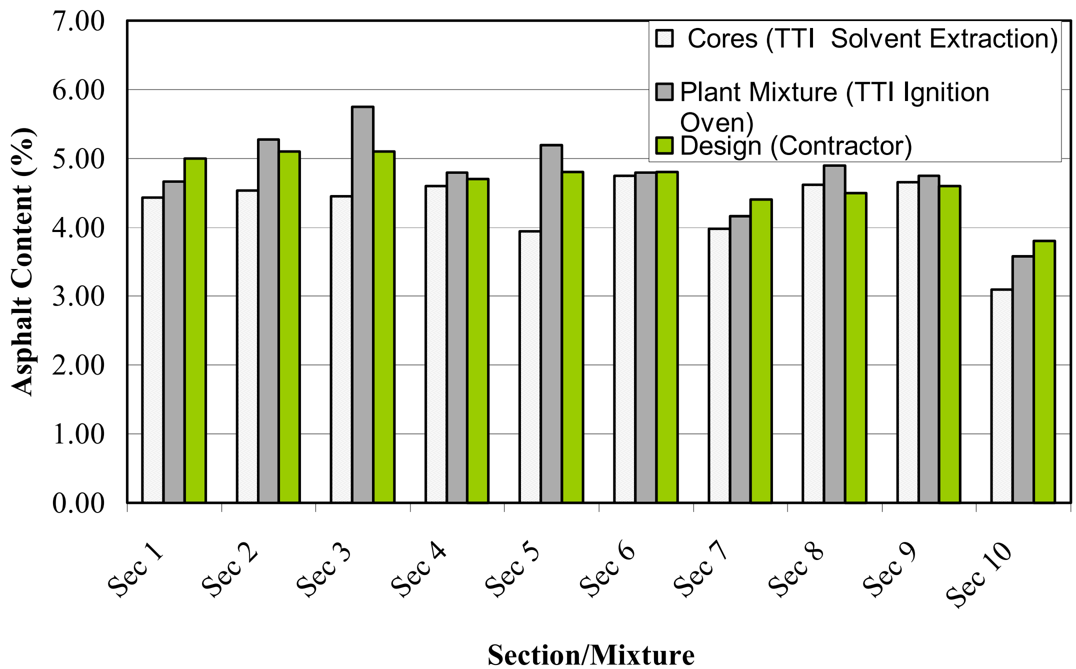

Figure 21. Comparison of Asphalt Content and Rice Specific Gravity.

Table 20. Design and Extracted Gradation for Superpave Mixtures, Sections 1-3 (TTI).

Sieve Size (mm)	Spec. Req.	Section 1 (Percent Passing)			Section 2 (Percent Passing)			Section 3 (Percent Passing)		
		Design	Extract	Diff.	Design	Extract	Diff.	Design	Extract	Diff.
19.00	100	100.0	100	0.0	100.0	100	0.0	100.0	100	0.0
12.50	90-100	92.0	93.9	1.9	92.1	93.2	1.1	93.7	92.5	-1.2
9.50		84.8	84.0	-0.8	79.4	80.8	1.4	81.7	76.8	-4.9
4.75		52.4	53.3	0.9	49.0	47.2	-1.8	45.5	49.3	3.8
2.36	25-58	30.9	30.3	-0.6	29.2	29.0	-0.2	31.4	33.7	2.3
1.18	10-25	20.4	20.2	-0.2	22.4	23.3	0.9	21.0	24.6	3.6
0.60	3-13	13.9	14.4	0.5	18.9	20.7	1.8	17.7	19.5	1.8
0.30		8.8	10.6	1.8	14.9	17.5	2.6	11.8	14.7	2.9
0.15		4.5	8.5	4.0	10.2	13.8	3.6	8.2	11.7	3.5
0.075	2-10	3.2	5.9	2.7	6.5	8.1	1.6	5.6	8.2	2.6

Table 21. Design and Extracted Gradation for CMHB Mixtures, Sections 4-6 (TTI).

Sieve Size	Spec. Req.	Section 4 (Percent Passing)			Section 5 (Percent Passing)			Section 6 (Percent Passing)		
		Design	Extract	Diff.	Design	Extract	Diff.	Design	Extract	Diff.
7/8 in	98-100	100.0	100.0	0.0	100.0	100.0	0.0	100.0	100.0	0.0
5/8 in	95-100	99.7	96.3	-3.4	100.0	100.0	0.0	99.6	100.0	0.4
3/8 in	50-70	64.5	71.9	7.4	65.4	69.8	4.4	65.6	62.6	-3.0
#4	30-45	34.3	44.7	10.4	38.0	38.4	0.4	34.2	37.7	3.5
#10	15-25	21.8	24.7	2.9	24.0	24.7	0.7	24.0	23.8	-0.2
#40	6-20	16.2	17.8	1.6	16.4	18.7	2.3	14.5	14.1	-0.4
#80	6-18	9.8	11.8	2.0	10.7	14.8	4.1	9.1	10.0	0.9
#200	5-8	6.4	7.5	1.1	6.4	8.7	2.3	5.9	6.3	0.4

Table 22. Design and Extracted Gradation for Type C Mixtures, Sections 7-9 (TTI).

Sieve Size	Spec. Req.	Section 7 (Percent Passing)			Section 8 (Percent Passing)			Section 9 (Percent Passing)		
		Design	Extract	Diff.	Design	Extract	Diff.	Design	Extract	Diff.
7/8 in	98-100	100.0	100.0	0.0	100.0	100.0	0.0	100.0	100.0	0.0
5/8 in	95-100	99.8	100.0	0.2	100.0	100.0	0.0	99.8	100.0	0.2
3/8 in	70-85	79.1	84.6	5.5	75.8	81.6	5.8	80.7	80.3	-0.4
#4	43-63	51.4	61.7	10.3	49.2	55.4	6.2	46.2	55.4	9.2
#10	30-40	34.0	38.7	4.7	31.5	35.4	3.9	30.9	35.2	4.3
#40	10-25	17.9	19.7	1.8	18.2	21.7	3.5	15.6	17.9	2.3
#80	3-13	10.0	12.4	2.4	11.7	17.7	6.0	9.6	12.6	3.0
#200	1-6	5.3	7.2	1.9	5.8	9.4	3.6	5.8	8.3	2.5

Table 23. Design and Extracted Gradation for Type B Mixture, Section 10 (TTI).

Sieve Size	Spec. Req.	Section 10 (Percent Passing)		
		Design	Extract	Difference
7/8 in	95-100	100.0	100.0	0.0
5/8 in	75-95	90.1	88.6	-1.5
3/8 in	60-80	79.4	75.9	-3.5
#4	40-60	52.9	49.7	-3.2
#10	27-40	31.9	29.9	-2.0
#40	10-25	19.4	18.8	-0.6
#80	3-13	9.8	11.6	1.8
#200	1-6	3.8	5.8	2.0

MIXTURE RANKING

One of the subtasks of this research project was to rank the mixtures based on the results from laboratory tests. Mixture ranking is not an easy, straightforward task. Each test is conducted at different loadings, using different test specimens and environmental conditions.

Furthermore, not all the tests yield a single result value that can be used for comparison. However, researchers prepared ranking tables. Researchers included APA, IDT, permeability, and HWTD (result from CTR/TxDOT [*13*]) tests for ranking of field cores. Dynamic modulus was included as an additional test for ranking of lab compacted specimens. All the mixtures (Sections 1 through 9) were ranked based on the tests performed using those mixtures.

The Type B mixture was excluded from ranking. Tables 24 and 25 show mixture rankings for field cores and lab compacted specimens, respectively. APA rut depth rankings were based on the average rut depths at the end of 8000 loading cycles; the mixture with the lowest rut depth is ranked as number 1. Similarly HWTD rut depth, permeability, and E*sin* rankings were prepared. The mixture with the highest IDT strength value was ranked as number 1. Similarly, the mixture with the highest APA creep slope, HWTD creep slope, and E*/sin* rankings were prepared. Lower creep slope or higher E*/sin* indicates better rut resistant mixture. Best mixes (i.e., No. 1) were considered those with:

Lowest	Highest
APA Rut Depth	IDT Strength
APA Creep Slope	E*/sinδ @130°F and 10 Hz
HWTD Rut Depth	
HWTD Creep Slope	
E*sinδ @ 40°F and 10 Hz	
Permeability	

Rankings in Table 24 (for field cores) reveal that there is general agreement between APA rut depth and APA creep slope; and HWTD rut depth and HWTD creep slope. Ranking by HWTD rut depth resembles that by permeability results. This result suggests that HWTD can measure both rutting and moisture susceptibility of the HMA mixture. Readers should consider the fact that higher permeability is not the only cause of moisture damage. The three lowest ranking mixtures (Sections 2, 5, and 6) using IDT results also received low ranking by APA, HWTD, and the permeability test. The high field air void contents (10.3, 10.5, and 9.1) of those (Sections 2, 5, and 6) mixtures are probably responsible for their low ranking. Overall, the Type C sandstone mixture performed best among the field cores.

Table 24. Mixture Ranking Based on Field Core Testing.

Section	Mixture	Ranking					
		APA		Permeability	IDT	HWTD	
		Rut Depth	Creep Slope			Rut Depth	Creep Slope
1	Superpave-Siliceous Gravel	3	7	7	6	5	5
2	Superpave-Sandstone	7	5	8	8	7	6
3	Superpave-Quartzite	4	9	2	3	3	1
4	CMHB-C-Siliceous Gravel	8	8	1	2	4	4
5	CMHB-C-Sandstone	9	6	9	9	8	8
6	CMHB-C-Quartzite	6	3	6	7	6	7
7	Type C-Siliceous Gravel	5	4	3	1	--	--
8	Type C-Sandstone	1	2	4	4	1	2
9	Type C-Quartzite	2	1	5	5	2	3

-- data not available from CTR

Table 25. Mixture Ranking Based on Lab Molded Specimen Testing.

Section	Mixture	Ranking							
		APA		Permeability	IDT	Dynamic Modulus		HWTD	
		Rut Depth	Creep Slope			E*/sinδ @ 130F 10 Hz	E*sinδ @ 40F 10 Hz	Rut Depth	Creep Slope
1	Superpave-Siliceous Gravel	7	7	5	5	3	7	4	4
2	Superpave-Sandstone	2	1	6	1	2	6	5	7
3	Superpave-Quartzite	5	4	2	9	9	2	7	6
4	CMHB-C-Siliceous Gravel	9	9	9	7	8	4	8	8
5	CMHB-C-Sandstone	8	8	8	3	4	9	2	2
6	CMHB-C-Quartzite	6	6	3	8	1	1	6	5
7	Type C-Siliceous Gravel	3	5	4	6	6	5	9	9
8	Type C-Sandstone	1	3	1	2	5	8	1	1
9	Type C-Quartzite	4	2	7	4	7	3	3	3

Rankings in Table 25 (lab compacted specimen) again show that Type C sandstone mixture (Section 8) performed the best in most test parameters. CMHB-C siliceous river gravel mixture (Section 4) performed the worst. Researchers did not find any clear pattern that particular mixture types (i.e., Superpave, CMHB or Type C) performed better or worse than other types.

MIXTURE GROUPING

The objective of this task was to identify statistically equivalent groups of mixtures in terms of rutting resistance, cracking resistance, and propensity to moisture-related damage using engineering properties determined in the laboratory. Researchers used the results from APA, and dynamic modulus test results to group rutting resistance of the mixtures. HWTD test data could not be used for mixture grouping as they were performed with only one set of specimens. The researchers used dynamic modulus and IDT test results for evaluating the mixtures' cracking resistance. Moisture damage potential of mixtures was evaluated using the results from the HWTD and permeability tests. Dynamic modulus was used for both rutting and fatigue property characterizations. Researchers selected $|E^*|$ value at 130°F and 10 Hz for rutting characterization and $|E^*|$ value at 40°F and 10 Hz for fatigue cracking characterization. Researchers prepared groupings for both field cores and lab compacted specimens. The Duncan Multiple Range Test was used to place the mixtures into statistically similar groups (*16*). Type B mixture was not included in the groupings.

Tables 26 and 27 exhibit the results from Duncan's test for field cores and lab compacted specimens, respectively. Statistically equivalent groups of material properties are indicated by matching numbers when the tables are read horizontally. Lower group number indicates better mixture (with respect to rutting, fatigue, or moisture damage potential).

APA rut depth and permeability test results were more sensitive than other tests for field cores. These two tests divided the nine mixtures into four groups. IDT strength and APA creep slope created only two groups. The apparent failure of these test procedures to discriminate among the mixtures could be attributed to the fact that all of the nine mixtures possess good quality, as mentioned earlier. Section 5 mixture was placed in the lowest groups by three tests parameters.

Table 26. Duncan Group Based on Field Core Results.

Test/ Parameter	Duncan Group								
	Superpave			CMHB-C			Type C		
	Sec 1	Sec 2	Sec 3	Sec 4	Sec 5	Sec 6	Sec 7	Sec 8	Sec 9
	SR	SS	QT	SR	SS	QT	SR	SS	QT
APA Rut Depth	2, 3	3, 4	2, 3	3, 4	4	3, 4	2, 3	1	1, 2
APA Creep Slope	1	1	1	1	1	1	1	2	2
IDT Strength Value	1	2, 3	1	1	3	1, 2	1	1	1
Permeability Value	2	3	1	1	4	1, 2	1, 2	1, 2	1, 2

SR-Siliceous River Gravel, SS-Sandstone, QT-Quartzite

Table 27. Duncan Group Based on Lab Compacted Specimen Results.

Test/ Parameter	Duncan Group								
	Superpave			CMHB-C			Type C		
	Sec 1	Sec 2	Sec 3	Sec 4	Sec 5	Sec 6	Sec 7	Sec 8	Sec 9
	SR	SS	QT	SR	SS	QT	SR	SS	QT
APA Rut Depth	1, 2	1, 2	1, 2	3	2	1, 2	1, 2	1	1, 2
APA Creep Slope	1	3	1, 2, 3	1	1	1	1, 2	2, 3	2, 3
E* at 130°F and 10 Hz	1, 2	1	2	1, 2	1, 2	1, 2	1, 2	1, 2	1, 2
E*/sinδ at 130°F and 10 Hz	1, 2	1	2	1, 2	1, 2	2	1, 2	1, 2	1, 2
E* at 40°F and 10 Hz	1, 2, 3	1, 2, 3	1	1, 2, 3	3	1	1, 2, 3	2, 3	1, 2
E*sinδ at 40°F and 10 Hz	1, 2, 3	2, 3	1	1, 2	1, 2, 3	1	1, 2, 3	3	1, 2, 3
IDT Strength Value	2	1	2, 3	2	1	2, 3	2	1	2
Permeability Value	1, 2	1, 2	1	2	2	1, 2	1, 2	1	1, 2

SR-Siliceous River Gravel, SS-Sandstone, QT- Quartzite

Table 27 does not reveal any dramatic result. Maximum number of groups created by the test parameters for lab compacted specimens are three and in some cases only two. Again, most of the mixtures fall into more than one group for a given test parameter. The lab compacted specimens are less sensitive to grouping than its counterpart. The lab compacted specimens are prepared with tighter air void control.

CHAPTER 5: CONCLUSIONS AND RECOMMENDATIONS

GENERAL

In the Atlanta District, TxDOT constructed nine test sections on IH-20 in Harrison County. Nine test sections using nine (three mixture type × three aggregate type) different mixtures were constructed as surface course. The test sections were built by TxDOT with a future objective of predicting HMA performance from measured properties and to develop simple, practical, and reliable test procedures for evaluating the quality of finished asphalt concrete pavements on the basis of predicted performance. Several agencies participated in the testing and data collection process. The particular objective of this project (0-4203) was to document the as-built properties and populate a database to be used in a future project for evaluating relationships between pavement performance and measured properties during construction. This project conducted several laboratory tests on field cores and lab compacted plant mix specimens. Researchers analyzed the APA, HWTD, permeability, IDT, and dynamic modulus test results for ranking and grouping the mixtures. These results were compared with other as-built properties.

CONCLUSIONS

Based on the test results and analysis, the following conclusions are made.

- All nine surface mixtures and one base mixture exhibited overall good performance in all of the tests performed. In most cases, their measured properties are found to be statistically similar.
- Permeability was found to be sensitive to air void content of the pavement cores. The field cores that had high air voids exhibited high permeability. Permeability increased exponentially when the air voids increased higher than 9.0 percent.
- All the mixtures exhibited a narrow range of APA rut depths. This narrow range may not be sufficient to rank mixes in the order of their individual performance. However, these results were used for grouping the data into four groups for field cores and two groups for lab specimens, for predicting their relative performance.

It should be noted that the final APA rut depth value is a function of the initial deformation and subsequent rate of deformation expressed as creep slope. Two mixes may have the same final rut depth value at 8000 strokes but may have significantly different initial deformation levels and creep slopes. A mixture with steeper creep slope but with a low initial deformation value may have a tendency to exhibit better performance in the initial stages but poorer performance at later stages as compared to a mix with high initial deformation and flatter creep slope.

• The average coefficient of variation of IDT for the field samples (9.6 percent) was almost the same as that for lab samples (8.3 percent) and, in general, the coefficient of variation was between 1.0 to 14.5 percent for both the lab and the field samples. IDT values for the field samples were consistently and significantly less than those of the lab values. However, in both the cases, the range of IDT strengths was narrow.

• All mixes tested exhibited a close range of dynamic modulus values at a specified temperature. The shift functions of all the curves did not exhibit a large difference in terms of the sensitivity to change in temperature or loading rate. The Type B mixture used as a base course (Section 10) was found to have a consistently higher $|E^*|$ value as compared to the rest of the mixtures. Relatively low asphalt content might have contributed to a high dynamic modulus value for Type B mixture.

• The result of the HWTD test agrees well with both the APA results and permeability results (assuming permeability is directly related to moisture damage). This suggests that HWTD can identify both rutting and moisture damage potential in HMA mixtures.

• No particular mixture type (Superpave, CMHB-C, or Type C) could be identified as best or worst. The Type C sandstone mixture exhibited the overall best performance. It performed best in tests conducted using both field cores and lab compacted specimens. In general, the siliceous river gravel mixture performed worse than other two aggregate types.

• Grouping of statistically equivalent mixtures did not yield any distinct grouping among the mixture types or aggregate types.

RECOMMENDATIONS

These documented as-built properties will be helpful for subsequent research to predict performance and/or correlate observed field performance with measured material properties.

During the construction of HMA pavement, more emphasis should be provided to ensure that the compacted layers meet the target air voids and that plant mixtures meet the target asphalt contents. Researchers recommend constructing test pavements with different (low to high) qualities to obtain better performance prediction curves. Dynamic modulus test results and other known as-built properties make these test sections ideal candidates for proposed AASHTO 2002 Design Guide validation sites. Future research should correlate observed field performance with measured properties.

REFERENCES

1. Fernando, E., V. Prabhakar, T. Scullion, and S. Nazarian. *Predicting Hot-Mix Performance from Measured Properties: Phase I Report*. Report No. FHWA/TX-00/1708-1, Texas Transportation Institute, College Station, Texas, May 2000.
2. Epps, J. A., et al. Recommended Performance-Related Specification for Hot-Mix Asphalt Construction: Results of the WesTrack Project. *NCHRP Report 455*. Transportation Research Board, Washington D.C., 2002.
3. Yildirim, Y., and T. W. Kennedy. *Hamburg Wheel Tracking Device Results on Plant and Field Cores Produced Mixture*. Report No. TX/02-4185-2 (Draft), Center for Transportation Research, The University of Texas at Austin, Austin, Texas, 2002.
4. Nazarian, S., D. Yuan, V. Tandon, and M. Arellano. *Quality Management of Flexible Pavement Layers with Seismic Methods.* Report No. TX-02-1735-3F (Draft), Center for Highway Materials Research, The University of Texas at El Paso, El Paso, Texas, December 2002.
5. Epps, J. A., P. E. Sebaaly, J. Penaranda, M. R. Maher, M. B. McCann, and A. J. Hand. Compatibility of a Test for Moisture-Induced Damage with Superpave Volumetric Mix Design. *NCHRP Report 444*, National Cooperative Research Program, Transportation Research Board, Washington, D.C., 2000.
6. Izzo, R. P., and J. W. Button. *Permeability of Coarse Matrix-High Binder Mixtures and Its Effects on Performance*. Report No. FHWA/TX-97/1238-1F, Texas Transportation Institute, College Station, Texas, April 1997.
7. "Standard Provisional Test Method for Measurement of Permeability of Bituminous Paving Mixtures Using a Flexible Wall Permeameter," American Society for Testing and Materials. *2001 Annual Book of ASTM Standards* Vol. 04.03, Pennsylvania, USA.
8. Cooley Jr., L. A., P. S. Kandhal, M. S. Buchanan, F. Fee, and A. Epps. Loaded Wheel Testers in the United States: State of the Practice. *Transportation Research E-Circular No. E-C016*, Transportation Research Board, National Research Council, Washington, D.C., July 2000.
9. Asphalt Pavement Analyzer User's Guide. Pavement Technology, Inc., Covington, Georgia, 1998.

10. Witczak, M.W., et al. Simple Performance Test for Superpave Mix Design. *NCHRP Report 465*, Transportation Research Board, National Research Council, Washington D.C., 2002.
11. Guddati, M. N., Z. Feng, and Y. R. Kim. Toward Micromechanics-Based Procedure to Characterize Fatigue Performance of Asphalt Concrete. *Transportation Research Record 1789*, Transportation Research Board, National Research Council, Washington, D.C., 2002.
12. American Association of State Highway and Transportation Officials. *Standard Specifications for Transportation Materials and Methods of Sampling and Testing*. Part II, Method of Sampling and Testing, Washington D.C., 2000.
13. Yildirim, Y., and T. W. Kennedy. *Correlation of Field Performance to Hamburg Tracking Device Result*. Report No. TX/02-4185-1, Center for Transportation Research, The University of Texas at Austin, Austin, Texas, October 2001.
14. Pellinen, T. K., M. W. Witczak, and R. F. Bonaquist. Asphalt Mix Master Curve Construction Using Sigmoidal Fitting Function with Non-linear Least Squares Optimization. 15th ASCE Engineering Mechanics Conference, Columbia University, New York, June 2002.
15. Mallick, R. B., L. A. Cooley, M. Teto, and R. Bradbury. Development of a Simple Test for Evaluation of In-Place Permeability of Asphalt Mixes. *International Journal of Pavement Engineering 2001/7 2(2)*. Gordon and Breach Science Publishers, Inc., 50 West 23rd Street, New York, 2001.
16. Milton, J. S., and J. C. Arnold. *Introduction to Probability and Statistics: Principles and Applications for Engineering and Computing Sciences*. 3rd Edition, Irwin McGraw-Hill, New York, 1995.

APPENDIX A:
MIXTURE DESIGN DATA

Mix Design AO111 (H01-07)
Optimum Asphalt Content = 5.0%

	TxDOT	Contractor
Stability	43	
TEX-531-C TSR	0.97	0.96
Conditioned Strength	132 PSI	134 PSI
GR	2.442	2.426
DENSITY	95.4	96.0

Aggregate Characteristics

(C.A.TY D)	FLAT & ELONGATED PARTICLES = 0.0%
(C.A.TY C)	FLAT & ELONGATED PARTICLES = 0.0%
SCREENINGS	FINE AGGREGATE ANGULARITY = 46
SAND EQUIVALENT	(COMBINED) = 86

Mixture Summary

Asphalt Content %	Sp.Grav. of Specimen @N_{des}	Maximum Specific Grav., Gr	Effective Gravity, Ge	Theoretical Sp. Grav, Gt	Density from Gt	VMA % (Tex-207-F)	VFA %	Dust to Asphalt Ratio, DP
4.5	2.316	2.440	2.608	2.442	94.8	15.3	66.2	0.7
5.0	2.328	2.425	2.611	2.425	96.0	15.3	73.9	0.6
5.5	2.333	2.410	2.614	2.408	96.9	15.6	80.0	0.6

Interpolated Optimum Mixture Properties @ 96% Density

Optimum Asphalt Content	5.1%
Voids in Mineral Aggregate, VMA	15.3%
Voids Filled with Asphalt, VFA	73.9%
Dust to Asphalt Ratio, DP	0.6

Specific Gravity of Asphalt=1.03
Material Passing #200 Sieve= 3.2

Density @ N_{ini}, N_{des}, & N_{max} @ 5.1%Asphalt Content

	Height Sample 'A'	Height Sample 'B'	Test Results	Specifications
$N_{initial}$-Gyrations	126.8	125.7	86.9%	89.0 Maximum
N_{design}-Gyrations	114.0	113.8	96.3%	96.0 +/- 1%
$N_{maximum}$-Gyrations	112.5	112.6	97.5%	98.0 Maximum

	Sample 'A'	Sample 'B'	Average
Ga @ N_{max}=	2.371	2.360	2.366
Gr @ OAC=	2.426	2.426	2.426

Figure A1. Section 1 Mixture Design Summary.

Mix Design AO112 (H01-08)
Optimum Asphalt Content = 5.1%

	TxDOT	Contractor
Stability	51	
TEX-531-C TSR	0.92	0.83
Conditioned Strength	136 PSI	206 PSI
GR	2.387	2.366
DENSITY	97.1	96

Aggregate Characteristics

(C.A.TY D)	FLAT & ELONGATED PARTICLES = 0.9%
(C.A.TY C)	FLAT & ELONGATED PARTICLES = 0.9%
SCREENINGS	FINE AGGREGATE ANGULARITY = 50
SAND EQUIVALENT	(COMBINED) = 56

Mixture Summary

Asphalt Content %	Sp. Grav. of Specimen @ N_{des}	Maximum Specific Grav., Gr	Effective Gravity, Ge	Theoretical Sp. Grav, Gt	Density from Gt	VMA % (Tex-207-F)	VFA %	Dust to Asphalt Ratio, DP
4.5	2.26	2.388	2.546	2.389	94.6	15.3	64.6	1.4
5.0	2.276	2.369	2.543	2.676	95.9	15.1	73.1	1.3
5.5	2.279	2.361	2.553	2.356	96.7	15.5	78.7	1.2

Interpolated Optimum Mixture Properties @ 96% Density

Optimum Asphalt Content	5.1%
Voids in Mineral Aggregate, VMA	15.4%
Voids Filled with Asphalt, VFA	73.14%
Dust to Asphalt Ratio, DP	1.3

Specific Gravity of Asphalt=1.03
Material Passing #200 Sieve= 6.5

Density @ N_{ini}, N_{des}, & N_{max} @ 5.1% Asphalt Content

	Height Sample 'A'	Height Sample 'B'	Test Results	Specifications
$N_{initial}$-Gyrations	128.5	129.7	86%	89.0 Maximum
N_{design}-Gyrations	115.1	115.6	96%	96.0 +/- 1%
$N_{maximum}$-Gyrations	113.7	114.2	97%	98.0 Maximum

	Sample 'A'	Sample 'B'	Average
Ga @ N_{max}=	2.302	2.308	2.305
Gr @ OAC=	2.366	2.366	2.366

Figure A2. Section 2 Mixture Design Summary.

Mix Design AO112 (H01-08)
Optimum Asphalt Content = 5.1%

	TxDOT	Contractor
Stability	41	
TEX-531-C TSR	0.94	0.81
Conditioned Strength	135 PSI	170 PSI
GR	2.464	2.456
DENSITY	96.6	96.0

Aggregate Characteristics

(C.A.TY D)	FLAT & ELONGATED PARTICLES = 1.9%
(C.A.TY C)	FLAT & ELONGATED PARTICLES = 2.2%
SCREENINGS	FINE AGGREGATE ANGULARITY = 50
SAND EQUIVALENT	(COMBINED) = 67

Mixture Summary

Asphalt Content %	Sp. Grav. of Specimen @N_{des}	Maximum Specific Grav., Gr	Effective Gravity, Ge	Theoretical Sp. Grav., Gt	Density from Gt	VMA % (Tex-207-F)	VFA %	Dust to Asphalt Ratio, DP
4.5	2.348	2.476	2.651	2.476	94.8	15.4	66.4	1.2
5.0	2.355	2.458	2.651	2.458	95.8	15.6	73.1	1.1
5.5	2.375	2.441	2.652	2.440	97.3	15.4	82.5	1.0

Interpolated Optimum Mixture Properties @ 96% Density

Optimum Asphalt Content, OAC	5.1%
Voids in Mineral Aggregate, VMA	15.4%
Voids Filled with Asphalt, VFA	76.1%
Dust to Asphalt Ratio, DP	1.1

Specific Gravity of Asphalt=1.03
Material Passing #200 Sieve= 5.6

Density @ N_{ini}, N_{des}, & N_{max} @ 5.1% Asphalt Content

	Height Sample 'A'	Height Sample 'B'	Test Results	Specifications
$N_{initial}$-Gyrations	126.9	128.4	86.5%	89.0 Maximum
N_{design}-Gyrations	114.4	115.2	96.2%	96.0 +/- 1%
$N_{maximum}$-Gyrations	113.0	113.7	97.4%	98.0 Maximum

	Sample 'A'	Sample 'B'	Average
Ga @ N_{max}=	2.394	2.389	2.392
Gr @ OAC=	2.457	2.455	2.456

Figure A3. Section 3 Mixture Design Summary.

Mix Design AO114 (H01-15)
Optimum Asphalt Content = 4.7%

	TxDOT	Contractor
Stability		42
TEX-531-C TSR	0.99	0.91
Conditioned Strength	94 PSI	91 PSI
GR	2.420	2.414
DENSITY		96.0

Aggregate Characteristics

LIME	TEXAS HYDRATED LIME = 1.0%
SAND EQUIVALENT	(COMBINED) = 76

Mixture Summary

Asphalt Content %	Specific Gravity of Specimen @ N_{des}	Maximum Specific Gravity, Gr	Effective Specific Gravity, Ge	Theoretical Max. Specific Gravity, Gt	Density (from Gt)	VMA %
4.0	2.315	2.432	2.578	2.440	94.9	14.1
4.5	2.328	2.421	2.586	2.422	96.1	14.1
5.0	2.341	2.401	2.582	2.405	97.3	14.0
5.5	2.358	2.392	2.599	2.372	99.7	13.9
6.0	2.365	2.381	2.599	2.372	99.7	14.1

Effective Specific Gravity, (Ge)	2.587
Optimum Asphalt Content	4.7%
VMA @ Optimum Asphalt Content	14.1
Interpolated values at optimum density of	96.5%

Interpolated Values

Ga @ Optimum Asphalt Content	2.332
Gr @ Optimum Asphalt Content	2.414
Gt @ Optimum Asphalt Content	2.416

Figure A4. Section 4 Mixture Design Summary.

Mix Design A0116 (H01-17)
Optimum Asphalt Content = 4.8%

	TxDOT	Contractor
Stability		
TEX-531-C TSR	1.05	0.99
Conditioned Strength	120 PSI	138 PSI
GR	2.397	2.386
DENSITY		96.0

Aggregate Characteristics

LIME	TEXAS HYDRATED LIME = 1.0%
SAND EQUIVALENT	(COMBINED) = 65

Mixture Summary

Asphalt Content %	Sp. Grav. of Specimen @N_{des}	Maximum Specific Grav. Gr	Effective Gravity, Ge	Theoretical Max. Specific gr. Gt	Density (from Gt)	VMA %
4.0	2.290	2.413	2.556	2.412	94.9	14.0
4.5	2.302	2.393	2.552	2.395	96.1	13.9
5.0	2.305	2.379	2.555	2.378	96.9	14.3
5.5	2.318	2.369	2.563	2.362	98.1	14.2
6.0	2.313	2.339	2.545	2.346	98.6	14.9

Effective Specific Gravity, Ge	2.554
Optimum Asphalt Content	4.8%
VMA@ Optimum Asphalt Content	14.1
Interpolated values at optimum density of	96.5%

Interpolated Values

Ga @Optimum Asphalt Content	2.304
Gr @ Optimum Asphalt Content	2.386
Gt @ Optimum Asphalt Content	2.387

Figure A5. Section 5 Mixture Design Summary.

Mix Design AO115 (H01-16)
Optimum Asphalt Content = 4.8%

	TxDOT	Contractor
Stability		
TEX-531-C TSR	0.99	0.98
Conditioned Strength	113 PSI	96 PSI
GR	2.474	2.469
DENSITY		96.0

Aggregate Characteristics

LIME	TEXAS HYDRATED LIME = 1.0%
SAND EQUIVALENT	(COMBINED) = 74

Mixture Summary

Asphalt Content %	Specific Gravity of Specimen @ N_{des}	Maximum Specific Gravity, Gr	Effective Specific Gravity, Ge	Theoretical max. Specific Gravity, Gt	Density (from Gt)	VMA %
4.0	2.350	5.495	2.652	2.494	94.2	14.9
4.5	2.366	2.482	2.659	2.475	95.6	14.7
5.0	2.385	2.460	2.654	2.457	97.1	14.5
5.5	2.389	2.439	2.650	2.439	97.9	14.8
6.0	2.393	2.412	2.638	2.422	98.8	15.1

Effective Specific Gravity, (Ge)	2.650
Optimum Asphalt Content	4.8%
VMA @ Optimum Asphalt Content	14.6
Interpolated values at optimum density of	96.5%

Interpolated Values

Ga @ Optimum Asphalt Content	2.377
Gr @ Optimum Asphalt Content	2.469
Gt @ Optimum Asphalt Content	2.464

Figure A6. Section 6 Mixture Design Summary.

Mix Design AO117 (H01-18)
Optimum Asphalt Content = 4.4%

	TxDOT	Contractor
Stability	50	48
TEX-531-C TSR	1.06	.90
Conditioned Strength	131 psi	116 psi
GR	2.450	2.455
DENSITY	96.0	96.0

Aggregate Characteristics

LIME	TEXAS HYDRATED LIME = 1.0%
SAND EQUIVALENT	(COMBINED) = 69

Mixture Summary

Asphalt Content %	Specific Gravity of Specimen @ N_{des}	Maximum Specific Gravity, Gr	Effective Gravity, Ge	Theoretical max. Specific Gravity, Gt	Density (from Gt)	VMA %
3.5	2.320	2.480	2.613	2.484	93.4	14.5
4.0	2.341	2.469	2.622	2.466	94.9	14.2
4.5	2.359	2.451	2.621	2.449	96.3	14.0
5.0	2.370	2.433	2.621	2.431	97.5	14.0
5.5	2.375	2.411	2.615	2.414	98.4	14.3

Effective Specific Gravity, Ge	2.618
Optimum Asphalt Content	4.4 %
VMA @ Optimum Asphalt Content	14.0
Interpolated values at optimum density of	96.0%

Interpolated Values

Ga @ Optimum Asphalt Content	2.355
Gr @ Optimum Asphalt Content	2.455
Gt @ Optimum Asphalt Content	2.453

Figure A7. Section 7 Mixture Design Summary.

Mix Design AO119 (H01-20)
Optimum Asphalt Content = 4.5%

	TxDOT	Contractor
Stability	48	49
TEX-531-C TSR	0.96	0.83
Conditioned Strength	188 psi	121 psi
GR	2.421	2.405
DENSITY	95.2	96.0

Aggregate Characteristics

LIME	TEXAS HYDRATED LIME = 1.0%
SAND EQUIVALENT	(COMBINED) = 47

Mixture Summary

Asphalt Content %	Specific Gravity of Specimen @N_{des}	Maximum Specific Gravity, Gr	Effective Gravity, Ge	Theoretical max. Specific Gravity, Gt	Density (from Gt)	VMA %
3.5	2.274	2.438	2.565	2.438	93.3	14.5
4.0	2.285	2.420	2.564	2.421	94.4	14.5
4.5	2.307	2.405	2.566	2.404	96.0	14.1
5.0	2.315	2.388	2.566	2.387	97.0	14.3
5.5	2.322	2.370	2.564	2.371	97.9	14.5

Effective Specific Gravity, Ge	2.565
Optimum Asphalt Content	4.5 %
VMA @ Optimum Asphalt Content	14.1
Interpolated values at optimum density of	96.0%

Interpolated Values

Ga @ Optimum Asphalt Content	2.307
Gr @ Optimum Asphalt Content	2.405
Gt @ Optimum Asphalt Content	2.404

Figure A8. Section 8 Mixture Design Summary.

Mix Design AO118 (H01-19)
Optimum Asphalt Content = 4.6 %

	TxDOT	Contractor
Stability	43	51
TEX-531-C TSR	0.90	0.90
Conditioned Strength	141 Psi	129 Psi
GR	2.474	2.478
DENSITY	96.8	96.0

Aggregate Characteristics

LIME	TEXAS HYDRATED LIME = 1.0%
SAND EQUIVALENT	(COMBINED) = 69

Mixture Summary

Asphalt Content %	Specific Gravity of Specimen @ N_{des}	Maximum Specific Gravity, Gr	Effective Specific Gravity, Ge	Theoretical Max Specific Gravity, Gt	Density (from Gt)	VMA %
3.5	2.350	2.520	2.660	2.517	93.4	14.6
4.0	2.365	2.500	2.658	2.498	94.7	14.5
4.5	2.378	2.481	2.657	2.480	95.9	14.5
5.0	2.380	2.460	2.654	2.462	96.7	14.9
5.5	2.385	2.440	2..651	2.444	97.6	14.1

Effective Specific Gravity, Ge	2.656
Optimum Asphalt Content	4.6%
VMA @ Optimum Asphalt Content	14.6
Interpolated values at optimum density of	96.0%

Interpolated Values

Ga @ Optimum Asphalt Content	2.378
Gr @ Optimum Asphalt Content	2.478
Gt @ Optimum Asphalt Content	2.478

Figure A9. Section 9 Mixture Design Summary.

Mix Design AO120 (H01-21)
Optimum Asphalt Content = 3.8%

	TxDOT	Contractor
Stability	46	56
TEX-531-C TSR	0.92	0.94
Conditioned Strength	145 Psi	178 Psi
GR	2.530	2.520
DENSITY	97.0	96.0

LIME	TEXAS HYDRATED LIME = 1.0%
SAND EQUIVALENT	(COMBINED) = 89
SAND EQUIVALENT	(FIELD SAND) = 71

Mixture Summary

Asphalt Content %	Specific Gravity of Specimen @ N_{des}	Maximum Specific Gravity, Gr	Effective Specific Gravity, Ge	Theoretical Max. Specific Gravity, Gt	Density (from Gt)	VMA %
3.5	2.397	2.540	2.661	2.547	94.1	12.9
4.0	2.410	2.531	2.672	2.528	95.3	12.9
4.5	2.419	2.514	2.675	2.509	96.4	13.0
5.0	2.421	2.493	2.672	2.490	97.2	13.3
5.5	2.439	2.468	2.664	2.472	98.7	13.2

Effective Specific Gravity, Ge	2.669
Optimum Asphalt Content	3.8 %
VMA @ Optimum Asphalt Content	13.0
Interpolated values at optimum density of	96.0%

Interpolated Values

Ga @ Optimum Asphalt Content	2.416
Gr @ Optimum Asphalt Content	2.520
Gt @ Optimum Asphalt Content	2.516

Figure A10. Section 10 (Base Course) Mixture Design Summary.

APPENDIX B: LABORATORY TEST RESULTS (TTI)

Table B1. IDT Test Results for Lab Molded Specimens.

Sec-tion	Sample ID	Height (inch)	Diameter (inch)	Load (lb)	IDT Strength (psi)	Air Void	Avg. IDT Strength (psi)	Std. Dev.	Cv %
1	3A	2.407	4.0	2578	170.6	7.5	174.0	10.3	5.9
	3B	2.484	4.0	2586	165.8	6.6			
	2B	2.371	4.0	2763	185.6	6.7			
2	2A	2.173	4.0	3078	225.6	7.8	226.4	7.5	3.3
	2B	2.337	4.0	3439	234.3	7.9			
	3A	2.361	4.0	3252	219.4	7.9			
3	5A	2.324	4.0	2248	154.1	6.0	154.2	1.5	1.0
	9B	2.436	4.0	2382	155.8	6.4			
	8B	2.387	4.0	2289	152.7	6.0			
4	1A	2.118	4.0	2291	172.3	6.1	168.9	24.9	14.7
	7B	2.442	4.0	2943	191.9	6.5			
	1B	1.975	4.0	1766	142.5	6.9			
5	1A	2.09	4.0	2805	213.7	6.6	205.2	14.3	6.9
	2A	2.097	4.0	2808	213.2	6.5			
	2B	2.099	4.0	2488	188.8	7.8			
6	1A	2.146	4.0	1894	140.6	7.8	159.1	21.8	13.7
	2A	2.132	4.0	2054	153.5	7.8			
	3A	2.147	4.0	2469	183.1	6.3			
7	2A	2.178	4.0	2584	188.9	7.6	173.6	20.1	11.6
	7A	2.439	4.0	2309	150.8	7.3			
	6B	2.416	4.0	2747	181.1	7.2			
8	4A	2.026	4.0	2864	225.1	7.5	213.7	10.4	4.9
	4B	1.964	4.0	2608	211.4	7.7			
	3B	2.035	4.0	2616	204.7	7.0			
9	1A	2.064	4.0	2520	194.4	7.2	176.1	16.1	9.1
	6A	2.436	4.0	2590	169.3	7.1			
	5A	2.396	4.0	2475	164.5	7.2			
10	7B	2.387	4.0	1815	121.1	6.4	138.8	16.7	12.1
	7A	2.441	4.0	2159	140.8	6.4			
	6A	2.034	4.0	1972	154.4	7.4			

Cv – Coefficient of Variation

Table B2. IDT Test Results for Roadway Core Specimens.

Section	Sample ID	Height (inch)	Diameter (inch)	Load (lb)	IDT Strength (psi)	Air Void	Avg. IDT Strength (psi)	Std. Dev.	Cv %
1	#10	2.158	4	1168	86.2	8.6	91.1	9.25	10.15
	#11	2.125	4	1306	97.9	9.0			
	#12	2.114	4	1069	80.5	9.0			
	#13	2.114	4	1324	99.7	8.9			
2	#10	2.571	4	1108	68.6	11.1	75.2	8.48	11.28
	#11	2.550	4	1074	67.1	10.1			
	#12	2.563	4	1326	82.4	10.4			
	#13	2.603	4	1350	82.6	10.6			
3	#10	2.110	4	1269	95.8	6.5	101.3	7.51	7.41
	#11	2.177	4	1518	111.0	6.8			
	#12	2.152	4	1399	103.5	6.6			
	#13	2.214	4	1321	95.0	7.2			
4	#10	2.033	4	1116	87.4	4.7	103.2	11.48	11.13
	#11	1.990	4	1415	113.2	5.1			
	#12	1.950	4	1345	109.9	4.9			
	#13	1.970	4	1264	102.2	5.2			
5	#10	2.226	4	870	62.2	9.4	72.1	10.46	14.49
	#11	2.216	4	898	64.5	9.7			
	#12	2.310	4	1218	84.0	9.2			
	#13	2.297	4	1123	77.8	9.1			
6	#10	2.336	4	1320	90.0	8.3	88.2	3.06	3.46
	#11	2.329	4	1244	85.0	8.8			
	#12	2.314	4	1255	86.4	8.9			
	#13	2.307	4	1327	91.6	8.3			
7	#10	2.273	4	1542	108.0	8.4	103.6	4.07	3.93
	#11	2.313	4	1426	98.2	8.0			
	#12	2.290	4	1500	104.3	8.4			
	#13	2.267	4	1477	103.7	8.5			
8	#10	2.146	4	1400	103.9	8.1	99.9	14.48	14.50
	#11	2.155	4	1213	89.6	8.6			
	#12	2.137	4	1172	87.3	8.9			
	#13	2.143	4	1596	118.6	8.3			
9	#10	1.962	4	1327	107.7	9.2	97.8	10.06	10.28
	#11	1.984	4	1176	94.4	9.3			
	#12	1.987	4	1295	103.8	9.6			
	#13	1.951	4	1044	85.2	9.6			

Table B3. Florida Permeability Test Results for Lab Molded Specimens.

Section	Specimen ID	Height (cm)	Area (sq. cm)	Time (sec)	Temp Correction Factor	Flow (cm)	Permeability (cm/sec)	Permeability (in/sec)	Avg. Permeability (in/sec)	Std. Dev.	Cv %
1	#1	7.55	174.44	230.55	0.965	63	3.08E-03	1.21E-03	1.38E-03	2.60E-04	18.8
	#2	7.56	175.93	220.28	0.965	63	3.19E-03	1.26E-03			
	#3	7.56	175.71	164.82	0.965	63	4.28E-03	1.68E-03			
2	#1	7.59	174.73	266.98	0.965	63	2.66E-03	1.05E-03	1.39E-03	4.84E-04	34.9
	#2	7.59	155.98	161.26	0.965	63	4.93E-03	1.94E-03			
	#3	7.60	173.87	240.13	0.965	63	2.97E-03	1.17E-03			
3	#1	7.60	175.32	278.97	0.965	63	2.54E-03	1.00E-03	8.11E-04	2.31E-04	28.5
	#2	7.66	175.98	504.53	0.965	63	1.41E-03	5.53E-04			
	#3	7.66	176.55	316.17	0.965	63	2.24E-03	8.80E-04			
4	#1	7.65	176.86	181.42	0.965	63	3.89E-03	1.53E-03	1.99E-03	1.04E-03	52.5
	#2	7.65	176.70	221.04	0.965	63	3.19E-03	1.26E-03			
	#3	7.65	176.63	87.22	0.965	63	8.10E-03	3.19E-03			
5	#1	7.68	176.44	138.70	0.965	63	5.11E-03	2.01E-03	1.87E-03	5.67E-04	30.4
	#2	7.64	176.86	118.12	0.965	63	5.97E-03	2.35E-03			
	#3	7.67	177.09	223.66	0.965	63	3.15E-03	1.24E-03			
6	#1	7.62	175.15	188.02	0.965	63	3.78E-03	1.49E-03	1.01E-03	5.02E-04	49.5
	#2	7.54	176.09	259.00	0.965	63	2.71E-03	1.07E-03			
	#3	7.64	175.36	574.03	0.965	63	1.24E-03	4.87E-04			
7	#1	7.57	175.13	264.46	0.965	63	2.67E-03	1.05E-03	1.19E-03	4.67E-04	39.4
	#2	7.65	175.44	350.04	0.965	63	2.03E-03	7.99E-04			
	#3	7.64	175.00	164.34	0.965	63	4.33E-03	1.71E-03			
8	#1	7.64	174.86	463.88	0.965	63	1.54E-03	6.05E-04	7.91E-04	1.62E-04	20.4
	#2	7.63	175.33	316.52	0.965	63	2.24E-03	8.83E-04			
	#3	7.65	176.27	314.07	0.965	63	2.25E-03	8.87E-04			
9	#1	7.69	176.12	171.50	0.965	63	4.14E-03	1.63E-03	1.45E-03	5.43E-04	37.4
	#2	7.68	176.77	147.79	0.965	63	4.79E-03	1.88E-03			
	#3	7.67	176.55	330.38	0.965	63	2.14E-03	8.43E-04			
10	#1	7.72	175.08	216.78	0.965	63	3.30E-03	1.30E-03	1.65E-03	3.02E-04	18.3
	#2	7.69	175.77	153.76	0.965	63	4.63E-03	1.82E-03			
	#3	7.63	174.83	153.47	0.965	63	4.64E-03	1.83E-03			

Cv – Coefficient of Variation

Table B4. Florida Permeability Test Results for Roadway Core Specimens.

Section	Spec. ID	Height (cm)	Area (sq.cm)	Time (sec)	Temp correction factor	Flow (cm)	Permeability (cm/sec)	Permeability (in/sec)	Avg. Permeability (in/sec)	Std. Dev.	Cv %
1	#1	5.39	176.79	62.77	0.965	63	8.91E-03	3.51E-03	3.90E-03	3.40E-04	8.71
	#2	5.29	176.32	52.71	0.965	63	1.05E-02	4.14E-03			
	#3	5.24	173.46	54.49	0.965	63	1.03E-02	4.04E-03			
2	#1	6.06	174.23	25.38	0.965	63	2.42E-02	9.54E-03	1.11E-02	1.39E-03	12.57
	#2	5.99	171.91	21.37	0.965	63	2.90E-02	1.14E-02			
	#3	6.17	172.75	20.15	0.965	63	3.11E-02	1.23E-02			
3	#1	5.50	173.96	128.33	0.965	63	4.49E-03	1.77E-03	1.70E-03	2.59E-04	15.21
	#2	5.62	176.25	118.32	0.965	63	4.88E-03	1.92E-03			
	#3	5.56	175.72	159.84	0.965	63	3.60E-03	1.42E-03			
4	#1	5.09	174.09	134.00	0.965	63	4.08E-03	1.61E-03	1.45E-03	6.75E-04	46.67
	#2	5.17	175.87	106.24	0.965	63	5.15E-03	2.03E-03			
	#3	4.97	174.48	299.20	0.965	63	1.79E-03	7.05E-04			
5	#1	5.62	172.87	11.47	0.965	63	5.14E-02	2.02E-02	2.28E-02	2.33E-03	10.22
	#2	6.32	173.41	10.76	0.965	63	5.90E-02	2.32E-02			
	#3	6.31	173.60	10.06	0.965	63	6.30E-02	2.48E-02			
6	#1	5.82	175.82	53.68	0.965	63	1.10E-02	4.35E-03	2.85E-03	1.62E-03	56.78
	#2	5.65	175.22	74.62	0.965	63	7.82E-03	3.08E-03			
	#3	5.73	173.50	206.93	0.965	63	2.87E-03	1.13E-03			
7	#1	6.17	176.16	130.06	0.965	63	4.73E-03	1.86E-03	1.95E-03	4.85E-04	24.95
	#2	6.18	175.88	161.21	0.965	63	3.83E-03	1.51E-03			
	#3	6.17	175.98	98.32	0.965	63	6.27E-03	2.47E-03			
8	#1	5.34	175.10	87.38	0.965	63	6.42E-03	2.53E-03	2.05E-03	5.47E-04	26.69
	#2	5.42	174.99	153.75	0.965	63	3.69E-03	1.45E-03			
	#3	5.36	174.65	102.61	0.965	63	5.50E-03	2.17E-03			
9	#1	5.17	174.90	76.59	0.965	63	7.18E-03	2.83E-03	2.25E-03	5.60E-04	24.89
	#2	5.14	175.16	97.72	0.965	63	5.60E-03	2.20E-03			
	#3	5.11	175.51	125.10	0.965	63	4.35E-03	1.71E-03			

Cv-Coefficient of Variation

Table B5. Dynamic Modulus – Section 1.

Fre-quency	40°F		70°F		100°F		130°F	
	Avg. E* ($\times 10^3$ psi)	Avg. δ (degree)	Avg. E* ($\times 10^3$ psi)	Avg. δ (degree)	Avg. E* ($\times 10^3$ psi)	Avg. δ (degree)	Avg. E* ($\times 10^3$ psi)	Avg. δ (degree)
25Hz	2,475	9.25	1,777	32.64	618	47.68	200	39.36
10Hz	2,447	13.85	1,378	23.53	487	37.45	179	30.74
5Hz	2,217	12.90	1,213	26.76	400	32.01	136	38.00
1Hz	1,796	13.84	882	24.73	244	34.00	77	32.13
0.5Hz	1,626	15.78	768	29.67	192	32.25	66	36.69
0.1Hz	1,283	18.74	519	32.45	127	36.94	47	32.49

Table B6. Dynamic Modulus – Section 2.

Fre-quency	40°F		70°F		100°F		130°F	
	Avg. E* ($\times 10^3$ psi)	Avg. δ (degree)	Avg. E* ($\times 10^3$ psi)	Avg. δ (degree)	Avg. E* ($\times 10^3$ psi)	Avg. δ (degree)	Avg. E* ($\times 10^3$ psi)	Avg. δ (degree)
25Hz	3,315	-	2,261	25.67	718	36.62	311	31.72
10Hz	2,923	11.15	1,855	27.26	574	34.52	232	34.55
5Hz	2,736	14.63	1,553	22.62	454	38.94	168	35.26
1Hz	2,363	14.00	1,110	24.51	269	30.58	92	31.33
0.5Hz	2,213	14.51	973	29.51	220	36.19	74	33.71
0.1Hz	1,735	19.94	628	32.87	133	36.02	46	28.92

Table B7. Dynamic Modulus – Section 3.

Fre-quency	40°F		70°F		100°F		130°F	
	Avg. E* ($\times 10^3$ psi)	Avg. δ (degree)	Avg. E* ($\times 10^3$ psi)	Avg. δ (degree)	Avg. E* ($\times 10^3$ psi)	Avg. δ (degree)	Avg. E* ($\times 10^3$ psi)	Avg. δ (degree)
25Hz	2,512	-	1,613	31.16	611	35.09	156	36.31
10Hz	2,095	11.85	1,329	24.49	472	31.68	109	41.98
5Hz	1,869	12.85	1,136	22.90	336	32.58	87	33.07
1Hz	1,408	18.26	799	26.45	209	31.94	55	25.69
0.5Hz	1,265	19.63	686	30.63	169	33.73	46	27.64
0.1Hz	910	22.17	446	34.02	101	31.70	34	22.12

Table B8. Dynamic Modulus – Section 4.

Frequency	40°F		70°F		100°F		130°F	
	Avg. E* (×10^3 psi)	Avg. δ (degree)	Avg. E* (×10^3 psi)	Avg. δ (degree)	Avg. E* (×10^3 psi)	Avg. δ (degree)	Avg. E* (×10^3 psi)	Avg. δ (degree)
25Hz	2,667	-	1,406	27.99	500	41.63	172	38.46
10Hz	2,190	13.33	1,209	24.76	393	37.43	135	32.87
5Hz	2,047	13.61	1,008	29.87	317	32.07	102	32.44
1Hz	1,590	17.64	709	29.96	185	35.24	58	31.86
0.5Hz	1,419	19.74	593	32.51	151	37.71	49	31.60
0.1Hz	1,050	21.84	378	36.68	92	38.25	34	32.14

Table B9. Dynamic Modulus – Section 5.

Frequency	40°F		70°F		100°F		130°F	
	Avg. E* (×10^3 psi)	Avg. δ (degree)	Avg. E* (×10^3 psi)	Avg. δ (degree)	Avg. E* (×10^3 psi)	Avg. δ (degree)	Avg. E* (×10^3 psi)	Avg. δ (degree)
25Hz	2,802	-	1,668	26.53	636	41.27	172	47.73
10Hz	2,607	16.76	1,415	24.37	458	33.78	162	31.95
5Hz	2,415	14.07	1,255	23.26	373	27.88	118	44.50
1Hz	1,934	14.62	841	24.75	209	34.43	69	29.60
0.5Hz	1,729	18.17	741	26.68	168	35.94	58	17.70
0.1Hz	1,324	22.09	473	29.88	102	35.16	40	27.05

Table B10. Dynamic Modulus – Section 6.

Frequency	40°F		70°F		100°F		130°F	
	Avg. E* (×10^3 psi)	Avg. δ (degree)	Avg. E* (×10^3 psi)	Avg. δ (degree)	Avg. E* (×10^3 psi)	Avg. δ (degree)	Avg. E* (×10^3 psi)	Avg. δ (degree)
25Hz	2,041	24.81	1,419	31.90	571	31.77	198	35.82
10Hz	2,113	11.53	1,311	24.60	487	27.90	193	27.56
5Hz	1,874	13.55	1,118	23.94	394	26.71	143	25.74
1Hz	1,533	15.29	826	23.05	256	29.79	83	28.81
0.5Hz	1,335	16.38	695	28.75	204	32.39	72	30.31
0.1Hz	1,065	17.97	478	29.68	135	33.13	51	27.72

Table B11. Dynamic Modulus – Section 7.

Frequency	40°F		70°F		100°F		130°F	
	Avg. E* ($\times 10^3$ psi)	Avg. δ (degree)	Avg. E* ($\times 10^3$ psi)	Avg. δ (degree)	Avg. E* ($\times 10^3$ psi)	Avg. δ (degree)	Avg. E* ($\times 10^3$ psi)	Avg. δ (degree)
25Hz	3,359	-	1,719	24.03	668	49.14	220	62.61
10Hz	2,595	12.34	1,503	25.79	512	33.67	162	37.98
5Hz	2,433	14.20	1,265	27.78	390	33.46	117	35.02
1Hz	1,959	16.64	924	27.24	234	32.80	67	29.82
0.5Hz	1,793	18.29	761	30.49	196	35.46	57	34.28
0.1Hz	1,396	19.31	512	35.24	122	35.13	40	31.21

Table B12. Dynamic Modulus – Section 8.

Frequency	40°F		70°F		100°F		130°F	
	Avg. E* ($\times 10^3$ psi)	Avg. δ (degree)	Avg. E* ($\times 10^3$ psi)	Avg. δ (degree)	Avg. E* ($\times 10^3$ psi)	Avg. δ (degree)	Avg. E* ($\times 10^3$ psi)	Avg. δ (degree)
25Hz	3,256	-	1,916	19.94	884	45.01	245	44.06
10Hz	3,160	10.96	1,714	21.39	658	32.15	169	37.67
5Hz	2,936	10.04	1,543	18.07	563	29.27	139	37.80
1Hz	2,388	12.25	1,116	17.46	328	31.26	77	29.34
0.5Hz	2,115	15.26	1,028	24.20	275	31.83	63	31.20
0.1Hz	1,722	15.86	689	30.02	173	35.42	42	29.50

Table B13. Dynamic Modulus – Section 9.

Frequency	40°F		70°F		100°F		130°F	
	Avg. E* ($\times 10^3$ psi)	Avg. δ (degree)	Avg. E* ($\times 10^3$ psi)	Avg. δ (degree)	Avg. E* ($\times 10^3$ psi)	Avg. δ (degree)	Avg. E* ($\times 10^3$ psi)	Avg. δ (degree)
25Hz	2,673	-	1,507	27.40	496	36.87	209	48.31
10Hz	2,407	8.15	1,193	24.05	358	32.53	139	33.64
5Hz	2,130	12.83	1,025	24.73	283	32.97	106	32.54
1Hz	1,702	15.03	718	22.16	173	31.28	68	30.08
0.5Hz	1,579	14.63	618	29.73	140	33.80	56	32.38
0.1Hz	1,210	18.12	395	31.43	91	33.58	39	28.80

Table B14. Dynamic Modulus – Section 10 (Type B Base).

Fre-quency	40°F		70°F		100°F		130°F	
	Avg. E* ($\times 10^3$ psi)	Avg. δ (degree)	Avg. E* ($\times 10^3$ psi)	Avg. δ (degree)	Avg. E* ($\times 10^3$ psi)	Avg. δ (degree)	Avg. E* ($\times 10^3$ psi)	Avg. δ (degree)
25Hz	3,781	-	2,573	28.84	1,125	42.93	366	46.00
10Hz	3,071	-	1,867	19.45	706	34.67	311	42.00
5Hz	2,946	12.96	1,754	24.71	602	33.10	194	34.24
1Hz	2,466	13.22	1,240	26.87	372	30.76	118	41.95
0.5Hz	2,224	15.08	1,143	26.08	331	34.41	105	35.49
0.1Hz	1,767	15.83	782	29.06	204	33.41	73	33.20

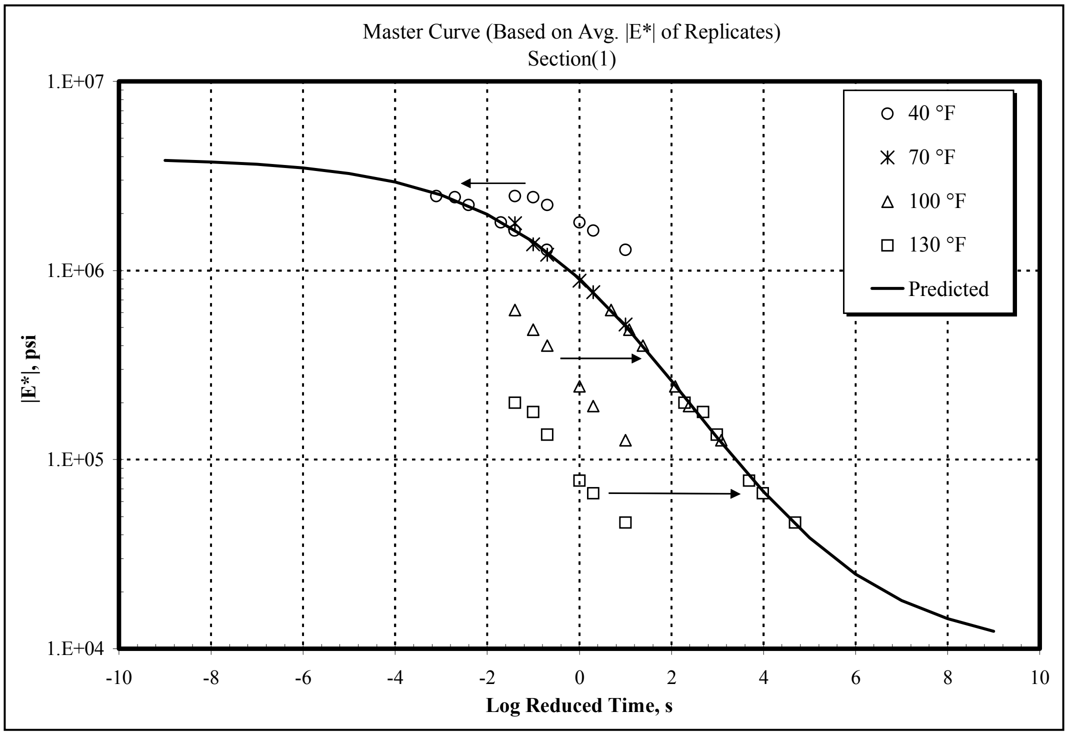

Figure B1. Dynamic Modulus Master Curve for Section 1.

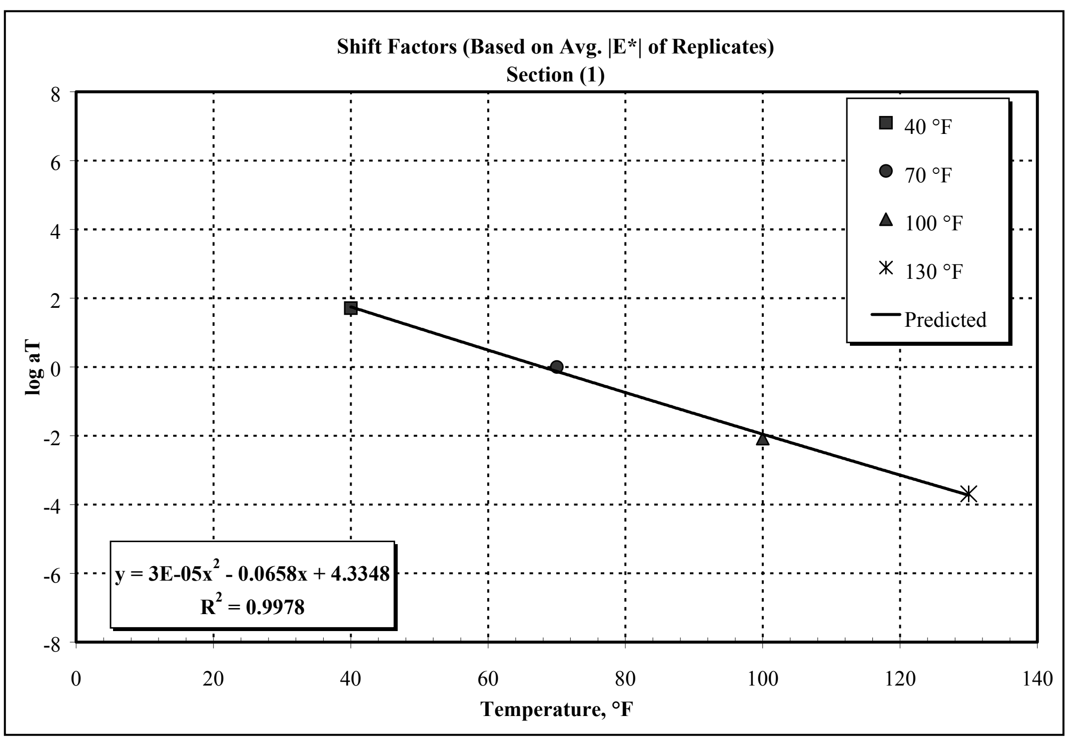

Figure B2. Dynamic Modulus Shift Factors for Section 1.

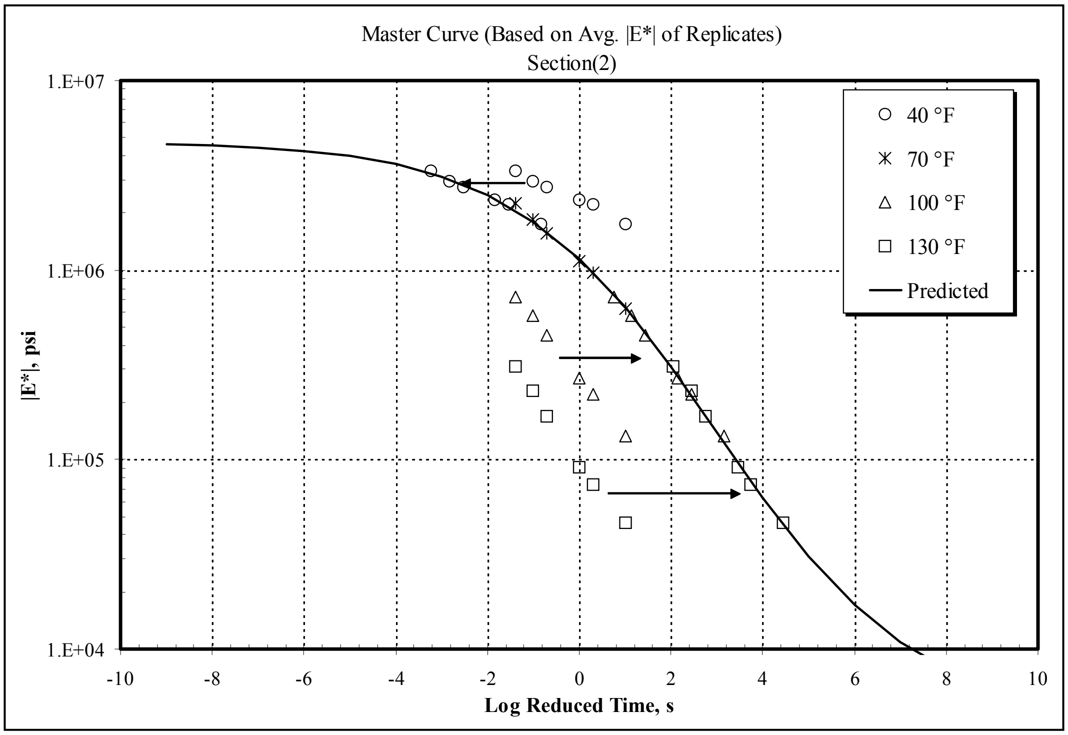

Figure B3. Dynamic Modulus Master Curve for Section 2.

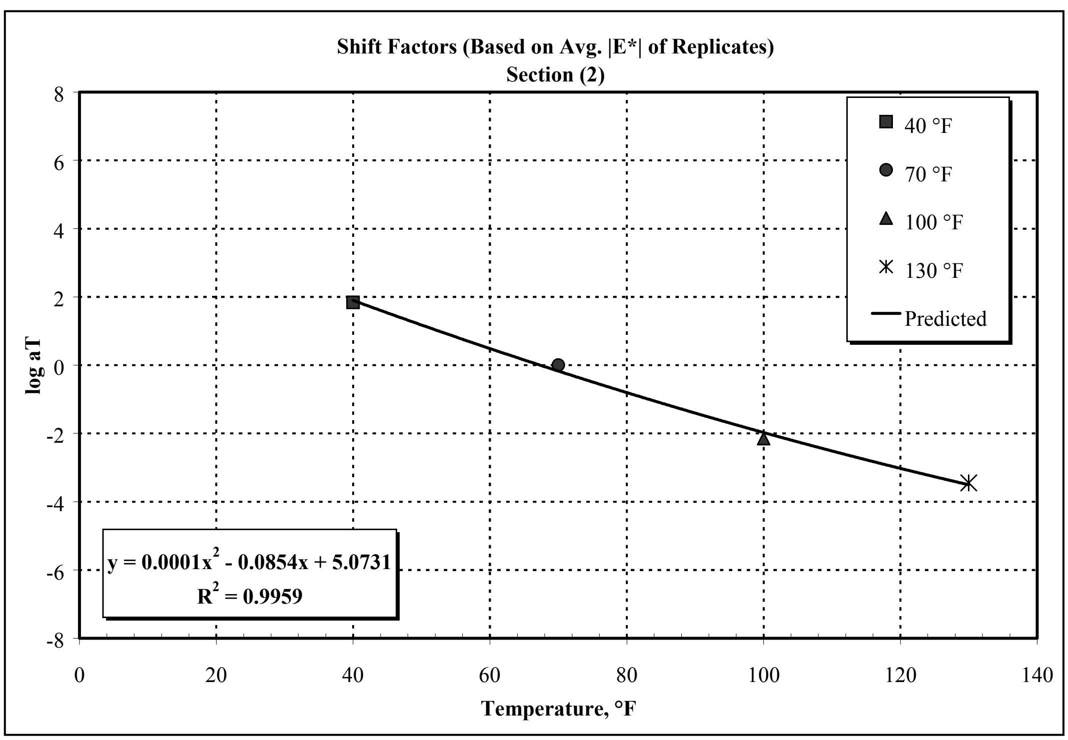

Figure B4. Dynamic Modulus Shift Factors for Section 2.

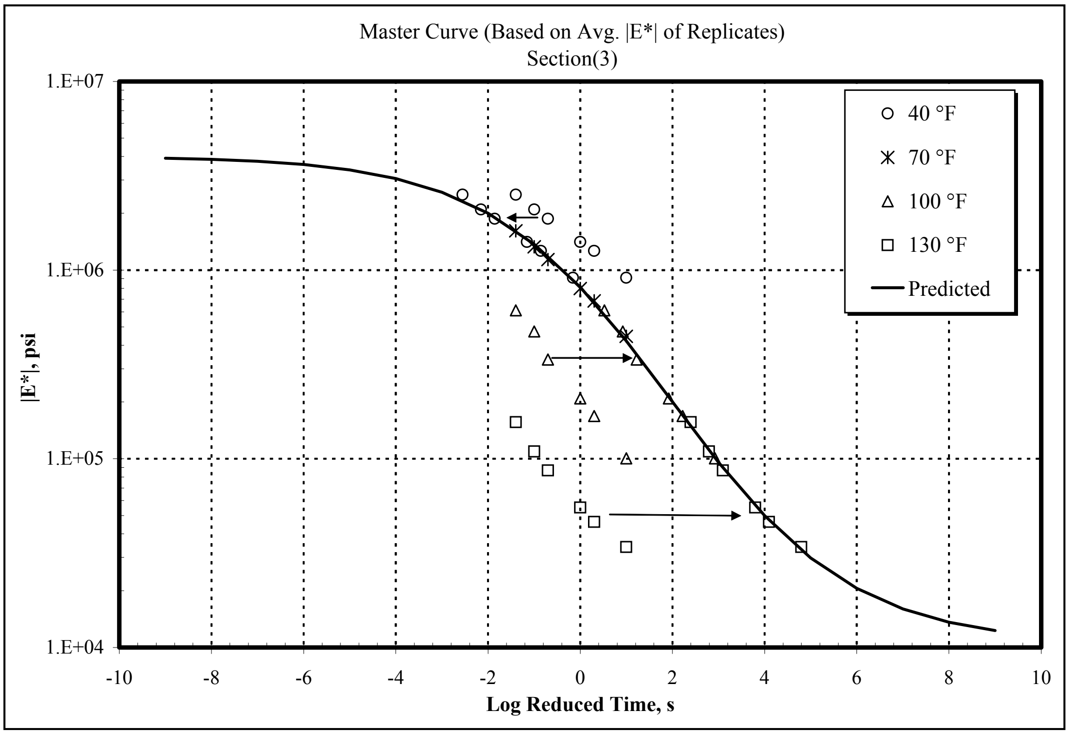

Figure B5. Dynamic Modulus Master Curve for Section 3.

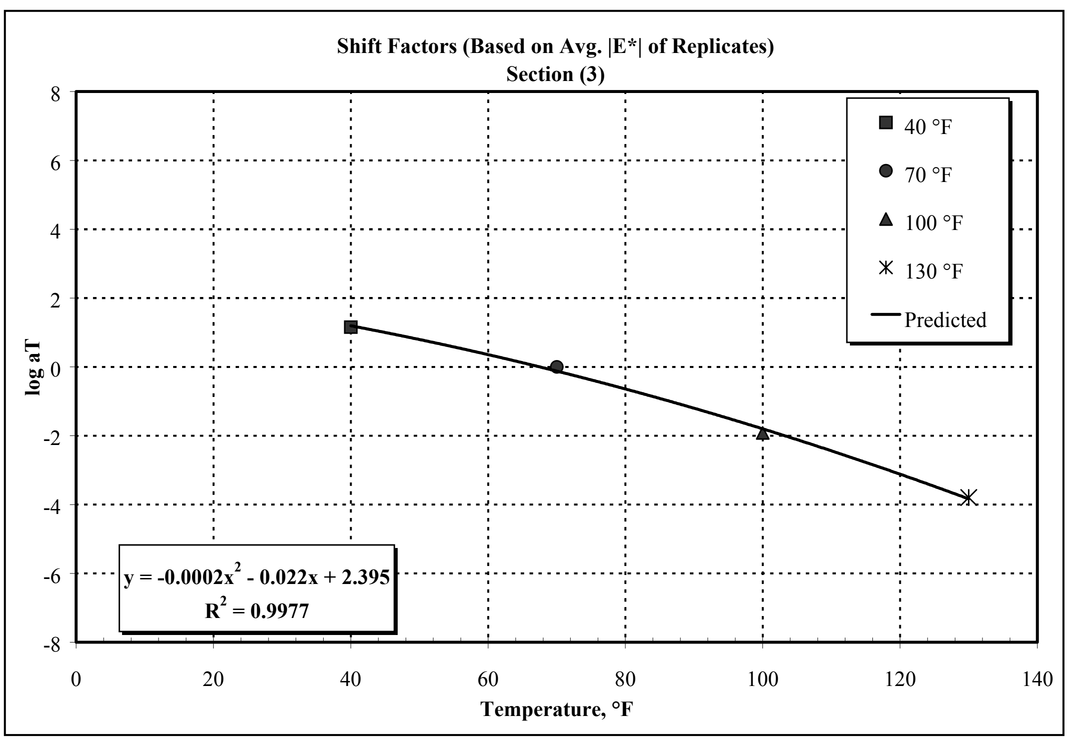

Figure B6. Dynamic Modulus Shift Factors for Section 3.

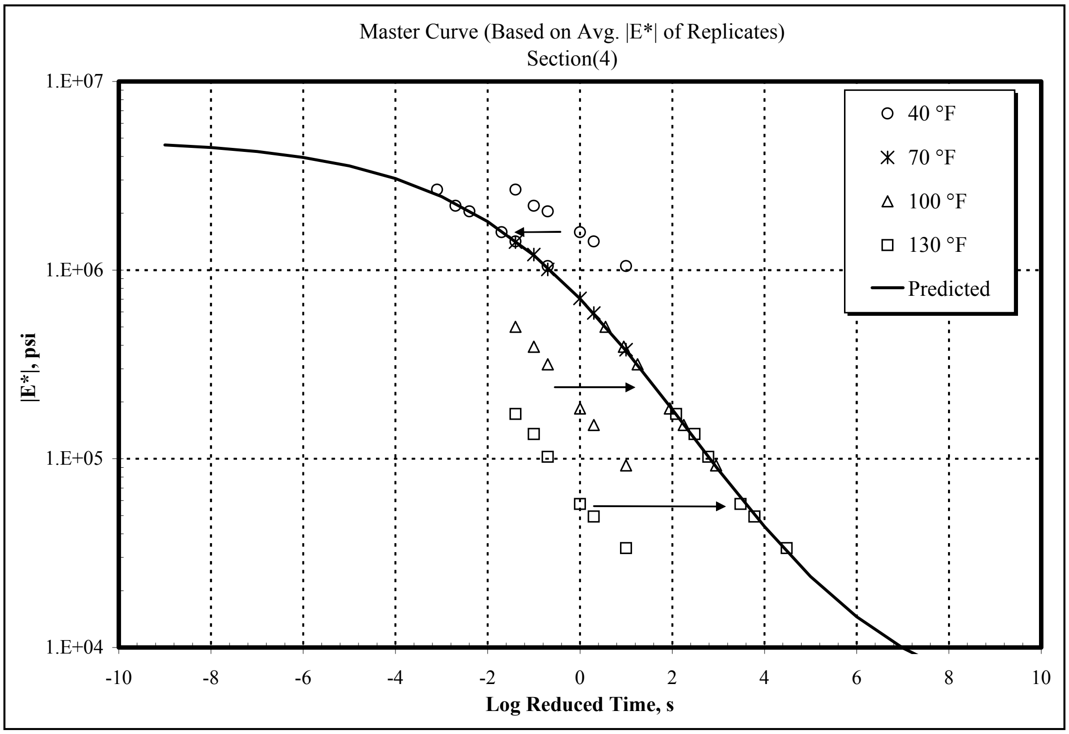

Figure B7. Dynamic Modulus Master Curve for Section 4.

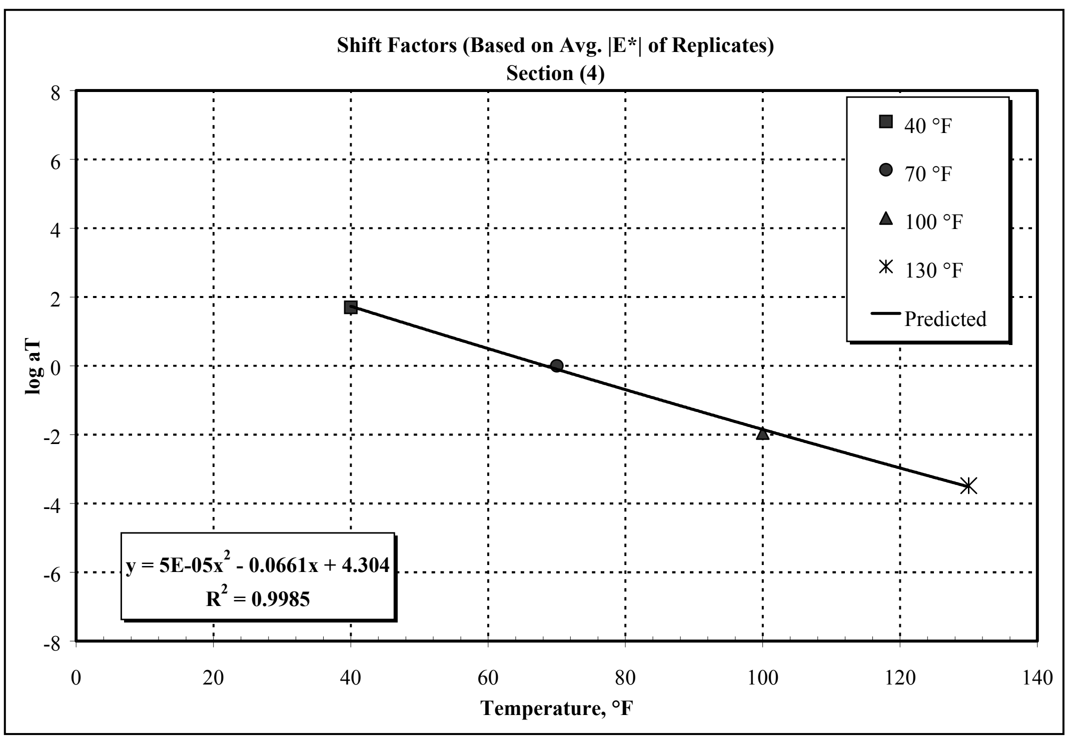

Figure B8. Dynamic Modulus Shift Factors for Section 4.

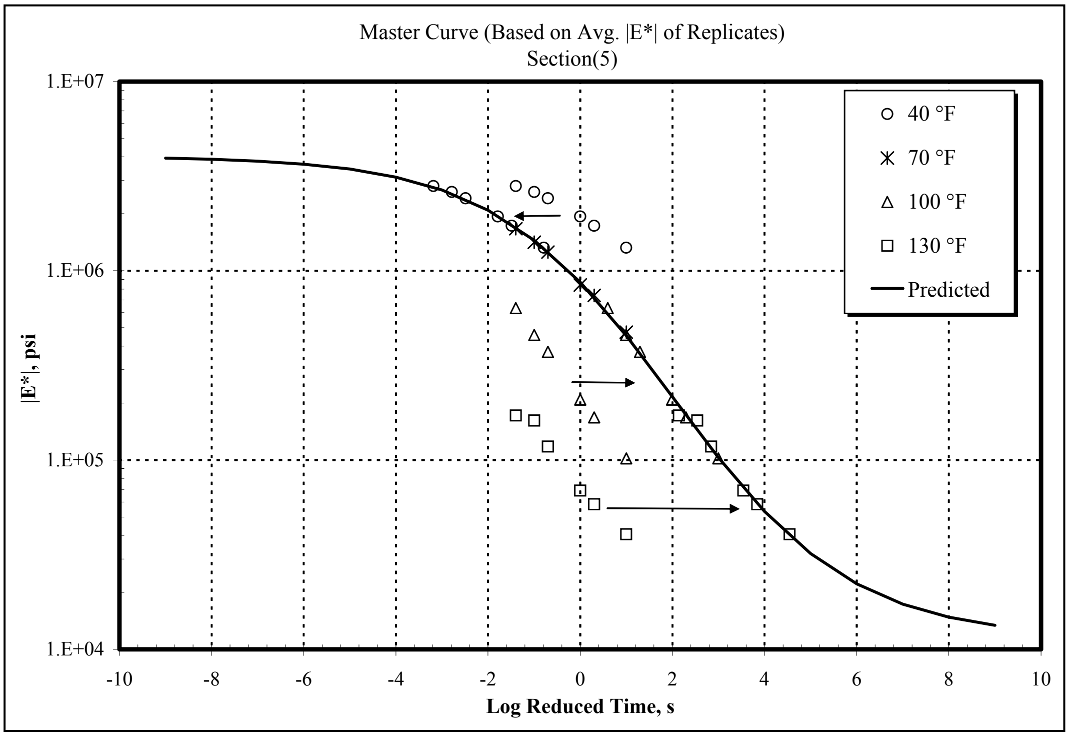

Figure B9. Dynamic Modulus Master Curve for Section 5.

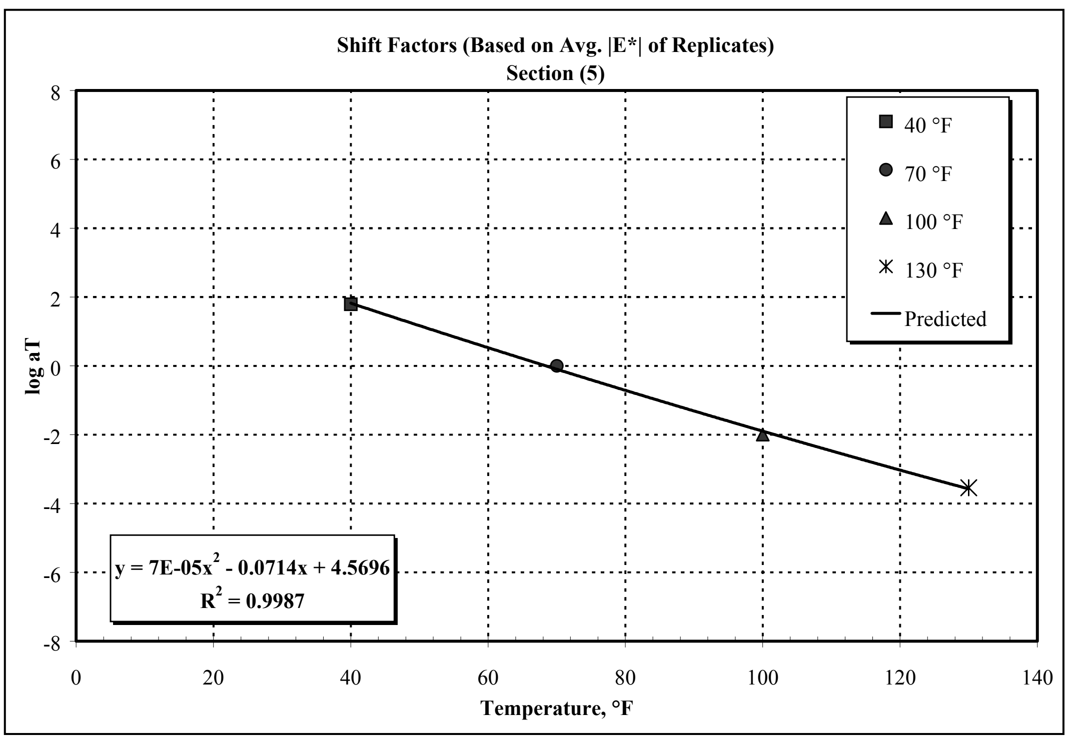

Figure B10. Dynamic Modulus Shift Factors for Section 5.

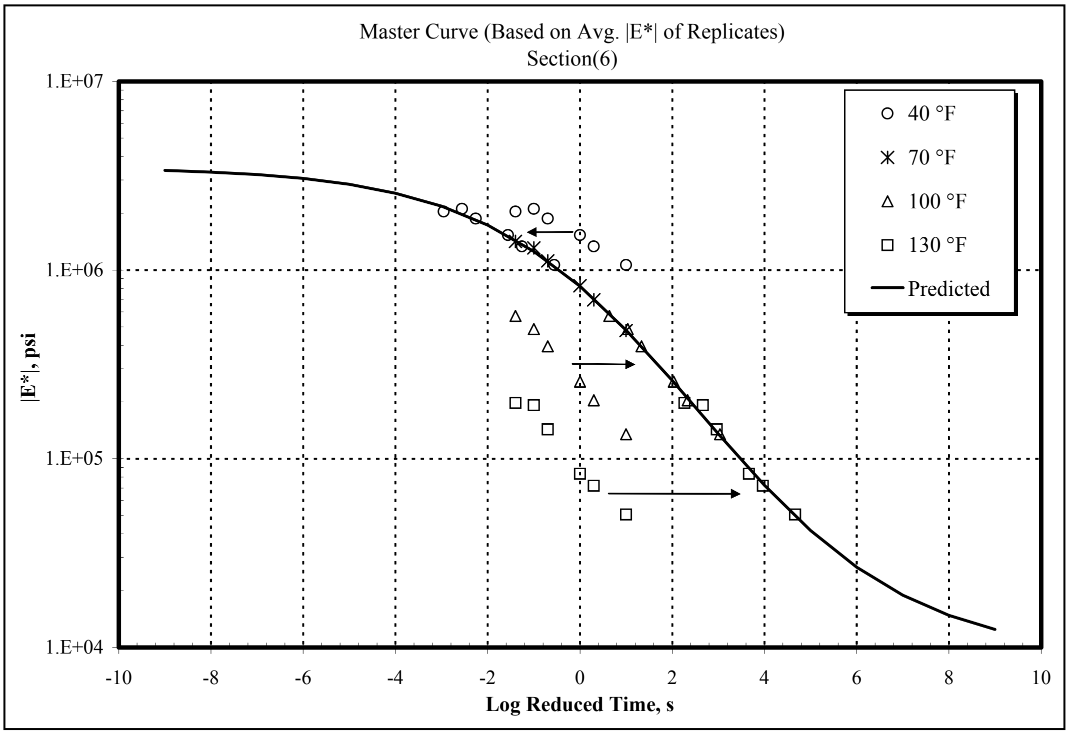

Figure B11. Dynamic Modulus Master Curve for Section 6.

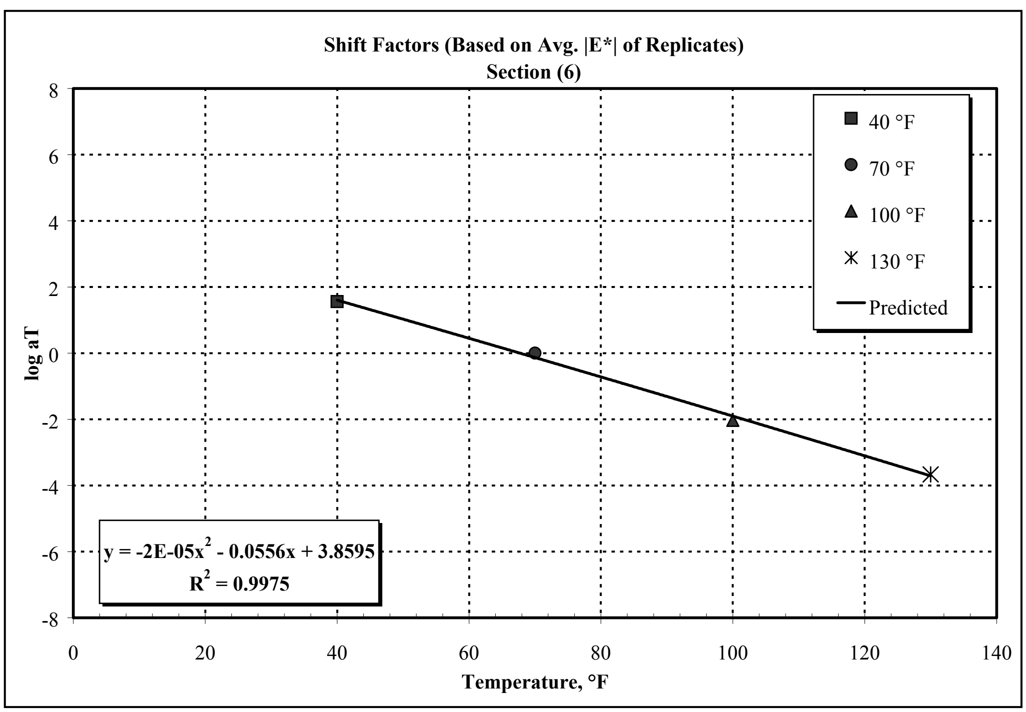

Figure B12. Dynamic Modulus Shift Factors for Section 6.

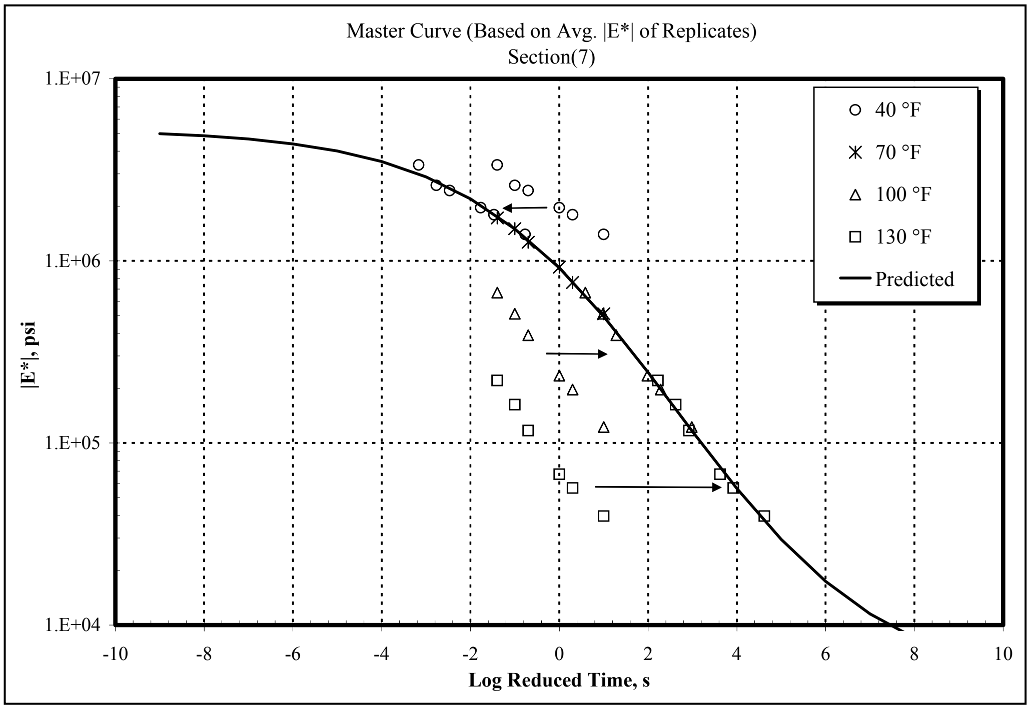

Figure B13. Dynamic Modulus Master Curve for Section 7.

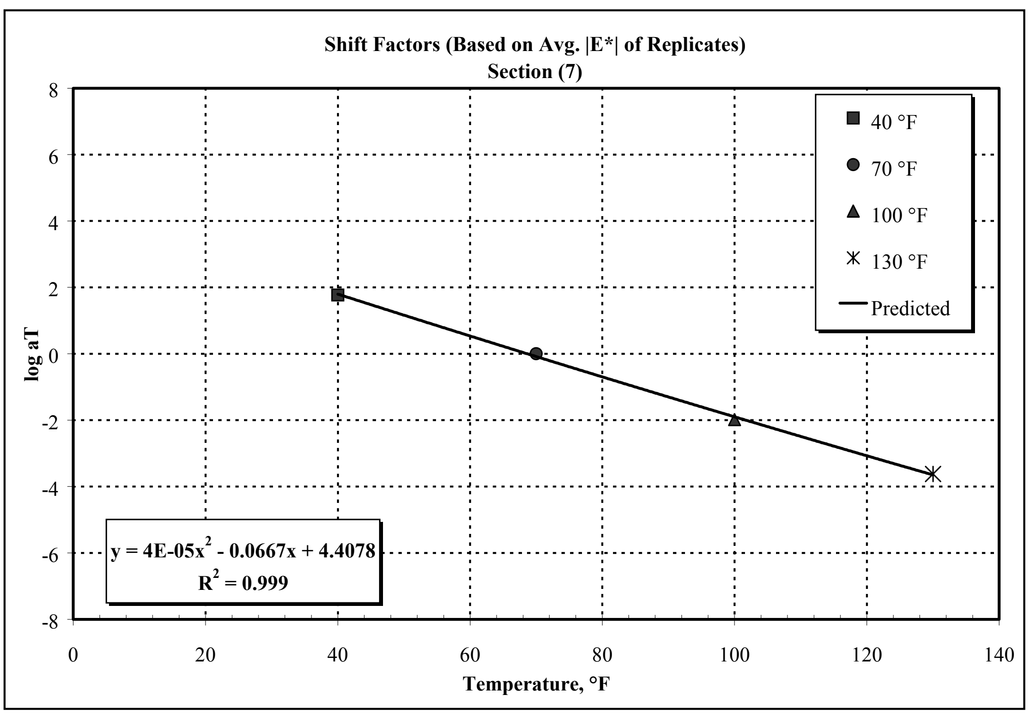

Figure B14. Dynamic Modulus Shift Factors for Section 7.

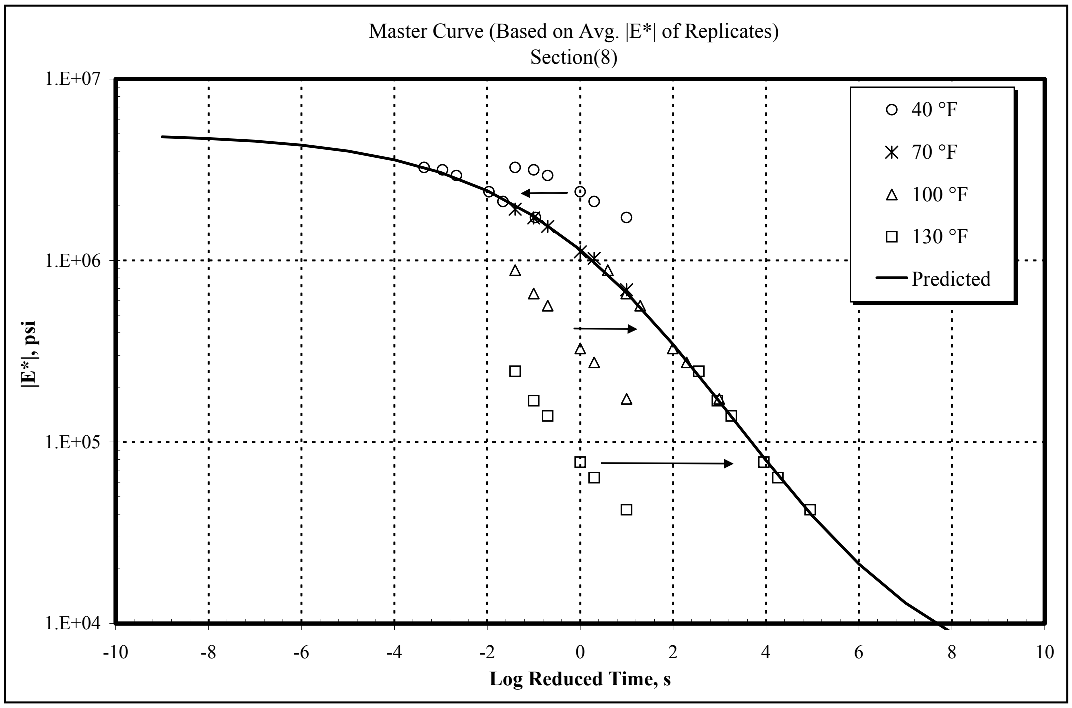

Figure B15. Dynamic Modulus Master Curve for Section 8.

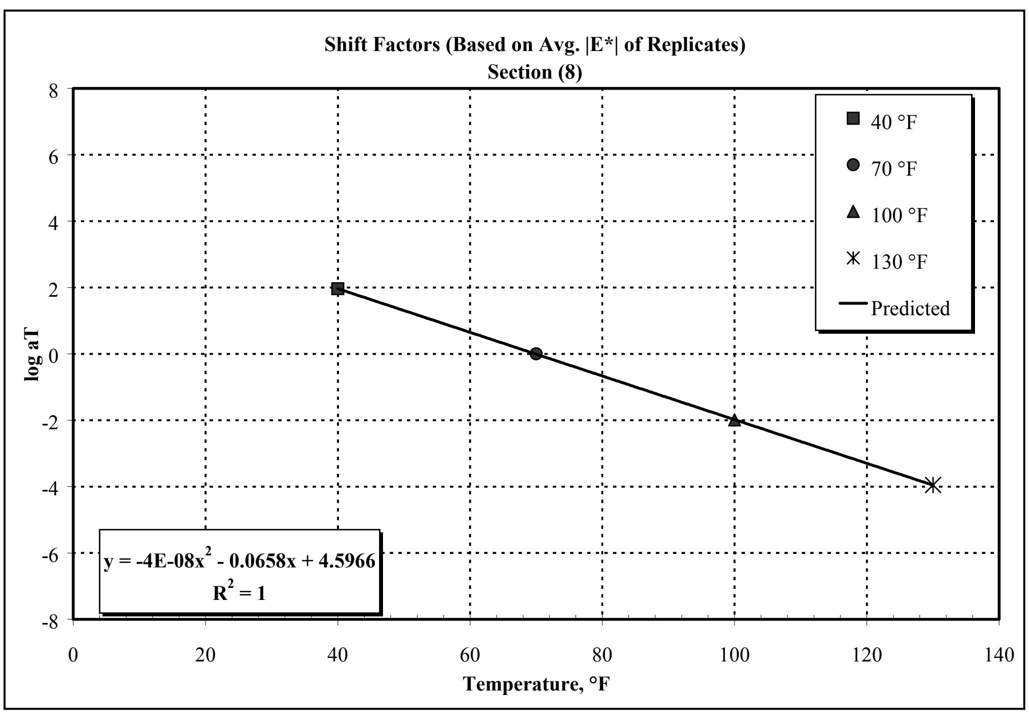

Figure B16. Dynamic Modulus Shift Factors for Section 8.

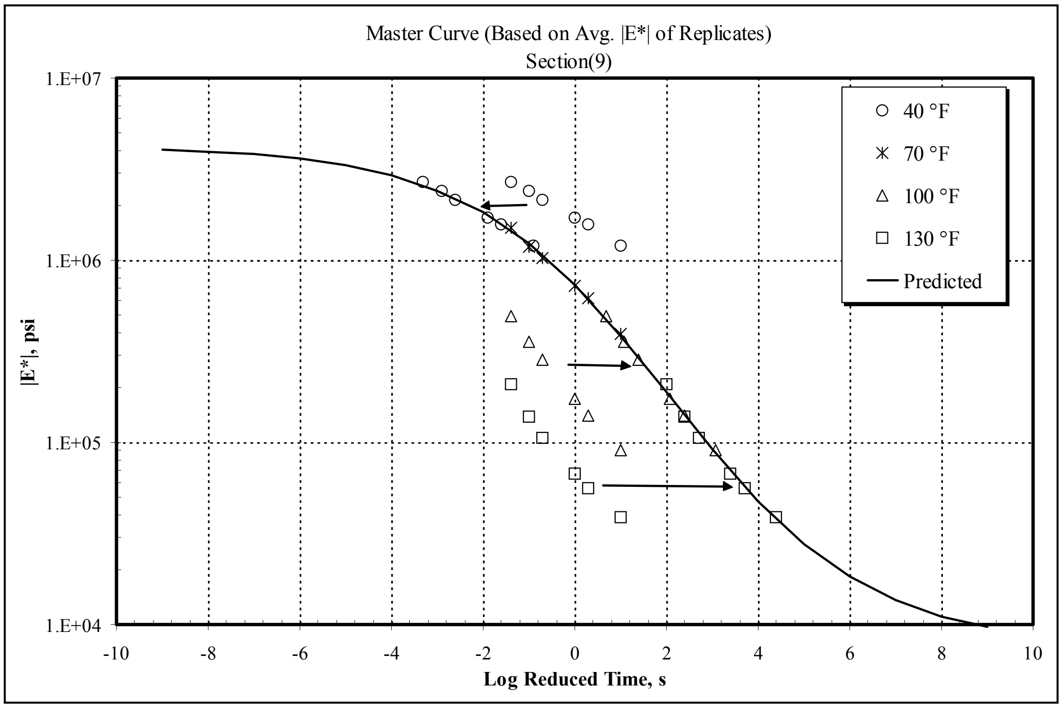

Figure B17. Dynamic Modulus Master Curve for Section 9.

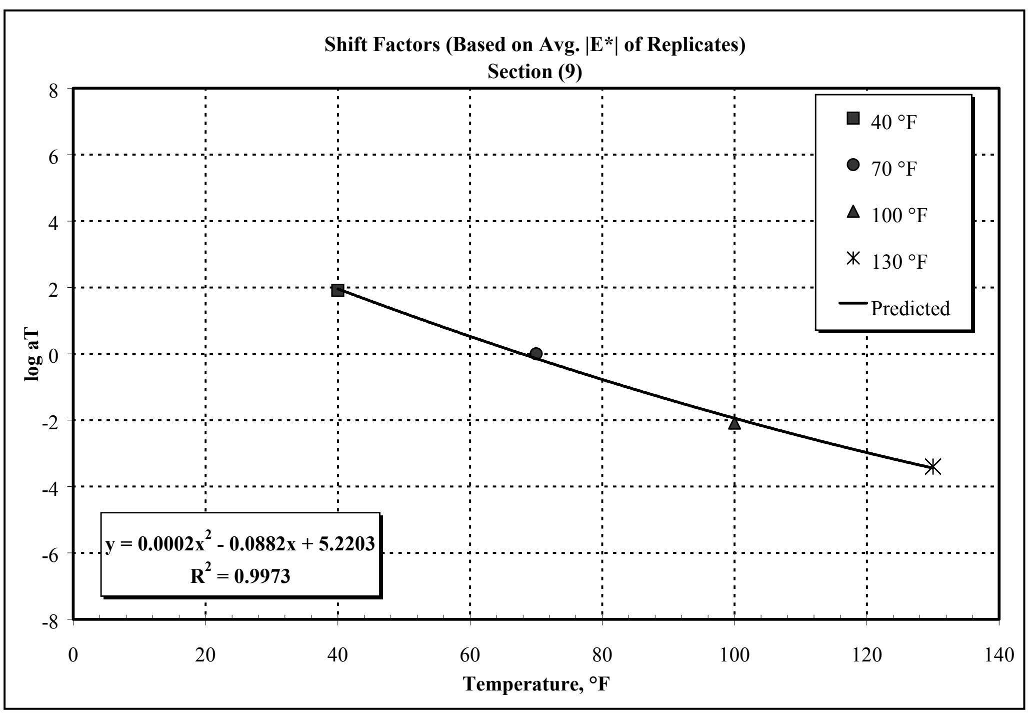

Figure B18. Dynamic Modulus Shift Factors for Section 9.

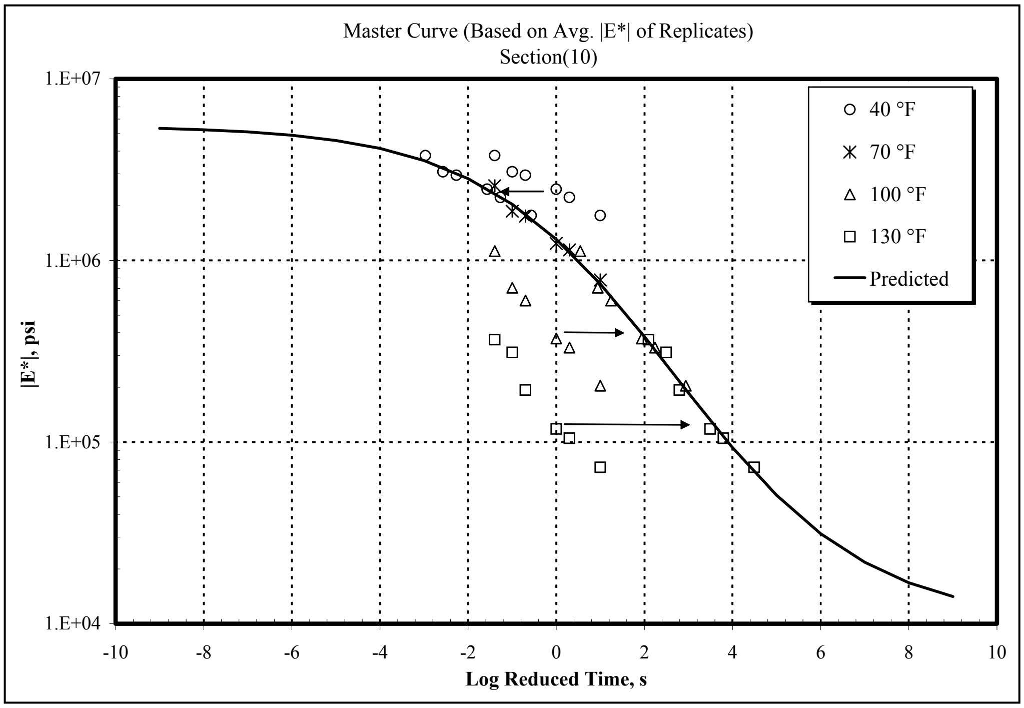

Figure B19. Dynamic Modulus Master Curve for Section 10.

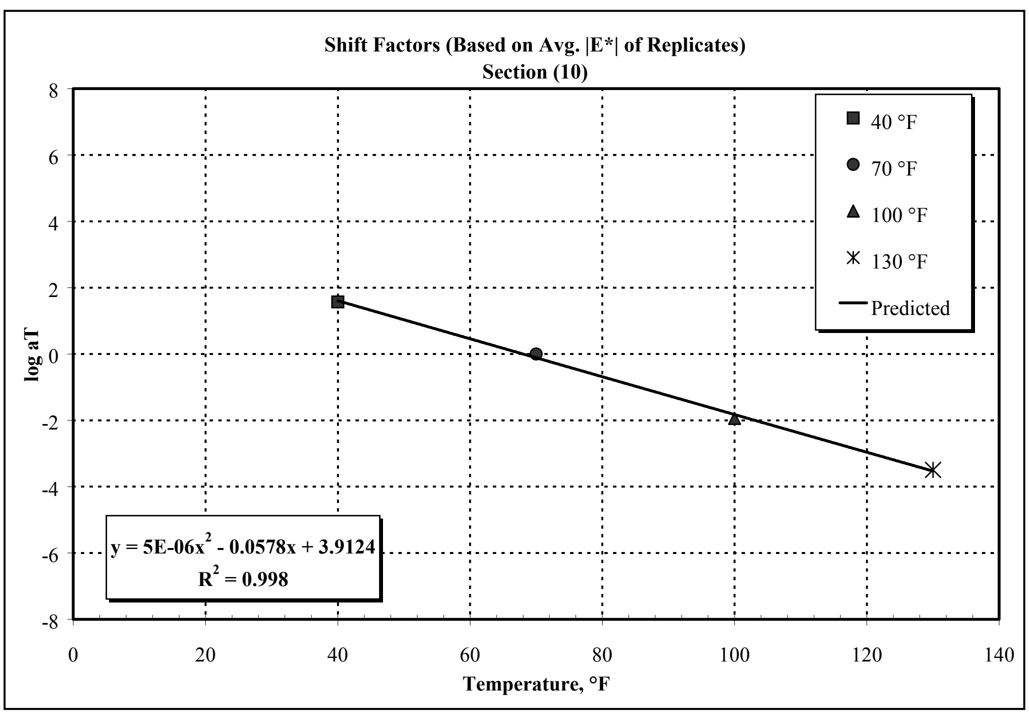

Figure B20. Dynamic Modulus Shift Factors for Section 10.

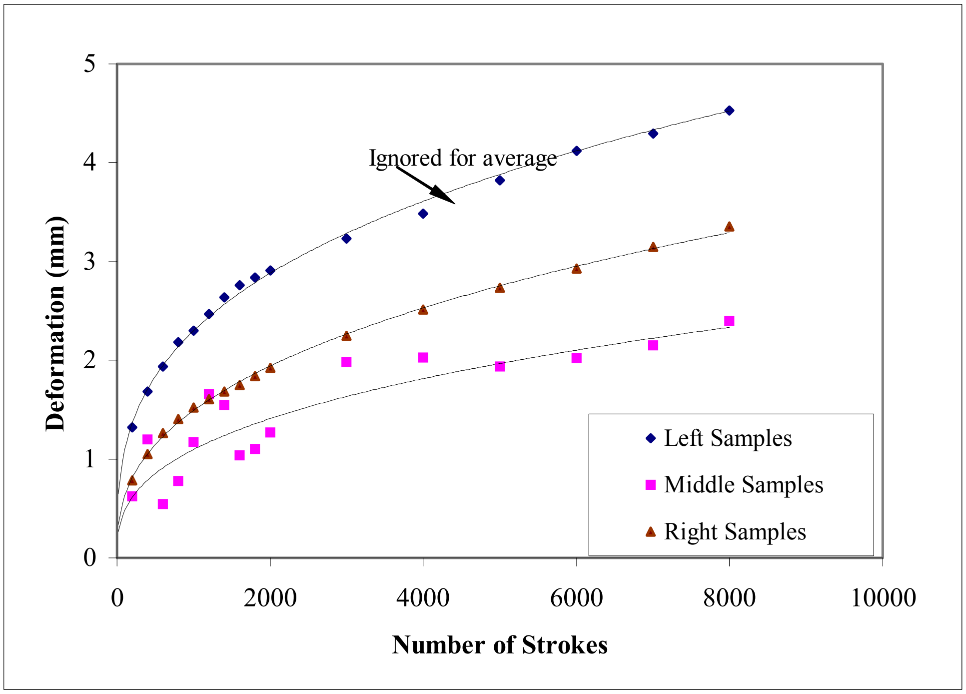

Figure B21. Section 1 APA Rut Test on Field Cores.

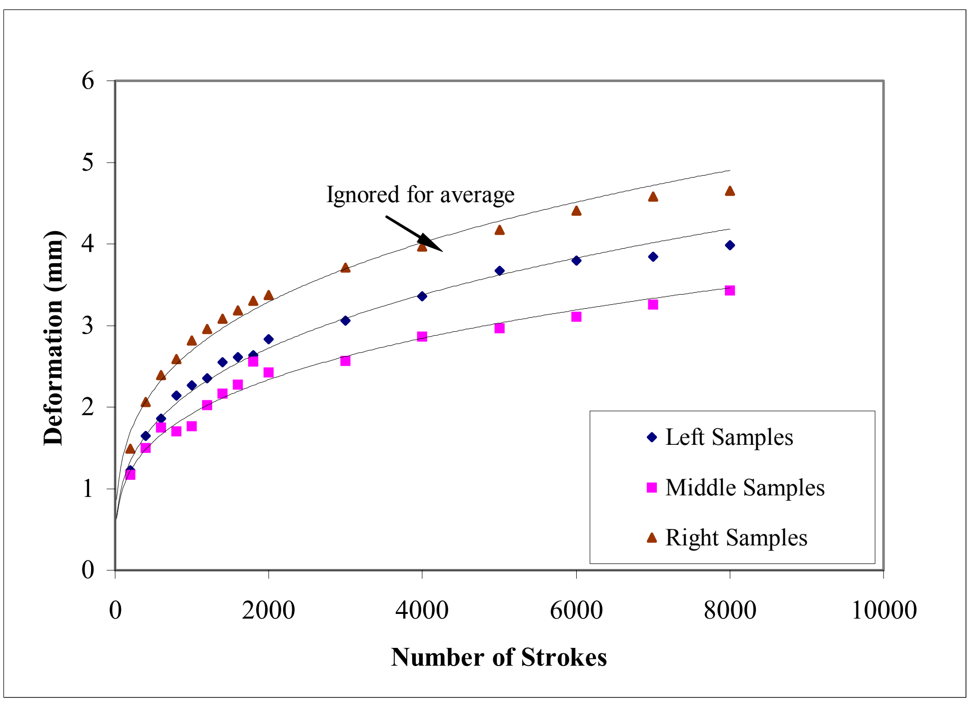

Figure B22. Section 2 APA Rut Test on Field Cores.

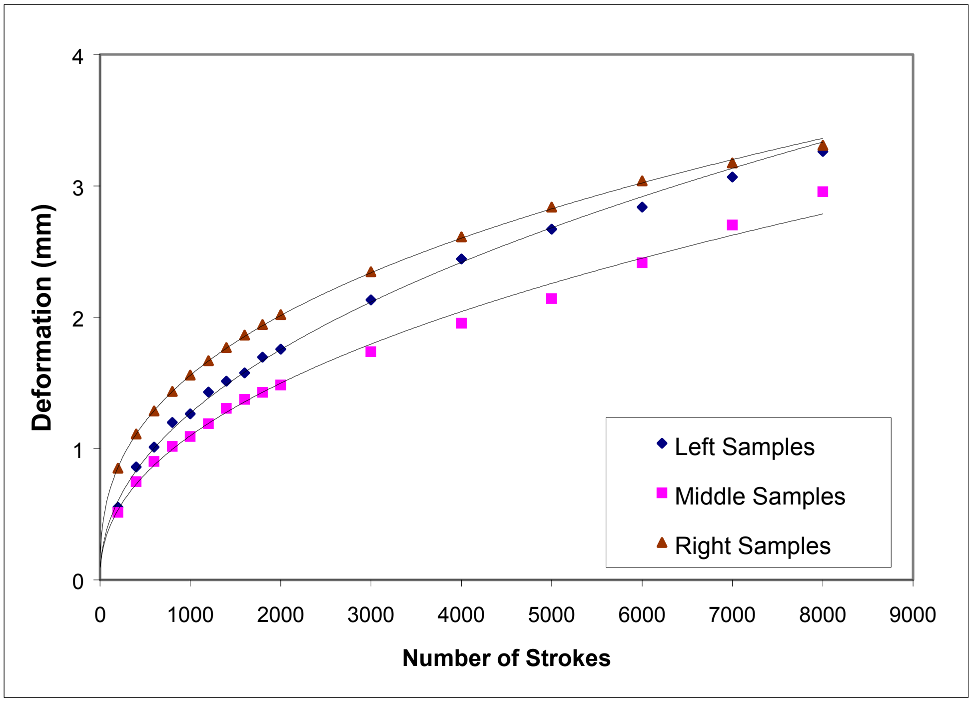

Figure B23. Section 3 APA Rut Test on Field Cores.

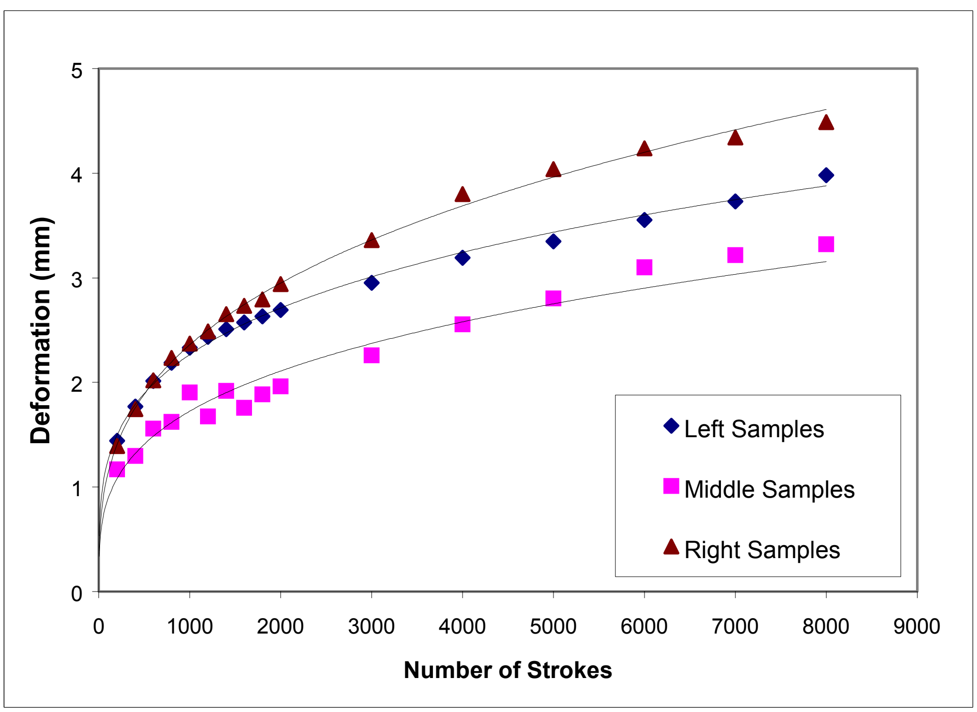

Figure B24. Section 4 APA Rut Test on Field Cores.

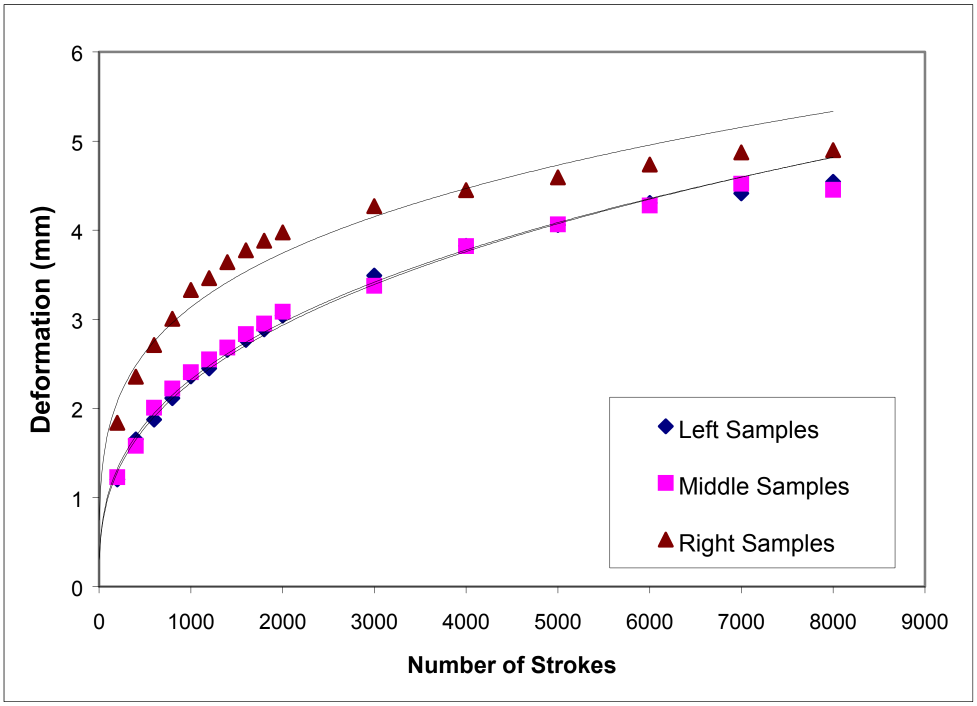

Figure B25. Section 5 APA Rut Test on Field Cores.

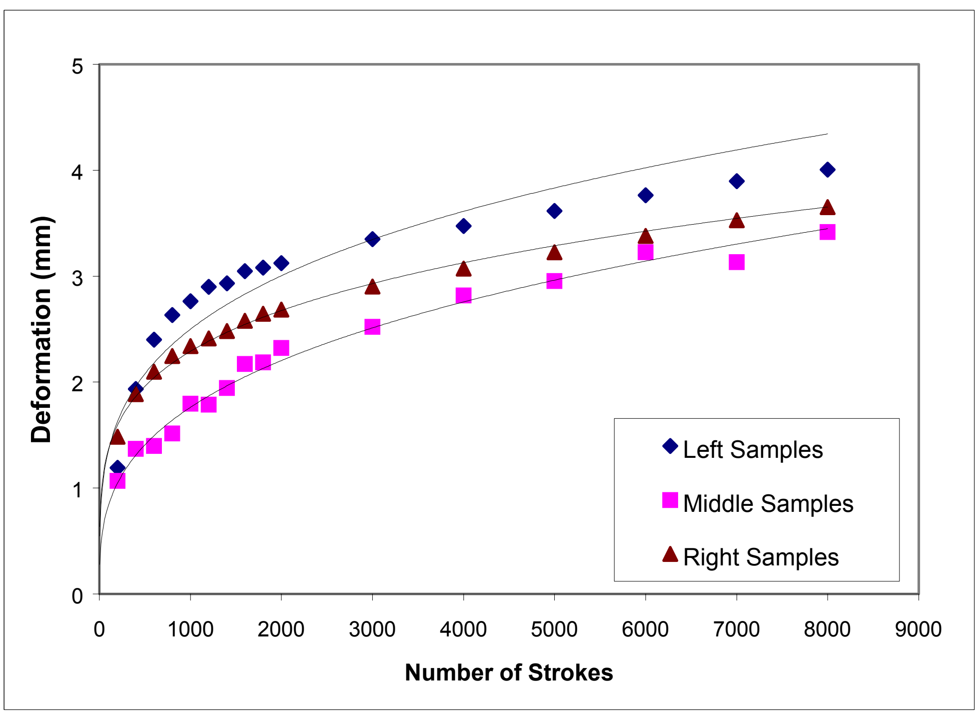

Figure B26. Section 6 APA Rut Test on Field Cores.

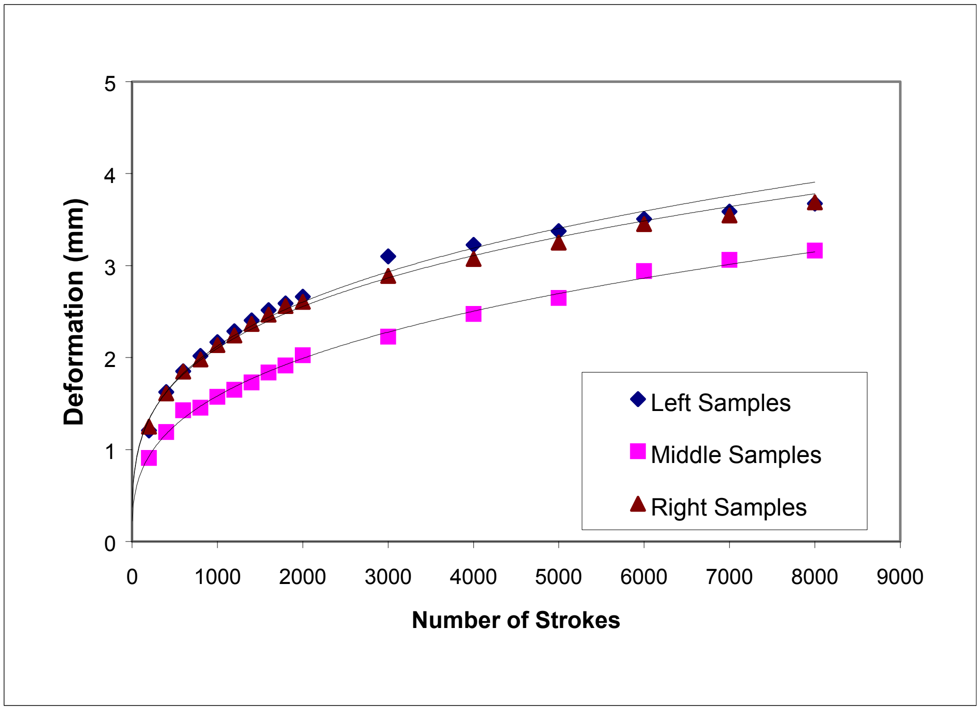

Figure B27. Section 7 APA Rut Test on Field Cores.

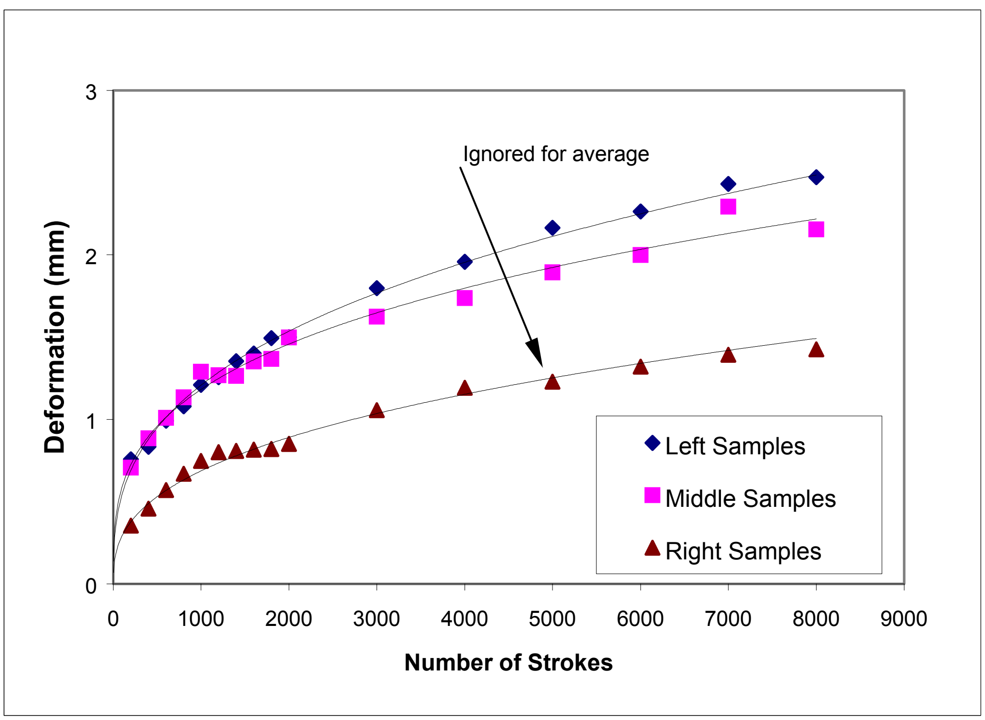

Figure B28. Section 8 APA Rut Test on Field Cores.

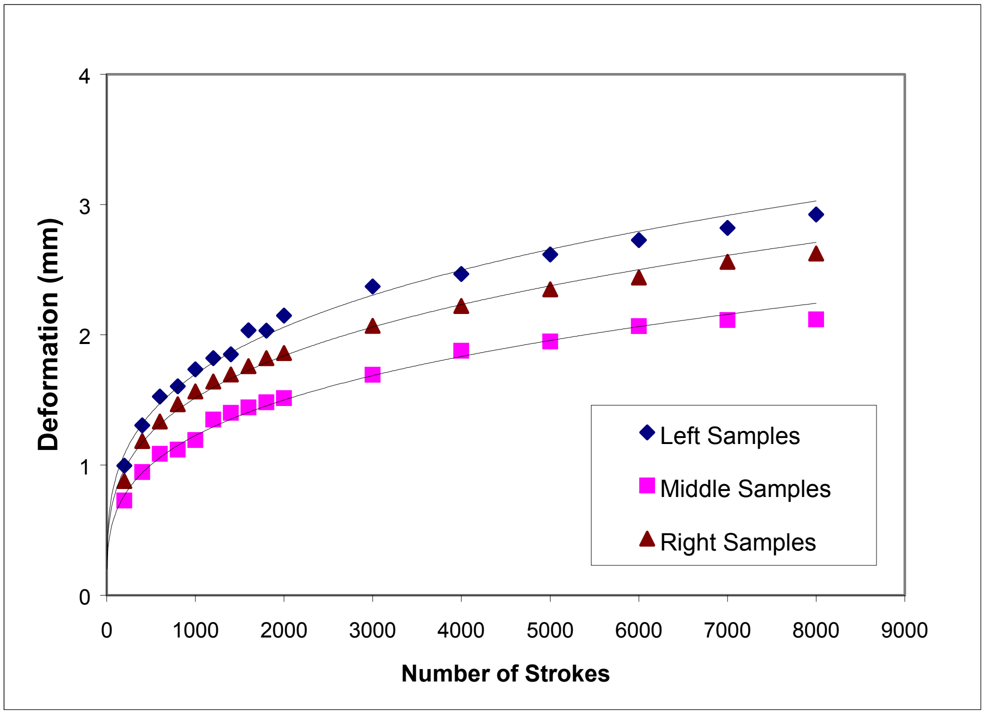

Figure B29. Section 9 APA Rut Test on Field Cores.

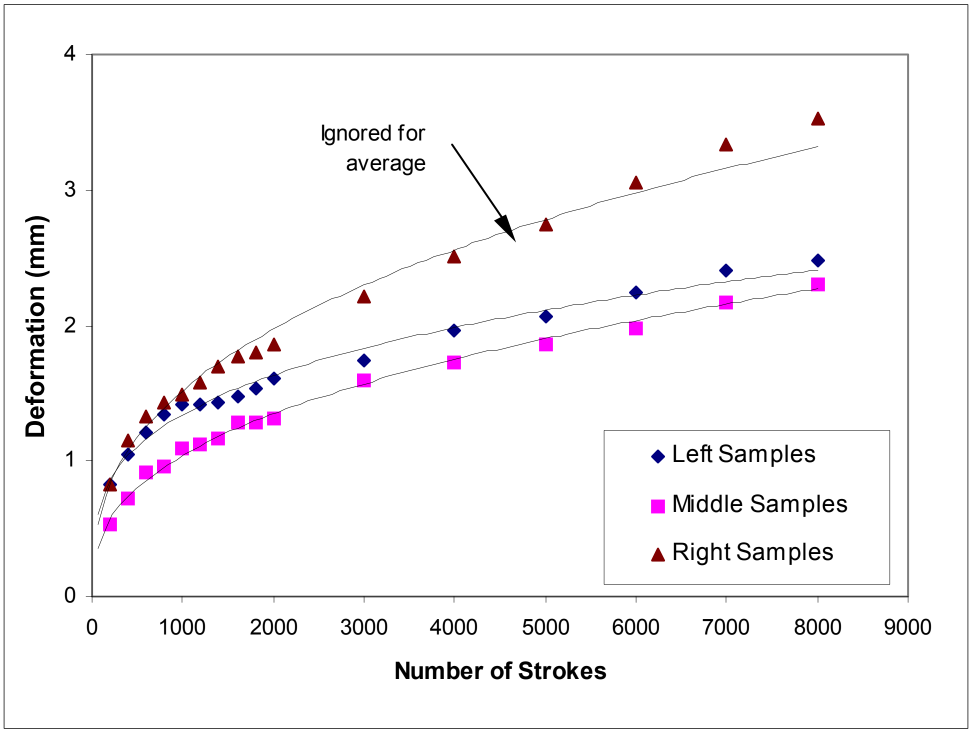

Figure B30. Section 1 APA Rut Test on Lab Molded Specimens.

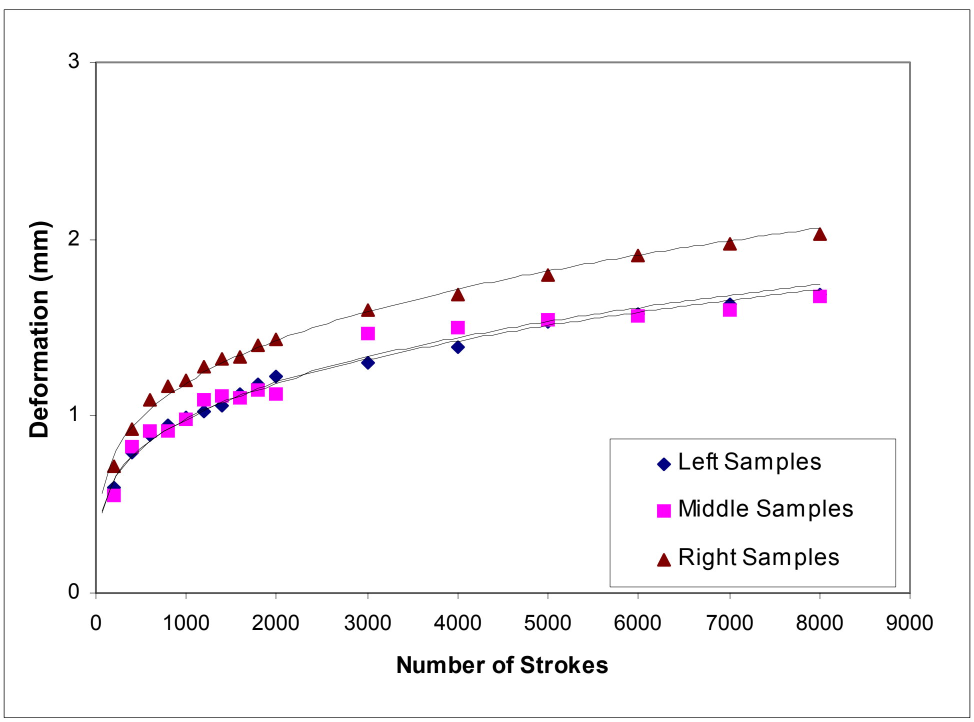

Figure B31. Section 2 APA Rut Test on Lab Molded Specimens.

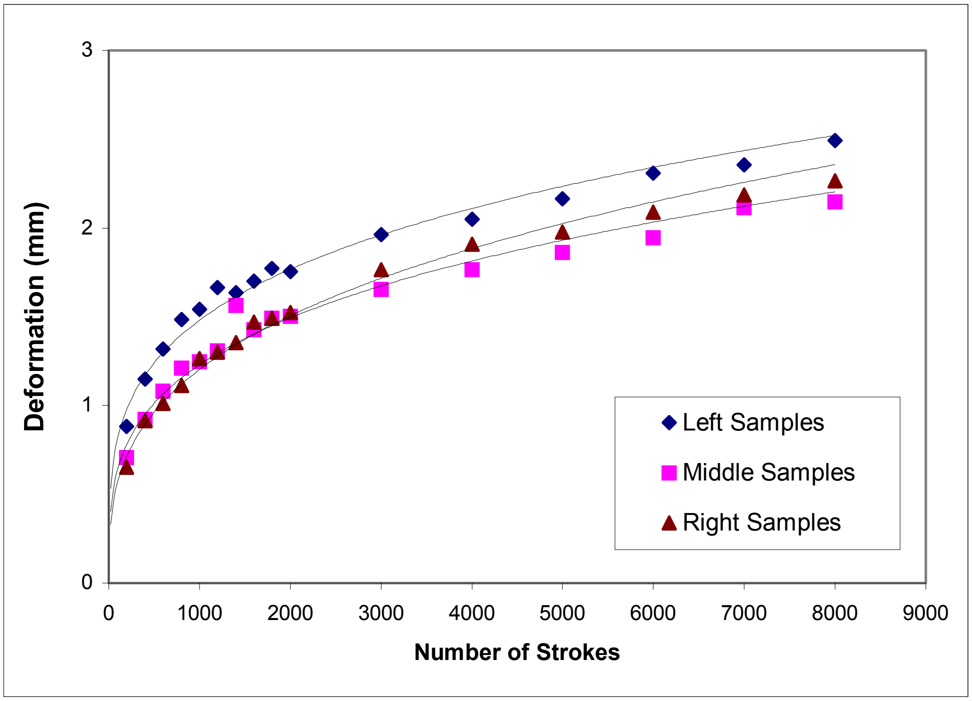

Figure B32. Section 3 APA Rut Test on Lab Molded Specimens.

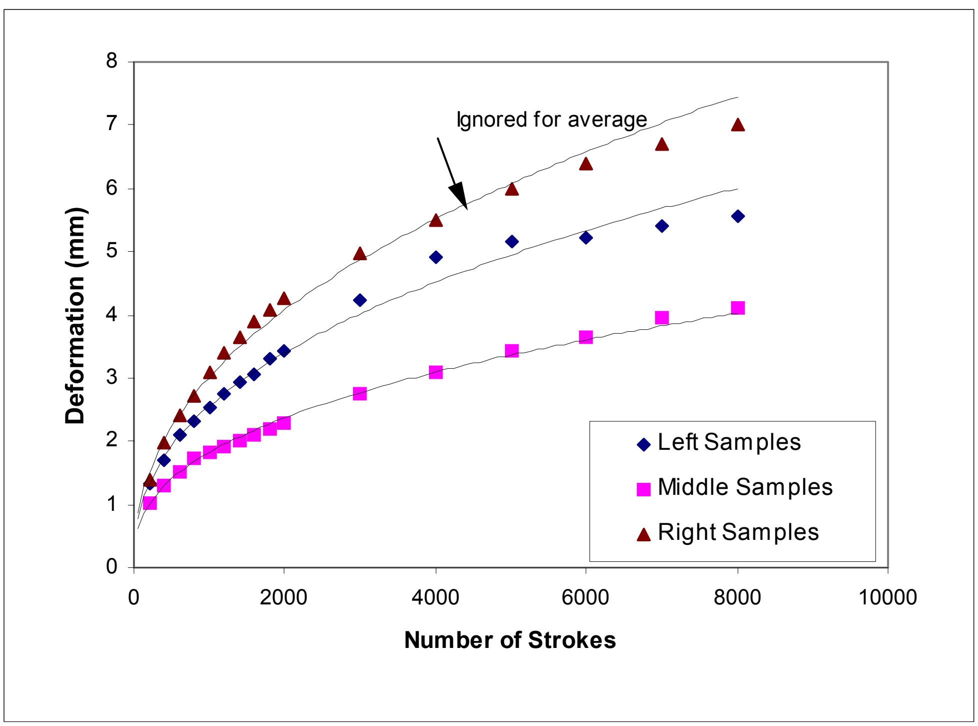

Figure B33. Section 4 APA Rut Test on Lab Molded Specimens.

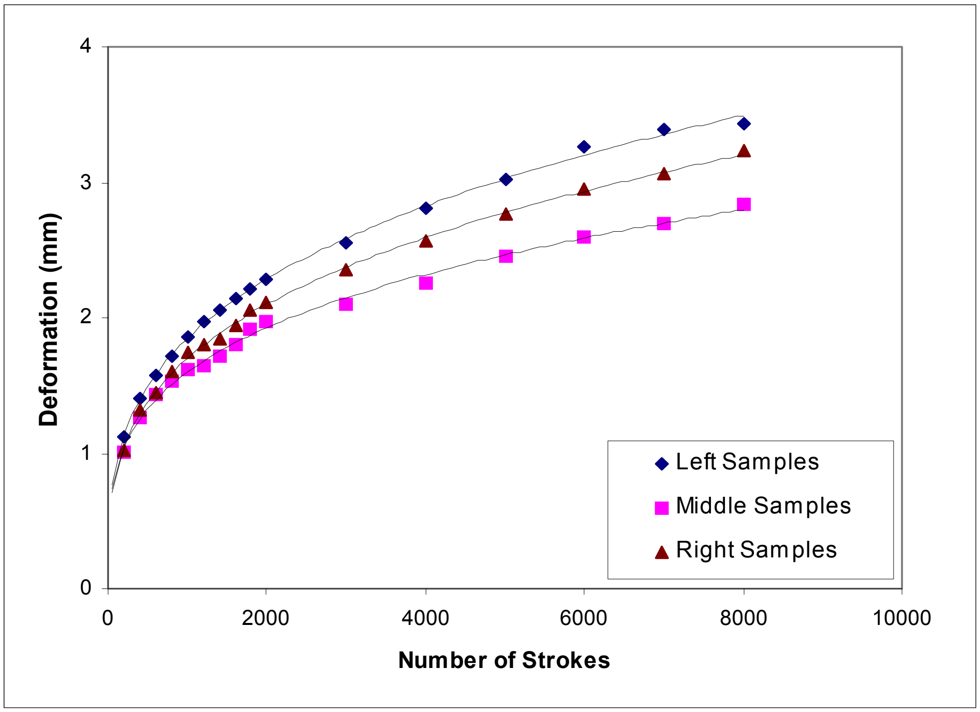

Figure B34. Section 5 APA Rut Test on Lab Molded Specimens.

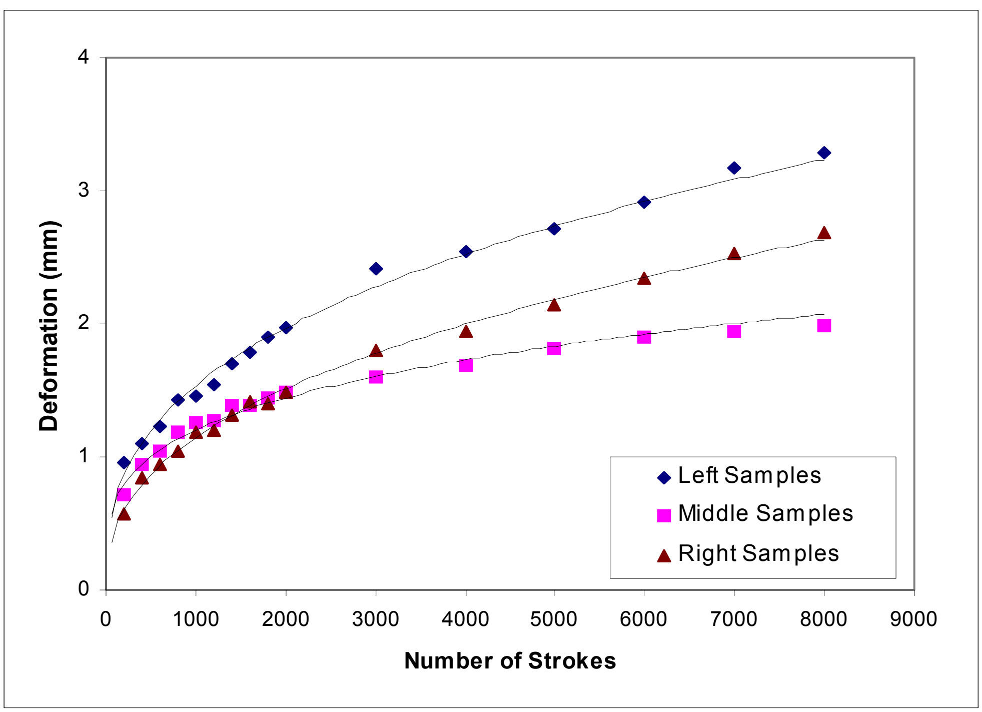

Figure B35. Section 6 APA Rut Test on Lab Molded Specimens.

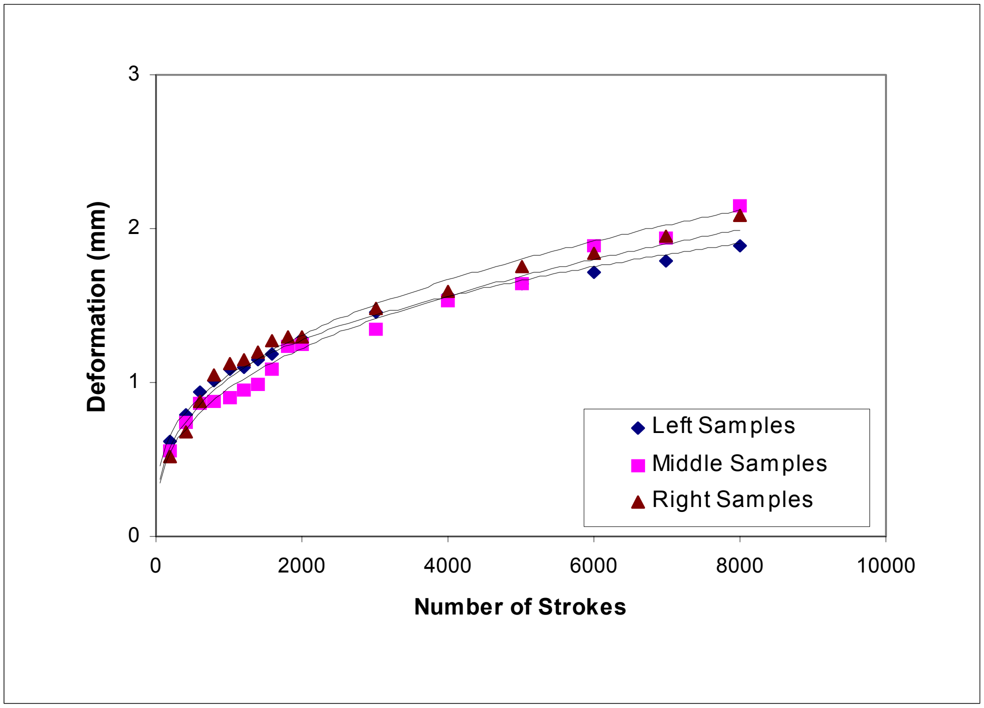

Figure B36. Section 7 APA Rut Test on Lab Molded Specimens.

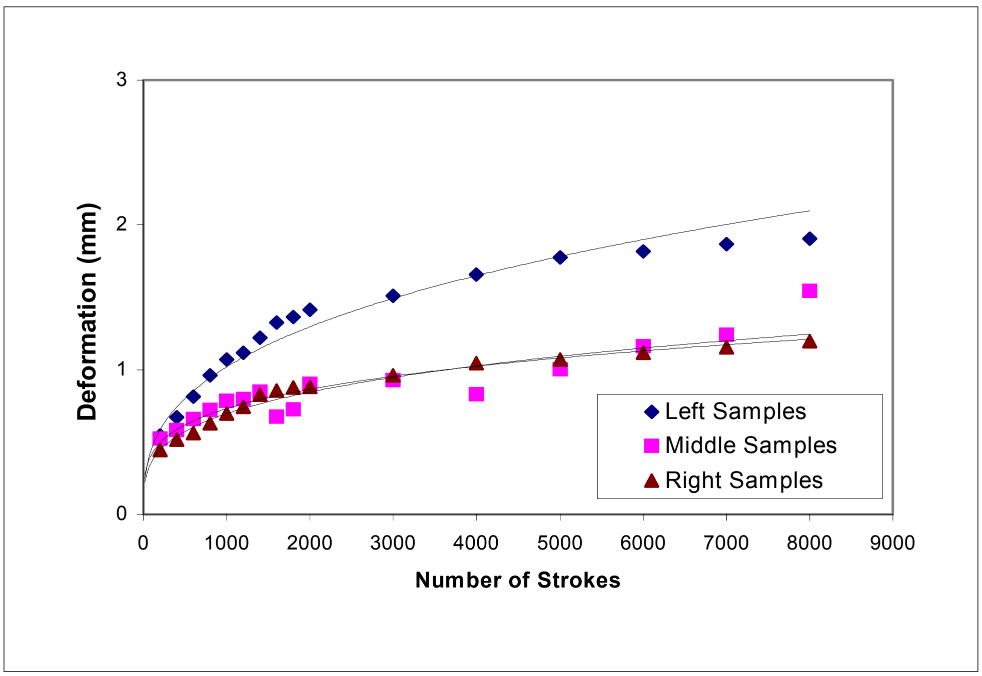

Figure B37. Section 8 APA Rut Test on Lab Molded Specimens.

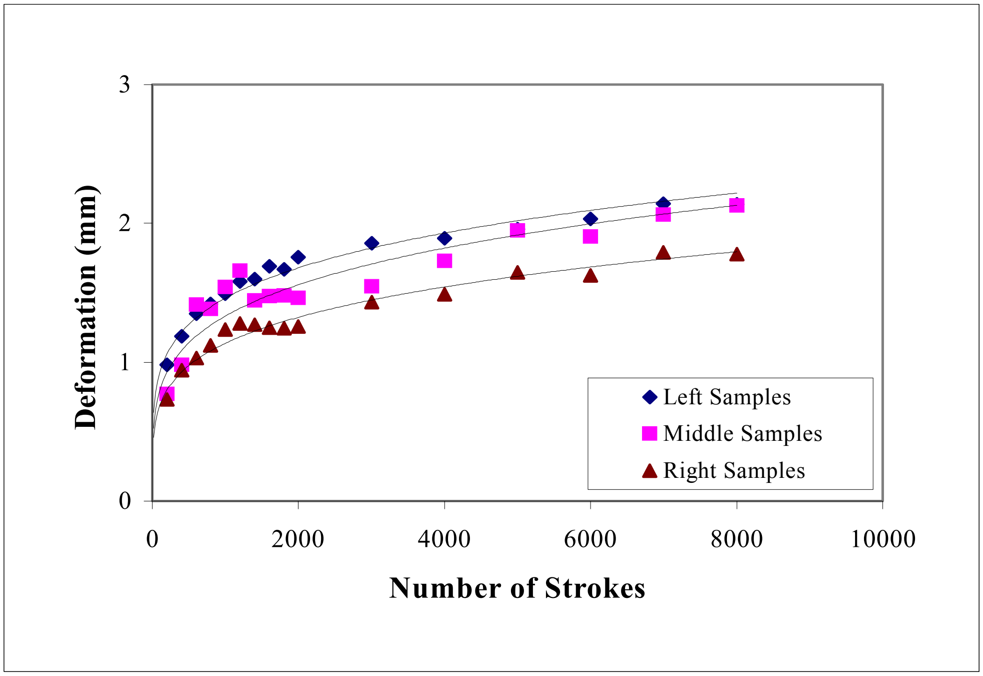

Figure B38. Section 9 APA Rut Test on Lab Molded Specimens.

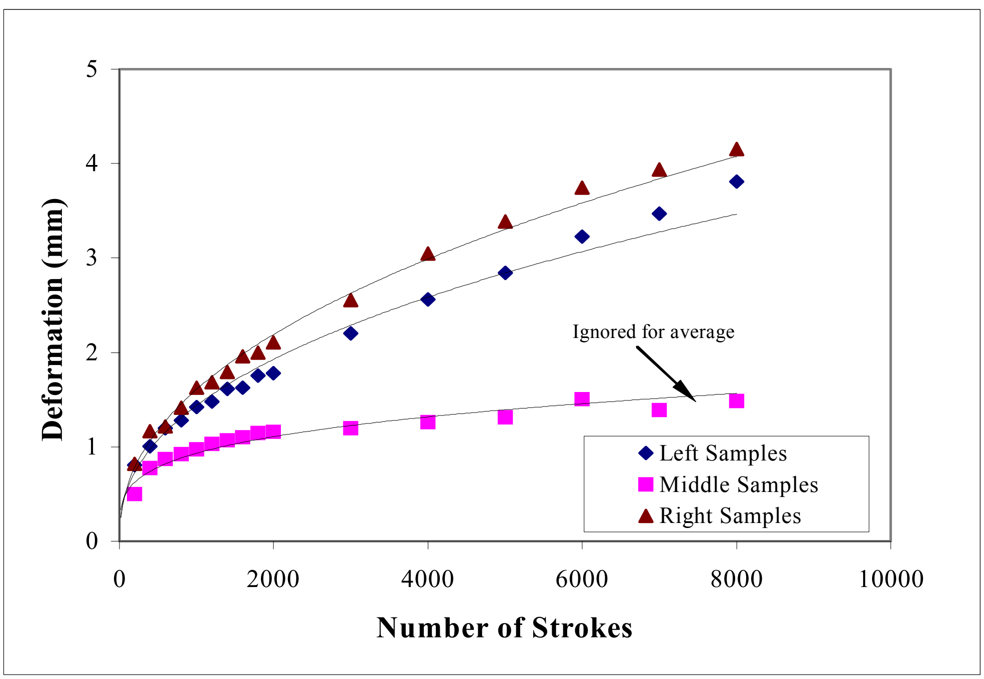

Figure B39. Section 10 APA Rut Test on Lab Molded Specimens.

APPENDIX C:
TEST RESULTS FROM OTHER AGENCIES

Table C1. Comparison of Superpave Design and Extracted Gradation (TxDOT).

Sieve Size	Spec. Req.	Section 1 (% passing)			Section 2 (% passing)			Section 3 (% passing)		
		Design	Extract	Diff.	Design	Extract	Diff.	Design	Extract	Diff.
19.00	100	100.0	100.0	0.0	100.0	--	--	100.0	100.0	0.0
12.50	90-100	92.0	94.4	2.4	92.1	--	--	93.7	96.7	4.0
9.50		84.8	86.0	1.2	79.4	--	--	81.7	81.8	0.1
4.75		52.4	56.3	3.9	49.0	--	--	45.5	51.7	6.2
2.36	25-58	30.9	32.3	1.4	29.2	--	--	31.4	35.0	3.6
1.18	10-25	20.4	21.0	0.6	22.4	--	--	21.0	25.0	4.0
0.60	3-13	13.9	14.6	0.7	18.9	--	--	17.7	19.7	2.0
0.30		8.8	11.0	2.2	14.9	--	--	11.8	14.9	3.1
0.15		4.5	8.3	3.8	10.2	--	--	8.2	11.0	2.8
0.075	2-10	3.2	6.5	3.3	6.5	--	--	5.6	8.2	2.6

-- data not available

Table C2. Comparison of CMHB Design and Extracted Gradation (TxDOT).

Sieve Size	Spec. Req.	Section 4 (% passing)			Section 5 (% passing)			Section 6 (% passing)		
		Actual	Extract	Diff.	Actual	Extract	Diff.	Actual	Extract	Diff.
7/8 in	98-100	100.0	100.0	0.0	100.0	100.0	0.0	100.0	100.0	0.0
5/8 in	95-100	99.7	100.0	0.3	100.0	100.0	0.0	99.6	100.0	0.4
3/8 in	50-70	64.5	74.3	9.8	65.4	66.2	0.8	65.6	57.8	-7.8
#4	30-45	34.3	41.8	7.5	38.0	33.8	-4.2	34.2	34.9	0.7
#10	15-25	21.8	20.8	-1.0	24.0	21.3	-2.7	24.0	21.5	-2.5
#40	6-20	16.2	15.1	-1.1	16.4	15.9	-0.5	14.5	12.5	-2.0
#80	6-18	9.8	10.0	0.2	10.7	12.0	1.3	9.1	8.9	-0.2
#200	5-8	6.4	6.2	-0.2	6.4	7.1	0.7	5.9	5.9	0.0

Table C3. Comparison of Design and Extracted Gradation (TxDOT).

Sieve Size	Spec. Req.	Section 7 (% passing)			Section 8 (% passing)			Section 9 (% passing)		
		Actual	Extract	Diff.	Actual	Extract	Diff.	Actual	Extract	Diff.
7/8 in	98-100	100.0	100.0	0.0	100.0	100.0	0.0	100.0	100.0	0.0
5/8 in	95-100	99.8	99.0	-0.8	100.0	100.0	0.0	99.8	99.6	-0.2
3/8 in	70-85	79.1	82.2	3.1	75.8	77.5	1.7	80.7	81.3	0.6
#4	43-63	51.4	61.7	10.3	49.2	48.7	-0.5	46.2	54.4	8.2
#10	30-40	34.0	37.3	3.3	31.5	31.5	0.0	30.9	34.3	3.4
#40	10-25	17.9	18.9	1.0	18.2	19.3	1.1	15.6	17.5	1.9
#80	3-13	10.0	12.1	2.1	11.7	15.5	3.8	9.6	12.4	2.8
#200	1-6	5.3	7.5	2.2	5.8	8.7	2.9	5.8	8.9	3.1

Table C4. Comparison of Type B Mixture Design and Extracted Gradation (TxDOT).

Sieve Size	Spec. Req.	Section 10 (% passing)		
		Actual	Extract	Difference
7/8 in	95-100	100.0	100.0	0.0
5/8 in	75-95	90.1	94.5	3.4
3/8 in	60-80	79.4	85.1	5.7
#4	40-60	52.9	57.6	4.7
#10	27-40	31.9	32.9	1.0
#40	10-25	19.4	20.2	0.8
#80	3-13	9.8	12.1	2.3
#200	1-6	3.8	6.6	2.8

Table C5. Density of Compacted Specimen (TxDOT QA).

Section	Percent Density	Specification Limit		Asphalt Content (%) (Nuclear Gauge)
		Minimum	Maximum	
1	94.8%	95.0%	97.0%	4.6
2	--	95.0%	97.0%	--
3	95.6%	95.0%	97.0%	4.6
4	94.2%	95.0%	97.0%	4.5
5	96.2%	95.0%	97.0%	4.3
6	94.4%	95.0%	97.0%	4.3
7	95.1%	95.0%	97.0%	4.3
8	95.4%	95.0%	97.0%	4.3
9	94.8%	95.0%	97.0%	4.1
10	95.8%	95.0%	97.0%	3.4

-- data not availabe

Table C6. Location of Field Cores.

Section	Station	Direction and Lane	Location in Lane	Core Dia. (inch)	Thickness (inch)
1 + 10	1241+60	EB OL	Center	6	2
2 + 10	1294+00	WB OL	Center	4 & 6	2 1/2
3 + 10	1166+50	WB OL	Center	4 & 6	2 1/8
4 + 10	1250+30	EB OL	Center	6	1 7/8
5 + 10	1250+80	WB OL	Center	4 & 6	2 1/8
6 + 10	1160+00	EB OL	Center	6	2 1/8
7 + 10	1306+70	EB OL	Center	6	2 1/4
8 + 10	1194+00	WB OL	Center	4 & 6	2 1/4
9 + 10	1199+00	EB OL	Center	6	1 7/8

Table C7. Summary Hamburg Test Results (TxDOT-During Mixture Design).

Section	Deformation @20,000 Passes (inches)	Creep Slope (Passes/inch deformation) 10^3
1	0.12	402
2	0.07	752
3	0.09	802
4	0.10	378
5	0.06	1149
6	0.10	650
7	0.10	471
8	0.06	1008
9	0.09	--
10	0.11	--

-- data not available

Table C8. Type B Base Course Longitudinal Joint Density (TxDOT).

Lot No.	Lane	Station	Density (pcf)		
			Left	Middle	Right
4-1	EB OS	1172+50	139.7	142.6	140.0
4-2	EB OS	1221+46	139.9	141.6	140.3
4-3	EB OS	1252+74	139.3	143.3	139.3
4-4	EB OS	1279+28	140.6	140.0	142.4
5-1	WB IS	1303+06	No Joint	141.7	141.6
6-1	WB IS	1302+23	No Joint	143.8	139.9
6-2	WB IS	1274+53	No Joint	144.6	142.7
6-3	WB IS	1239+18	No Joint	138.1	137.6
6-4	WB IS	1171+15	No Joint	143.8	139.9
7-1	WB IS	1148+76	No Joint	139.1	142.6
7-3	EB IS	1141+70	144.8	141.4	143.3
7-4	EB IS	1155+60	144.1	143.3	141.3
8-1	EB IS	1223+35	143.9	142.8	143.6
8-4	EB IS	1264+99	142.8	142.4	141.7

Table C9. Surface Course Longitudinal Joint Density (TxDOT).

Type of Mixture	Section No.	Lot No.	Station	Lane	Density (pcf)		
					Left	Middle	Right
CMHB- Martin Marietta	6	1-1	1154+50	EB IS	No Joint	133.8	134.7
CMHB- Martin Marietta	6	1-2	1135+94	EB IS	No Joint	129.5	132.5
CMHB- Martin Marietta	6	1-3	1163+38	EB OS	128.3	136.6	132.5
CMHB-Meridian, Sawyer	5	1-1	-	WB IS	No Joint	126.3	127.8
CMHB-Meridian, Sawyer	5	1-2	-	WB IS	No Joint	119.9	118.0
CMHB-Meridian, Sawyer	5	1-3	-	WB OS	117.1	117.7	117.3
CMHB-Hanson, Prescott	4	-	-	-	-	-	-
Type C- Martin Marietta	9	1-1	1201+22	EB IS	No Joint	132.9	128.7
Type C- Martin Marietta	9	1-2	1195+12	EB OS	128.2	130.8	127.4
Type C-Hanson, Prescott	7	1-1	-	WB IS	No Joint	132.9	128.7
Type C-Hanson, Prescott	7	1-2	-	WB IS	No Joint	119.8	122.9
Type C-Hanson, Prescott	7	1-3	-	WB OS	122.3	124.3	121.6
Type C-Meridian, Sawyer	8	1-1	1293+12	WB IS	No Joint	139.4	137.7
Type C-Meridian, Sawyer	8	1-2	1307+86	WB IS	No Joint	133.9	136.3
Type C-Meridian, Sawyer	8	1-3	1292+28	WB OS	137.5	140.3	137.2
Superpave-Hanson, Prescott	1	1-1	1221+90	EB IS	No Joint	134.9	136.7
Superpave-Hanson, Prescott	1	1-2	1224+80	EB IS	No Joint	135.8	135.2
Superpave-Hanson, Prescott	1	1-3	1242+40	EB OS	131.7	132.8	129.9
Superpave- Martin Marietta	3	1-1	1187+90	WB IS	No Joint	127.4	129.1
Superpave- Martin Marietta	3	1-2	1145+93	WB IS	131.3	131.4	133.4
Superpave-Meridian, Sawyer	2	1-1	-	WB OS	124.7	127.6	127.4

\- data not available

Table C10. Mixture Temperature before Laydown (TxDOT).

Section No.	No. of Temp. Reading	Average Temp. (°F)	Std. Deviation	Coefficient of Variation (%)
1	7	318.9	18.9	5.9
2	10	320.2	14.8	4.6
3	8	306.4	23.2	7.6
4	7	318.1	18.8	5.9
5	7	318.4	14.4	4.5
6	8	313.3	18.2	5.8
7	8	318.1	14.9	4.7
8	9	323.9	21.5	6.6
9	6	321.2	13.8	4.3
10	34	326.9	11.2	3.4

Table C11. Modulus Testing at UTEP.

Section	Mixture	Aggregate	Modulus of Asphalt Mixture					
			PSPA (Field Measurement)		Core (Ultrasonic-Lab Measurement))		Lab Compacted (Seismic Modulus-Lab)	
			Avg. (ksi)	Cv (%)	Avg. (ksi)	Cv (%)	Avg. (ksi)	Cv
1	Superpave	Siliceous	577	10.8	575	9.2	927	7.9
2	Superpave	Sandstone	560	5.9	593	5.2	--	--
3	Superpave	Quartz	621	7.7	626	10.7	957	3.2
4	CMHB-C	Siliceous	683	12.0	663	4.8	1043	1.9
5	CMHB-C	Sandstone	515	8.6	514	3.2	847	2.3
6	CMHB-C	Quartz	609	13.4	507	11.2	851	2.0
7	Type C	Siliceous	573	11.5	637	0.9	1088	3.7
8	Type C	Sandstone	531	8.0	542	4.8	914	9.4
9	Type C	Quartz	566	7.2	590	2.7	807	6.4

Cv – Coefficient of Variation